MRC Harwell Institute

An International Centre for Mouse Genetics

UNIVERSITY OF OXFORD

Study of sex determination in mice lacking candidate genes identified by human exome sequencing

A thesis presented for the degree of Doctor of Philosophy (DPhil)

Wolfson College, University of Oxford

Danielle Anjali Sagar

Mammalian Genetics Unit, MRC Harwell Institute

Department of Physiology, Anatomy and Genetics, University of Oxford

Supervisors:

Dr Andy Greenfield

Professor Shankar Srinivas

Michaelmas Term 2021

Word Count: 41,500

Abstract

Disorders of sex development (DSD) comprise a heterogeneous group of conditions in which human sex development is atypical. The research described in this thesis aims at improving our understanding of DSDs, in particular those characterised by abnormal gonad development (gonadal dysgenesis, GD), using the mouse as a model of human sex development. I discuss four genes (*TLE3*, *SEC31A*, *NCOR2* and *ZNRF3*) identified by exome sequencing screens of individuals with 46,XY GD and experiments aimed at assessing their candidacy as human testis-determining genes and, in the case of one (*ZNRF3*), exploring mechanisms that lead to mouse embryonic gonadal sex reversal in their absence.

Sexual development in the mouse starts at around 10 days *post coitum* (dpc), with the formation of the bipotential gonadal primordium on the surface of the mesonephros. At around 11.5 dpc, the gonad acquires a fate determined by the chromosomal sex of the individual – a process known as gonadal sex determination. In XY embryos, *SRY* expression from the Y chromosome results, by 14.5 dpc, in Sertoli cell differentiation and testis development. In XX embryos, in the absence of SRY, canonical WNT signals and FOXL2 cause granulosa cell specification and ovary development. Therefore, I examined mouse lines that lack function of the four genes discussed above during the period 11.5 to 14.5 dpc.

Loss of the transcriptional co-repressor TLE3 did not result in any overt gonadal phenotype. By contrast, loss of SEC31A, a component of the coat protein complex II (COPII), led to very early embryonic lethality, and I investigate the molecular and cellular basis of this lethality. *NCOR2* encodes a nuclear receptor co-repressor that mediates transcriptional silencing of target genes. Exome sequencing identified sequence variants in unrelated 46,XY and 46,XX individuals with DSD, across 3 continents, making it the strongest of the candidate genes. I describe subtle but clear defects in testis and ovary development in a mouse line lacking NCOR2 function, dependent on the mouse genetic background in which the loss-of-function phenotype was analysed. These data support a role for NCOR2 in human sexual development and DSD, and warrant further investigations.

Finally, I describe experiments aimed at understanding the role of the anti-WNT ubiquitin ligase ZNRF3 in mouse testis determination, a role that was reported during the research period covered by this thesis. I show cell proliferation defects in the *Znfr3* null XY gonad and discuss the relevance of these to the sex reversal phenotype. I also describe experiments aimed at being able to detect endogenous ZNRF3 protein, using antibody generation and CRISPR/Cas9-mediated epitope tagging of the endogenous gene. Finally, I describe data from an RNA sequencing (RNAseq) experiment aimed at identifying the transcriptional consequences of *Znrf3* ablation at the sex-determining stage of gonadogenesis.

I conclude by discussing the benefits and limitations of using the mouse model for study of primary sex determination in humans, the importance of genetic background and suggest ways in which the success rate of this approach might be improved in future, by incorporating new models.

Acknowledgements

I'd like to start by thanking my supervisor, Dr Andy Greenfield, for all the amazing support you have provided throughout my DPhil and for all the time and effort spent in helping me write this thesis. I am extremely grateful to you for constantly challenging me, providing advice, and teaching me how to use a comma.

Special thanks must also go to the rest of the Sexual Development lab. To Nick Warr for providing constant entertainment alongside your excellent teaching. And also to Pam Siggers, for always encouraging me and for being an endless fountain of knowledge on sexual development and lab techniques. I most definitely couldn't have done this DPhil without you two. Thank you to Rosie Little, for your constant friendship and ceaseless reassurance, I am so glad to have worked next to you for the last four years. Also to Raissa, David, Laura, Abi and Cathy thank you for your friendship and guidance. All of you made my time at MRC Harwell enjoyable, and I cannot thank you guys enough for that.

I am incredibly grateful to Jackie Harrison and the rest of the Ward 5 team for your tireless work managing my colonies, even during a global pandemic, I couldn't have done this work without you. My sincere gratitude also goes to the rest of the Mary Lyon centre and all its staff, for all the wonderful work they do. Thanks also to the Core services at MRC Harwell, particularly to Chris Esapa and Jeremy Sanderson, for your endless help. Also, thank you to the Molecular and Cellular Biology team for my CRISPR/Cas9 mice, and to Michelle Simon and Richard Reeves for all your amazing hard work with my RNAseq data.

Thank you to my incredible family for your unwavering support and encouragement. I could never have made it this far in life without your love and inspiration, and I am eternally grateful for all you have done for me. To my partner Jonny, thank you for always being there to offer support, and for your constant belief in me even when I didn't believe in myself. Your endless love and laughter made even the toughest times enjoyable.

Finally, thank you to the Medical Research Council for funding this DPhil.

Table of Contents

List of Figures

List of Tables

Abbreviations

129	129/SvEv
3'-UTR	3 prime untranslated region
AMH	Anti-Müllerian hormone
AR	Androgen receptor
B6J	C57BL/6J
BC	Backcross level
BMP	Bone morphogenetic protein
bp	Base pair
CAH	Congenital adrenal hyperplasia
CGD	Complete gonadal dysgenesis
ChIP	Chromatin immunoprecipitation
CLSD	Cranio-lenticulo-sutural dysplasia
COPII	Coat protein complex II
CRISPR/Cas9	Clustered regularly interspaced short palindromic repeats/ CRISPR-associated protein 9
DAD	Deacetylation activation domain
DHH	Dessert hedgehog
DIG	Digoxygenin
dpc	Days *post coitum*
DSD	Differences of sex development
EdU	5-ethynyl-2´-deoxyuridine
ENH13	Enhancer 13
ER	Endoplasmic reticulum
FBS	Foetal Bovine Serum
FGF9	Fibroblast growth factor 9
GCNF	Germ cell nuclear factor
GD	Gonadal dysgenesis
GEF	Guanine nucleotide-exchange
GOF	Gain-of-function
GVHD	Graft-versus-host disease
HDAC	Histone deacetylases
HID	Histone interaction domain
HISS	Heat Inactivated Sheep Serum
HMG	High mobility group
HSCs	Hematopoietic stems cells
IF	Immunofluorescence
iPSCs	Induced pluripotent stem cells
KO	Knock-out
LB	Lysogeny broth
LOF	Loss-of-function
MAPK	Mitogen activated protein kinase
NCOR2	Nuclear receptor co-repressor 2
NMD	Nonsense mediated decay

PAGE	Polyacrylamide gel electrophoresis
PBMCs	Peripheral blood mononuclear cells
PCAF	p300/CBP-associated factor
PGD	Partial gonadal dysgenesis
RA	Retinoic Acid
RAR	Retinoic acid receptor
RID	Receptor interaction domain
RIN	RNA integrity number
RNAseq	RNA sequencing
SARS-CoV-2	Severe acute respiratory syndrome coronavirus 2
SF1	Steroidogenic factor 1
SHARP	SMRT/HDAC1-associated repressor protein
TE	Trophectoderm
TESCO	Testis-specific enhancer of *Sox9*
TLE3	Transducin-like enhancer protein 3
ts	Tail somites
UGR	Urogenital ridge
WGS	Whole genome sequencing
WMISH	Wholemount In Situ Hybridisation
wt	Wildtype
ZGA	Zygotic genome activation
ZNRF3	Zinc and ringer finger 3
ZTAG	ZNRF3-MYC-HIS-B6J line

1 Introduction

1.1 Sexual reproduction

The majority of multicellular organisms reproduce sexually rather than asexually. Asexual reproduction involves an organism producing a clone of itself, and does not involve any differences in sex between organisms. In other words, each asexual organism is able to reproduce on its own without the need for a partner. The dominance of sexual reproduction across various multicellular organisms suggests that it offers some advantage. However, some of the obvious downsides in sexual reproduction include the need, as a species, to involve two or more distinct sexes; the requirement of finding a partner, hence slowing down the reproduction process; and the need to cultivate a means of halving parental DNA so that the offspring does not possess double the genome of the parent. The distinct sexes within each sexually reproducing species need differing reproductive organs, but they must not be so different physiologically that one may have a survival advantage over the other; otherwise the balance in the population would not be maintained, making it even more challenging to find a reproductive mate. So, with these factors in mind, sexual reproduction must offer a considerable advantage for it to have evolved.

Sexual reproduction offers the advantage of generating genetic variation, which can benefit the population in many ways. A major advantage that sexual reproduction has over asexual reproduction is that it enables the quick combination of genetic variants in novel ways that may be advantageous to the individual. It can also help with the spread of beneficial mutations, which can be acquired in one organism and be passed to multiple offspring through sexual reproduction. In this way, mutations are spread much faster than in asexual reproduction, where beneficial mutations can only be acquired if the parent organism attained them. On the other side, sexual reproduction also results in the quick spread of deleterious mutations, allowing for homozygosing of harmful genes, resulting in lethality and their removal from the population. These advantages have led to the widespread use of sexual reproduction, leading to the question of how different sexes are generated.

1.2 Sex determination

Sex determination is the process by which two distinct sexes are generated. It most commonly has a genetic basis, but can also be environmental. For example, temperature-sensitive sex determination is based on the temperature the egg is incubated at during certain periods of development, which affects gene expression and gonadal development. This form of sex determination is most commonly seen in egg-laying reptiles, such as the temperature-sensitive expression of *Dmrt1* in *Trachemys scripta,* which has been shown to impact sex determination (Ge et al. 2017, Weber et al. 2020).

Genetic sex determination is usually determined by differences in chromosomes, such as the ZW and XY sex chromosome system. The ZW system, most commonly found in birds, involves the presence of either a ZW (female) or a ZZ (male) set of set sex chromosomes. This system, studied in chickens, involves the presence of *Dmrt1* on the Z chromosome. Chickens who possess the ZZ genotype then have double the amount of *Dmrt1* expression, resulting in male sex determination (Smith et al. 2009). This dosage-dependent system differs from the XX/XY (XY) system which is found in mammals, such as mice and humans. In these mammals, the Y chromosome is a dominant male determinant, and dosage of the X chromosome does not influence sex determination. It is this form of sex determination, primarily that found in the mouse, which is the focus of this thesis.

1.3 Mammalian sex determination

Sex determination in humans occurs around 6 weeks of gestation, whilst in the mouse it starts at around 10 days *post coitum* (dpc) with the development of a bipotential gonadal primordium on the surface of the mesonephros. At this stage the developing gonad can adopt either the ovarian or testicular fate. In the presence of a Y chromosome, testis determination occurs due to the presence of the *SRY* gene on its short arm (Gubbay et al. 1990, Sinclair et al. 1990). *SRY* has been shown to be the only gene on the Y chromosome needed for testis determination, and can initiate male gonadal development in XX transgenic mice (Koopman et al. 1991).

1.3.1 Testis determination

Sry is expressed in the gonadal somatic cells between 10.5-12.0 dpc in mice. It encodes a transcription factor that upregulates *SOX9* (SRY box containing gene 9) expression, allowing differentiation of somatic cell precursors into Sertoli cells, the supporting cells of the testis. Strict control of spatio-temporal expression of *Sry* in mice is highly important for correct testis development, and studies have found a critical period during which it must be expressed to enable Sertoli cell differentiation (Hiramatsu et al. 2009). Further studies have also found that mutations affecting S*ry's* temporal expression pattern prevent proper testis determination. For example, a delay in S*ry* expression in *Mus domesticus* compared to *Mus musculus* has been shown to cause sex reversal in C57BL/6J mice who carry the Y chromosome from *domesticus* (Bullejos and Koopman 2005, Livermore et al. 2020).

Sry expression in mice is transient, with expression being undetectable by 12.5 dpc (Koopman et al. 1990). This is because *Sry's* primary function is to drive *Sox9* expression and allow for the establishment of the testis-determining pathway (Fig 1.1), which then works to maintain its own expression throughout development via a positive feedback loop (Barrionuevo et al. 2006). In addition to being transient, *Sry* is expressed in a specific spatial pattern. Initial expression starts in the centre of the gonad before spreading to the poles. At the peak of *Sry* expression, at around 18 tail somites (ts) (Materials and Method Fig 2.1) in the mouse, it is present along the length of the gonad. As expression fades it moves towards the poles before being undetectable by 12.5 dpc (Bullejos and Koopman 2001). Even the slightest delay in *SRY* expression may prevent it from reaching the poles of the gonad during the critical period, making the poles highly sensitised to XY sex reversal (Bullejos and Koopman 2005).

SRY was initially thought to activate *Sox9* transcription by binding testis-specific enhancer of *Sox9* core (TESCO), which is mediated by steroidogenic factor 1 (SF1). SF1 is encoded by the gene *Nr5a1*, and is only expressed in supporting cells (Sekido and Lovell-Badge 2008). Further to this, SF1 plays a role in testis development even after the transient expression of *Sry*, via the maintenance of *Sox9*. Much the

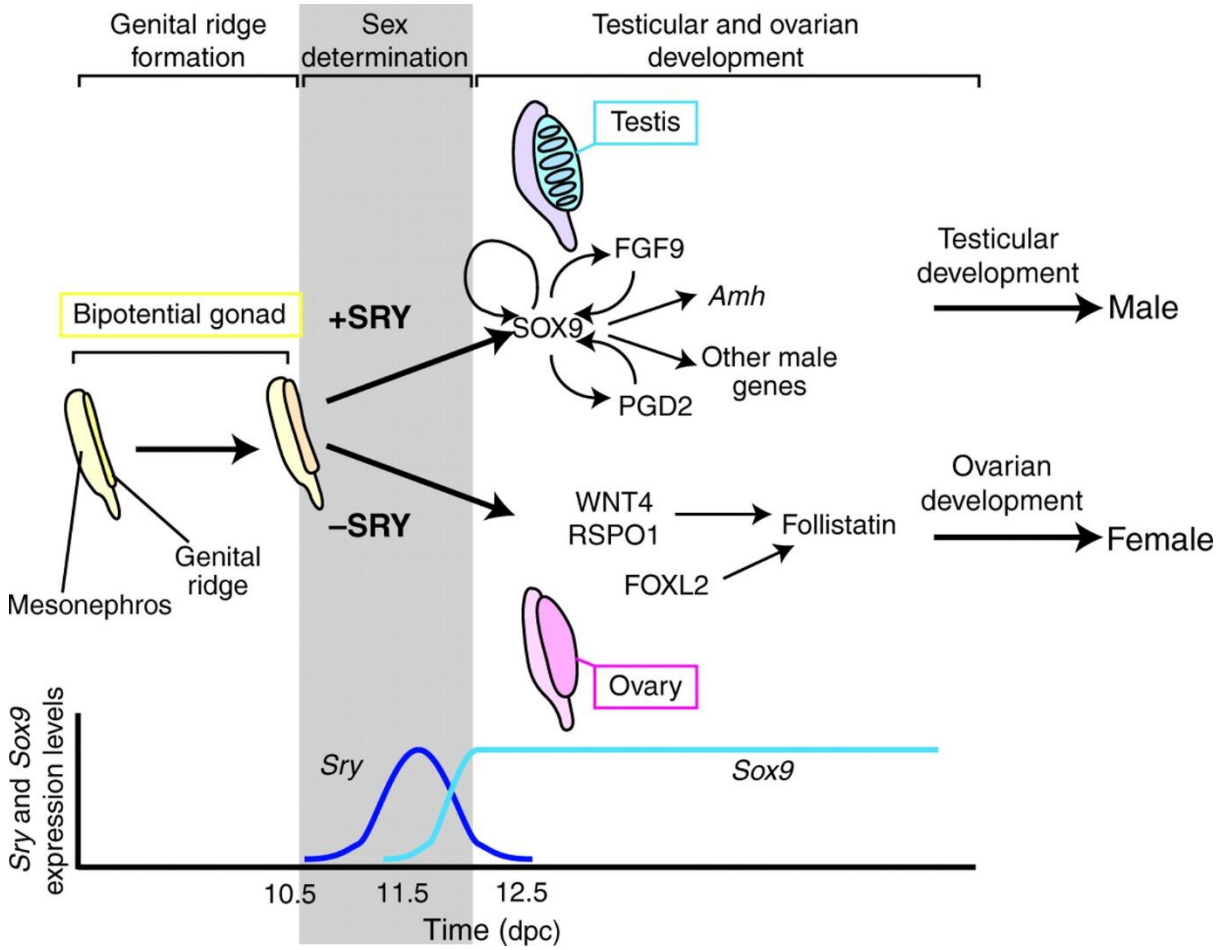

Figure 1.1. Sex Determination Pathway.
In XY gonads the presence of *Sry* results in *Sox9* and *Fgf9* expression which work in a positive feedback loop to maintain *Sox9* expression and enable testis determination. In the absence of *Sry*, in XX gonads, *Rspo1* exxpression enables the WNT/β-catenin signalling pathway which results in ovarian determination. (Kashimada and Koopman 2010)

same as SF1 enables SRY to bind to TESCO and upregulate *Sox9,* it also enables SOX9 to do the same, establishing a positive feedback loop with itself, allowing for maintained expression of *Sox9* throughout development of the gonad, even when SRY isn't present. TESCO deletion reduces *Sox9* expression in XY embryonic gonads to 60-40%, and when present alongside a conditional *Sox9* null allele this deletion results in ovotestes development (Gonen et al. 2017). More recent studies have discovered an additional and more important enhancer that enables *Sox9* maintenance; *Enhancer 13 (Enh13)* was discovered in the 2-megabase gene desert upstream of *Sox9*, and has been shown to be essential to initiate testis determination (Gonen et al. 2018). This initiation and maintenance of *Sox9*

is the central premise of testis determination, allowing for upregulation of downstream factors such as *Fgf9/Fgfr2,* and crucial Sertoli cell differentiation. Further highlighting the importance of *Sox9* in sex determination, is its connection with multiple cases of XY gonadal dysgenesis (GD) in humans. In addition to bone defects, a proportion of campomelic dysplasia patients also show male to female sex reversal, associated with mutations in *SOX9* (Unger, Scherer and Superti-Furga 1993, Foster et al. 1994). In addition, a case of female to male sex reversal was found in a patient with a duplication of *SOX9* (Huang et al. 1999). Subsequent studies of *Sox9* in mice showed it to be necessary and sufficient for testis determination, with complete loss causing XY gonadal sex reversal – the presence of ovarian tissue and structures within an XY gonad - and ectopic expression causing female to male (XX) gonadal sex reversal – the presence of testicular tissue and structures within an XX gonad - (Barrionuevo et al. 2006, Vidal et al. 2001).

Downstream targets of SOX9 are not as clearly characterised within the developing gonad. Chromatin immunoprecipitation (ChIP) experiments have highlighted many putative targets for SOX9, some of which have clear roles within the gonad (Rahmoun et al. 2017). However, detailed expression patterns of many of these genes and how they functionally interact with *Sox9* and each other are not yet available. Some target genes highlighted by ChIP experiments have known roles in sex development, including desert hedgehog (*Dhh*), fibroblast growth factor 9 (*Fgf9*) and anti-Müllerian hormone (*Amh*). *Dhh* is known to have a role in cell-type specification within the gonad; specifically, it has been shown to be secreted from Sertoli cells enabling steroidogenic cell precursors to differentiate into Leydig cells, within the developing gonad (Yao, Whoriskey and Capel 2002). *Amh* is known to encode anti-Müllerian hormone (AMH), a hormone which is secreted by Sertoli cells during testis development, enabling Müllerian duct regression (Arango, Lovell-Badge and Behringer 1999, Behringer, Finegold and Cate 1994). *Fgf9* is considered to be one of the major downstream targets of SOX9, and is thought to have a role in the continued maintenance of *Sox9* expression throughout gonadal development, with *Fgf9*-null gonads showing loss of *Sox9* expression between 11.5-12.5 dpc (Kim et al. 2006). Throughout gonadal development, *Fgf9* expression changes: at 11.5 dpc it is expressed in both the XX and XY

gonad; however, by 12.5 dpc expression is sexually dimorphic, and expression is restricted to the XY gonad by 13.5 dpc (Kim et al. 2006). More recent studies with *Fgf9* suggest that its role may not be to directly upregulate *Sox9,* as was previously suggested, but to negatively regulate *Wnt4,* a vital component of the ovarian pathway (Jameson, Lin and Capel 2012a). In this way, *Fgf9* promotes testis development and also prevents WNT4 from repressing *Sox9* expression. So, it is still involved in the maintenance of *Sox9* expression, just not as a direct positively-acting factor. This role of FGF9, is part of the mutual antagonism between the ovarian and testicular pathways which is now considered fundamental to mammalian sex determination (see later section on mutual antagonism).

1.3.2 Ovary determination

Ovarian development is often referred to as the 'default' pathway, which occurs whenever *SRY/SOX9* are not present. However, more recent studies suggest that the ovarian pathway is much less 'passive' than once thought, with many models highlighting how loss of key genes can lead to masculinisation of XX gonads.

In the XX gonad there is no *SRY* present due to the lack of a Y chromosome; this prevents upregulation of *SOX9* and its downstream components. However, there appears to be no single 'female determining gene'. Although less is known about ovarian development, it is considered that there are three major pro-ovarian genetic components: *RSPO1, WNT4* and *FOXL2.* Knocking out any of these genes in mice causes postnatal female-to-male sex reversal of varying degrees (Chassot et al. 2008, Vainio et al. 1999). These three genes are thought to be involved in two distinct genetic cascades within the developing gonad. *RSPO1* and *WNT4* function in canonical WNT signalling. XX mice lacking *Rspo1* or *Wnt4* develop a coelomic vessel, a structure that would normally only be seen in XY testis; and some degree of masculinisation also occurs post-natally (Chassot et al. 2008, Vainio et al. 1999).

The second is the *FOXL2* pathway, which is less clearly understood but considered equally vital for ovary development (Pannetier et al. 2016). Once ovarian fate is determined, supporting cell precursors differentiate into granulosa cells. The exact catalyst behind this specification is uncertain

but it is thought to require the *Foxl2* pathway, since *Foxl2* expression within the developing gonad does not appear until after sex determination has occurred (Auguste et al. 2011, Schmidt et al. 2004), making it a likely candidate. Further studies with *Foxl2* mouse mutants have shown that it is needed for granulosa cells to complete the squamous to cuboidal transition necessary for proper ovarian development and maintenance, confirming the likelihood of its role in ovarian germ cell development. Murine gonadal somatic cells are microscopically distinct by 12.5 dpc; however, germ cells remain microscopically indistinguishable until 13.5 dpc. It is considered that this is because granulosa cells must first develop to initiate germ cell differentiation. This specification pattern of germ cells differentiation after somatic cells correlates with *Foxl2* expression. All of this suggests that *Foxl2*'s role within the developing ovary is to enable germ cell specification after somatic cell differentiation. However, more recent studies have suggested that germ cells are in fact already sexually dimorphic by 11.5 dpc, (Mayère et al. 2021), and merely take longer to become microscopically distinct when compared to somatic cells. Further to the above potential role, *Foxl2* also has a role in post-determination in the maintenance of gonadal fate. As with the other two pro-ovarian factors, *Wnt4* and *Rspo1,* it required throughout the lifespan of the ovary to maintain ovarian fate. Loss of these core genes can result in partial sex reversal, even in adult ovaries, in a process known as cell fate reprogramming (Uhlenhaut et al. 2009).

When the germ cells become sexually dimorphic at 13.5 dpc, the ovarian germ cells initiate prophase of meiosis, whereas testicular germ cells arrest in the mitotic cell cycle and don't undergo meiosis until after birth. This transition into meiosis is initiated by *Stra8* expression, both embryonically for ovarian development and post-natally for testicular development (Koubova et al. 2006). As such, there is sexually dimorphic expression of *Stra8,* with it being expressed embryonically in the developing ovary from around 13.5 dpc, but not expressed in the testes until after birth. This sexual dimorphic expression makes *Stra8* a good marker of embryonic ovarian development, especially when contrasted against *Sox9* expression as a marker of testicular development.

1.4 Canonical WNT signalling in the developing gonad

As previously mentioned, WNT signalling is a vital part of sex determination. In particular, *Wnt4* has been highlighted in mouse studies as necessary for normal ovarian development in XX mice. Duplications of the distal region of human chromosome 1p have also been associated with male to female sex reversal in 46,XY patients (Elejalde et al. 1984, Wieacker et al. 1996). This region is known to contain *WNT4* and *RSPO1.* Other studies with *WNT4* have shown that it is involved in three distinct areas of sex development: formation of the Müllerian duct, differentiation of stromal cell lineage, and oocyte development. *WNT4* has also been shown to supress Leydig cell differentiation during ovarian development (Vainio et al. 1999), with more recent DSD cases showing that a loss in WNT4 function can cause female to male sex reversal in 46,XX patients (Mandel et al. 2008).

Murine studies have shown that *Wnt4* is expressed in both XX and XY gonads prior to sex determination; however, at around 11.5 dpc it becomes sexually dimorphic and restricted to XX gonads (Kim et al. 2006). Throughout gonad development it continues to be expressed in the somatic cells of the ovary, suggesting a continued role for *Wnt4* in the embryonic ovary (Vainio et al. 1999), however unlike *Foxl2* this has not been established by inactivating *Wnt4* in the adult ovary. This continued role is thought to be linked to the mutual antagonism between XX and XY pathways that is so central to gonadal development. Further to all this evidence for WNT4's role in ovarian development, downstream targets of WNT4 have also been shown to be upregulated during ovarian development. For example, *Axin2* which is activated through canonical WNT-signalling, is expressed in ovarian somatic cells (Chassot et al. 2008), solidifying the importance of WNT-signalling for ovarian development.

1.4.1 Canonical WNT signalling: β-catenin

As previously mentioned, WNT signalling in the XX gonad operates through *Rspo1/Wnt4.* This pathway activates canonical WNT signalling, a pathway that involves the activation and maintenance of β-catenin. β-catenin is encoded by the gene *Ctnbb1*, and it is the primary target of canonical WNT

signalling. Murine studies with β-catenin have shown that its ectopic expression in XY gonads can cause male to female sex reversal (Maatouk et al. 2008). Further to this work the same study also showed that stabilisation of β-catenin in a WNT-null gonad rescues the sex reversal phenotype. Meaning that *Wnt4* in the gonad is definitely acting through canonical signalling, rather than the other possible WNT-signalling pathways (Maatouk et al. 2008). β-catenin stabilisation causes upregulation of the canonical WNT-signalling pathway via a positive feedback system. When this occurs in the developing murine gonad the Sertoli cell lineage is unable to be maintained. This was shown in developing XY murine gonads where β-catenin was stabilised; at 11.5 dpc *Sox9* expression is normal however, by 12.5-13.5 dpc expression has completely disappeared leading to male to female sex reversal in these mice (Maatouk et al. 2008).

To further study the involvement of β-catenin in gonadal development, it was ablated in the SF1-positive population of somatic cells. In the XY gonad this did not affect Sertoli cell differentiation, confirming that whilst present in the developing testis it is dispensable, however in the XX gonad sex reversal was seen (Liu et al. 2009). The phenotype of the knockout closely resembled that of *Rspo1* and *Wnt4* knockout. Gene expression studies performed on the β-catenin knockout showed *Wnt4* expression to be reduced but *Rspo1* unaffected, placing the role of β-catenin between these two. All of the above mentioned work confirms the importance of β-catenin and the canonical WNT signalling pathway in ovarian development.

1.4.2 *RSPO1* and *ZNRF3*

Studies have shown that the secreted protein RSPO1, in association with LGR4/5, can promote WNT signalling; however, the direct mechanism of this was unclear until recently. WNT signalling is activated by binding of a WNT-protein ligand to a FRIZZLED family receptor which then passes a signal to the dishevelled protein inside the cell. Current studies show that RSPO1 can bind to ZNRF3, either via LGR4 or on its own, and block it from functioning as an E3 ubiquitin ligase that clears FRIZZLED from the cell membrane (Fig 4.1). In this way, RSPO1 can promote stabilisation of FRIZZLED receptor

and WNT signalling. However, without the presence of RSPO1, ZNRF3 is free to target the FRIZZLED receptor for degradation by ubiquitination, and as such diminish WNT signalling (Hao et al. 2012, Xie et al. 2013, Szenker-Ravi et al. 2018). Evidence exists that this pathway functions in the developing gonad, with the identification of 46,XY female patients who have missense mutations in *ZNRF3* (Harris et al. 2018). This highlights the importance of this E3 ubiquitin ligase in sex determination, and suggests that RSPO1 is functioning via ZNRF3 to promote canonical WNT signalling. Murine studies with *Znrf3*-null mice also reveal varying degrees of XY gonadal sex reversal, supporting what was observed in humans and indicating how RSPO1 may be functioning in the gonad (Harris et al. 2018). RSPO1 has been shown to be acting via the WNT/β-catenin signalling pathway during ovarian development; however, *Rspo1*-null mice have a more severe masculinisation phenotype than *Wnt4*-null mice (Chassot et al. 2008), suggesting that RSPO1 might be influencing sex determination through other mechanisms as well. All of this work highlights how vital *Wnt4, RSPO1* and in particular the canonical WNT pathway are to ovarian development.

1.5 Mutual Antagonism between the testis- and ovary-determining pathways

As previously mentioned, in the developing testis SOX9 upregulates *Fgf9,* which was initially thought to work in a positive feedback loop to maintain *Sox9* expression after *Sry* expression ceases. However, more recent studies looking at *Wnt4* and *Fgf9* double knockouts have found that FGF9 works to repress canonical WNT signalling, a pathway which has previously been shown as vital to ovarian development (Jameson et al. 2012a). Further studies have determined that FGF9 acts via the FGFR2 receptor, during gonadal development, to repress canonical WNT signalling and allow testis development (Bagheri-Fam et al. 2008, Siggers et al. 2014, Kim et al. 2007). This suggests that FGF9's role as a pro-testis factor is in fact more anti-ovarian factor. Further this, the same study showed that, in the absence of WNT4 signalling, FGF9/FGFR2 are not needed to maintain SOX9 expression. This highlights the importance of WNT4 in the function of FGF9/FGFR2, and falls in with current views that

antagonism between the two pathways is vital for proper sex determination, and that maybe FGF9's main role is to act in an anti-ovarian fashion.

This antagonism does not just work one way with pro-testicular factors repressing ovarian factors: it is mutual. This means that ovarian factors are also working to repress testicular factors. This was suggested early on when duplication of *WNT4* was shown to disrupt testis development in 46,XY patients leading to male to female sex reversal (Jordan et al. 2001). This antagonism was further confirmed again in studies previously discussed, in which stabilisation of β-catenin was shown to prevent SOX9 maintenance in the developing gonad by 12.5 dpc, leading to XY gonadal sex reversal (Maatouk et al. 2008). Interestingly, the XX gonadal sex reversal that *Wnt4*-null mice undergo cannot be rescued by *Fgf9* deletion (Bagheri-Fam et al. 2008, Jameson et al. 2012a). This suggests that WNT4 does not function in XX gonad development by opposing FGF9.

1.6 Cell lineages of the gonad

The developing gonad comprises four distinct cell lineages: the supporting cells, the interstitial/stromal cells, and the endothelial cells – all of which are somatic – and the germ cells. Primary (gonadal) sex determination occurs within the supporting cell lineage. The supporting cells arise from a common mesodermal progenitor within the urogenital ridge (UGR) along with the interstitial/stromal cells. The other two lineages are not produced in the urogenital ridge and must migrate in. Germ cells are the embryonic precursors of gametes, the haploid cells used in sexual reproduction, these migrate into the developing gonad from a region near the allantois. It is crucial that sex determination does not occur before these cells have migrated. This links back to the specific temporal expression pattern of key sex determining genes, and how any disruption to this expression can prevent correct determination. Prior to sex determination each lineage is bipotential and can adopt either a testicular or ovarian cell fate (Karl and Capel 1998, Coveney et al. 2008, Martineau et al. 1997). More recent single-cell RNAseq studies have confirmed that the somatic lineages of the

gonad arise from a single multipotent progenitor population at around 10.5 dpc (Stevant et al. 2018, Stevant et al. 2019).

The two most important lineages in sex determination of the gonad are the supporting cell lineage and the germ cell lineage. It is thought that primary sex determination within the supporting cell lineage occurs first and causes sex determination within the germ cell lineage. Murine supporting cells are microscopically different between XX and XY gonads by 12.5 dpc; however, germ cells are not distinct until 13.5 dpc (Koubova et al. 2006), supporting the theory that supporting cells differentiate first and then influence germ cell development. Further to this, studies have shown that it is the supporting cell lineage that is directly influenced by *SRY* expression, and not the germ cell lineage. Transgene studies using eGFP attached to the *Sry*-promoter have shown the presence of SRY causes somatic cells to differentiate into Sertoli cells, whereas the lack of SRY allows for granulosa cell development (Albrecht and Eicher 2001). Sertoli cells have then been shown to influence the microenvironment surrounding the germ cells, allowing for spermatozoa development within the embryonic testis (Griswold 1998).

Whilst the supporting and germ cell lineages are the most studied, the other lineages are also vital for gonadal development. For example, the endothelial cell lineage is known to be involved in the developing structure of the testis and also forms the coelomic vessel on the surface of the mesonephros (Romereim and Cupp 2016), a structure often used to show female to male sex reversal. However, the role of the supporting cell and germ cell lineages in primary sex determination makes them the focus of the work in this thesis.

1.7 Differences of sex development (DSD)

I have previously highlighted that many different genes are necessary for gonadal development. When these genes are mutated patients may present with DSDs. Up until recently this acronym stood for ‘Disorders of Sex Development’; however, after suggestions of stigma being attached to this term and

many patients highlighting that their DSD does not affect their health, the term now used is 'Differences of Sex Development' (Johnson et al. 2017). DSDs are conditions in which chromosomal, gonadal or phenotypic sex development occurs in an atypical fashion. DSDs are complex disorders often involving many genes, and can have a wide range of phenotypes, each with varying severity. Phenotypes can range from cryptorchidism, the most common phenotype seen in male births in the UK (1 in 25), to extremely rare 46,XY complete gonadal dysgenesis (CGD) with female external genitalia. DSDs are categorised into three groups: chromosomal DSD, 46,XX DSD and 46,XY DSD. Each group accounts for 12%, 26% and 62% of DSDs respectively (Lee et al. 2006).

1.7.1 Chromosomal DSD

Within the chromosomal category there are further subcategories such as mosaicism, Klinefelter syndrome and Turner syndrome. 45,X/46,XY mosaicism involve differences in genotype between cells within one individual. As with most DSDs the phenotypes associated are extremely variable and are thought to be due to the ratio of 45,X to 46,XY cells within the gonad itself (Kamel et al. 2015).

Klinefelter syndrome occurs in patients with 47,XXY karyotype. There are variations of this that have a more severe phenotype and are much rarer in occurrence, involving a 48,XXXY or 49,XXXXY karyotype. The prevalence of this syndrome is estimated at around 1 in 600-700 males (Bojesen, Juul and Gravholt 2003). Affected males present with androgen deficiency and incomplete spermatogenesis resulting in small testes, sparse body hair, tallness and infertility, although as previously mentioned the phenotype is very variable so patients do not always present with all the above. This phenotypic variation is thought to make Klinefelter syndrome significantly underdiagnosed, and many patients won't be diagnosed until puberty or even until they start trying to have children (Smyth and Bremner 1998).

Turner syndrome occurs in females who are missing an X chromosome, either completely or partially, and as such have a 45,X karyotype. The condition occurs at a frequency of 1 in 2500 female live births. The most common phenotypes affecting over 90% of patients are short stature and premature ovarian

failure. Other phenotypes involve webbed neck, low-set ears and skeletal abnormalities. A proportion of patients also have a nonverbal learning disorder, which has previously caused this syndrome to be associated with a low IQ (Bondy 2009).

1.7.2 46,XX DSD

46,XX DSDs are characterised by ambiguous or 'male' external genitalia in patients carrying the female complement of sex chromosomes. The most common form of 46,XX DSD is congenital adrenal hyperplasia (CAH). Patients with CAH have adrenal glands overproducing androgens, leading to aberrant formation of masculinised external genitalia. However, these patients usually have ovaries, Müllerian structures and can be fertile and able to give birth if treated correctly (Achermann et al. 2015, Dessens, Slijper and Drop 2005).

Another rarer group of 46,XX DSD patients possess testes (46,XX testicular DSD) or 'ovotestes' (46,XX ovotesticular DSD) i.e. varying degrees of gonadal masculinisation. This can be linked to the presence of *SRY* on the X chromosome due to a translocation event, as was seen in a familial case of 46,XX DSD in which a father had transmitted an *SRY*-bearing X chromosome to two of his children. One was a 46,XX male and the other a 46,XX ovotesticular DSD. Variable phenotypes were thought to be due to X-inactivation differences (Abbas et al. 1993). Genetic background is also likely to make a significant contribution to phenotypic variability. However, some 46,XX DSD patients do not possess *SRY* (Toublanc et al. 1993). These patients often possess loss of function mutations in genes which are central to ovarian development, such as *WNT4* or *RSPO1* (Mandel et al. 2008, Parma et al. 2006).

Further causes of 46,XX DSD have more recently been attributed to *SOX9* duplication (Cox et al. 2011). However, some causes are still unknown.

1.7.3 46,XY DSD

46,XY DSDs account for 62% of all DSDs, and can be due to abnormal hormone production and/or sensitivity. In androgen insensitivity syndrome, patients often have normal or even higher levels of

testosterone present but lack functional androgen receptor required to respond to this, resulting in ambiguous or female external genitalia (Mongan et al. 2015). The same phenotype is seen in patients with testosterone synthesis defects. These patients can often have testes within the abdomen that have not descended during development (Achermann et al. 2015). Another 46,XY DSD related to defects in endocrine function is Testicular Dysgenesis syndrome, which covers a range of problems caused by insufficient androgen production by the developing testis. It can result in cryptorchidism, hypospadias, low sperm count and testicular germ cell cancer (Sharpe 2020).

Another group of 46,XY DSDs involves aberrant testes determination during development leading to gonadal dysgenesis (GD). GD can either be complete (CGD), and involve female external genitalia, Müllerian structures and 'ovarian like' gonads, or partial (PGD) with a mix of ovarian and testicular structures present. Around 15% of CGD patients have mutations in *SRY*. A further 15% of 46,XY DSDs are caused by mutations within *NR5A1* , and 10% caused by *MAP3K1* variants. Other genes implicated in 46,XY DSD include *DMRT1*, *CBX2, GATA4, SOX9, DHH, WT1,WNT4, NR0B1, HHAT* and *ZNRF3* (Bashamboo and McElreavey 2016, Bashamboo et al. 2017, Harris et al. 2018, Callier et al. 2014). However, many causes of 46,XY GD are still unknown, and this thesis focuses on ways of closing this gap in our understanding.

1.7.4 Understanding DSDs

As previously mentioned, many causes of DSD are still unknown. Determining these causes offers many benefits, including providing clarity to patients and their families and revealing any associated risks. Some GD patients are at risk of developing gonadal germ cell tumours (Tam et al. 2016). In addition to providing important diagnoses, identifying novel causes of GD enables us to better understand the mechanisms behind gonadal development and disease, including how aberrant development may lead to tumours, potentially allowing at-risk patients to be identified before tumour growth begins.

The advent of cheaper and faster next generation sequencing techniques is enabling clinicians to identify potential candidate genes in patients who present with DSD of unknown cause. The most successful approach has been via exome sequencing, which highlights coding variants in patients who have DSD. 80-90% of known disease-causing variants are located within the exome, making this a good place to investigate first; whole genome sequencing methods are often more expensive and ineffective, although improved analytical tools are making this approach more realistic. Exome sequencing often identifies around 21,000 variants per person compared to the human reference genome; these can then be narrowed down using bioinformatic analysis to enable the identification of potential candidate genes, which can be studied in more detail using *in vitro* and *in vivo* models. A 2015 study provided a genetic diagnosis via exome sequencing in 35% of patient cases where all other genetic testing had been exhausted (Baxter et al. 2015, Lee et al. 2014). Specific examples for novel DSD diagnosis include: *NR5A1* mutations such as a R92W variant and, separately, a 3 base-pair (bp) deletion in exon 6 both discovered via exome sequencing gonadal dysgenesis patients (Bashamboo et al. 2016, Eggers et al. 2015), variants in *MAP3K1* including de novo R339Q in a patient with complete gonadal dysgenesis and P267L in a patient with ambiguous external genitalia, and variants in *WT1* comprising H469Q and R458Q (Baxter et al. 2015). A more recent example of the potential of exome sequencing was the discovery of a novel testis-determining gene, *ZNRF3* (Harris et al. 2018).

1.8 Mouse models of sex determination

As previously discussed, the sex determination system used by mammals is the genetic XY chromosome system. The pathways involved in this system are well conserved between humans and mice, with *SRY* being the male determining gene on which gonadal fate is decided in both organisms (Nef and Vassalli 2009, Morais da Silva et al. 1996). As such, mice are a widely used model organism for studying human sex determination. They can be used to study candidate genes or even to discover them. For example, forward genetic screens in mice have highlighted novel genes involved in mouse sex determination which can often be relevant to human gonadal development.

However, some discoveries made in mice are not easily translated into humans. One such discovery concerns the gene *Map3k4,* which was found to be necessary for mouse testis determination; but *MAP3K4* mutations have never been reported in human cases of 46,XY DSD (Siggers et al. 2014, Bogani et al. 2009). However, mutations in *MAP3K1* are one of the most frequently cited causes of 46,XY GD and DSD (Pearlman et al. 2010). This highlights how there are some important differences in sex determination between these two organisms. One of these important differences involves the testis-determining gene, *SRY;* whilst it is crucial in both organisms its mode of expression does vary. In mice, *Sry* expression has been shown to be transient with a peak at 18 ts (11.5 dpc), as previously discussed. However, in humans *SRY* expression is not transient and remains present throughout development and adulthood (Clepet et al. 1993). These differences do not render the mouse model obsolete, and it is still very useful in replicating and characterising human DSDs, but they are important to bear in mind.

A recent example of the usefulness of the mouse model was the discovery of a novel sex determining gene, *ZNRF3*. In this case, patients presented with 46,XY DSD of unknown cause; exome sequencing was then performed, which highlighted *ZNRF3* as a candidate gene. Global knockout studies subsequently performed in mice confirmed the importance of this gene for correct testis determination. An interesting point to note is that when the specific human mutation was replicated in mice using CRISPR/Cas9 the 46,XY sex reversal phenotype was not seen. This study highlights both the usefulness of the mouse model organism and its limitations (Harris et al. 2018).

The study just discussed was performed using C57BL/6J (B6J) mice. The strain of inbred mice used for model studies is important as the literature shows, but this particular strain is extremely important for sex determination studies because B6J mice are sensitised to disruptions to testis determination. This is thought to be due to higher levels of expression of pro-ovary genes in the B6J 11.5 dpc gonad when compared to 129S1/SvlmJ (129) mice (Munger et al. 2009, Correa et al. 2012). Another useful sub-strain of mice are those with a Y chromosome derived from *Mus domesticus,* kept on a congenic

B6J background (B6J.Y^{AKR}). These mice are highly sensitised to testis development disruptions as their Y chromosome is not fully compatible with B6J autosomes, resulting in transient ovotestes during development and small testes with reduced fertility post-natally (Washburn and Eicher 1989). All of these models and genetic tools reveal the mouse to be a useful model organism for modelling DSDs, with its conserved genetic pathways and variable genetic backgrounds. This thesis will focus on this model organism for all *in vivo* work. In particular, I will discuss the use of mouse models for the evaluation of several candidate DSD genes identified by human exome sequencing. I will also describe further studies on the role of ZNRF3 in testis determination.

2 Materials and methods

2.1 Mouse lines and genotyping

2.1.1 Chromosomal Sexing

All embryos were genotyped using a previously described assay (Warr et al. 2009).

2.1.2 *Znrf3*^{del}

Mice harbouring floxed *Znrf3* allele were a gift from Hans Clevers, as described in (Harris et al. 2018). The colony was genotyped by the Harwell GEMS core facility (Ramakrishna Kurapati). Embryos were genotyped with a gel-based assay using primers designed around exon 7 (Table 2.1) (Harris et al. 2018).

2.1.3 *Tle3*^{del}

Mice harbouring a floxed *Tle3* allele were kindly provided by Peter Tontonoz (Villanueva et al. 2013). Males were culled and their sperm harvested for IVF. Fertilised eggs were treated with soluble Cre [Excellegen] in order to generate null animals. The colony was genotyped by the Harwell GEMS core facility (Ramakrishna Kurapati), with embryos genotyped using a gel based assay designed around exon 3. The gel based assay consisted of 3 primers (Table 2.1), DreamTaq Green PCR Master Mix [ThermoFisher K1081], and water at a 0.75:5:4 ratio.

2.1.4 *Sec31a*^{del}

This allele was generated by the Harwell CRISPR team (Lydia Teboul) and genotyped by the Harwell GEMS core facility (Ramakrishna Kurapati). Embryos were also genotyped using a gel based method designed around exon 21 (Table 2.1). The gel based assay consisted of 3 primers (Table 2.1), DreamTaq Green PCR Master Mix [ThermoFisher K1081], and water at a 0.75:5:4 ratio.

2.1.5 *Ncor2*^{del}

This floxed line was imported (Shimizu et al. 2015), males were culled and their sperm harvested for IVF. Fertilised eggs were treated with soluble Cre [Excellegen] in order to generate null animals. The colony was genotyped by the Harwell GEMS core facility (Ramakrishna Kurapati), with embryos genotyped using a gel based assay designed around exon 3 (Table 2.1). The gel based assay consisted of 3 primers (Table 2.1), DreamTaq Green PCR Master Mix [ThermoFisher K1081], and water at a 0.75:5:4 ratio.

Tle3	F- GGGAACTCTACTGCCCTTGG F2- TTTGGGACAGTCGCAGACC R- AGGACCAGAGTCCCAACTGA	wt-414bp	del-370bp	flox-500bp
Sex	F- TGGATGGTGTGGCCAATG R- TGGATGGTGTGGCCAATG	Y-253bp	X-335bp	
Znrf3	F- CACACCCTGACCCTACGAA R- TTACCACACCCATACCCAACT R2- GTGGGCCATACTTCAAGGGAT	wt-324bp	del-205bp	flox-405bp
***Sec31a* 1055**	F- GCTCTCGCTTCTTCCTCGTT R- CCTGGAGGTGGGGGATTTTC R2- AGTCTGCCTCTACCCACCAT	wt-582bp	del-377bp	
***Sec31a* 423**	F- TCCAGTCCCTACTCGGCATT R- CCACTCTCTGTGGGTGCTAGA R2- TCGTTGCTGCAAAGCATACA	wt-812bp	del-389bp	
Ncor2	F- GGTCTACAAGGACCGTCAGG F2- GGAGACACTTGGAAAGTCCGT R- ACCTCAACCTCAGCCTGTTC	wt-455bp	del-380bp	flox-800bp

Table 2.1 Genotyping Primers
Table showing the primers used for genotyping lines.

2.1.6 *Znrf3*$^{MYC/6xHis}$

This allele was generated by the Harwell CRISPR team (Lydia Teboul) and genotyped by the Harwell GEMS core facility (Ramakrishna Kurapati). A single guide RNA (sgRNA) was used and the donor oligo consisted of a *Myc* sequence followed by *6x His* sequences. The sgRNA and Cas9 were injected into the 1-cell embryo, by pronuclear injection, as purified mRNA. Simultaneously the donor oligo, synthesised and purified by Polyacrylamide gel electrophoresis (PAGE) by Integrated DNA technologies, was injected. Embryos were then implanted, after 30 minutes' recovery, into pseudo-pregnant recipient females. F1 analysed using ddPCR to confirm donor oligos were inserted on target in the genome. Pups possessing the tagged allele were bred onto a C57BL6/J background to produce a colony. Once established, the colony was genotyped by the Harwell GEMS core facility (Ramakrishna Kurapati, Deen Quwailid).

2.2 Tissue collection and processing

2.2.1 Embryo collection and staging

In order to generate embryos at specific time-stages, vaginal plugs were checked the following morning. 12 noon on the day a plug was identified was considered to be 0.5 dpc. Dams were culled by cervical dislocation (Schedule One) and the uterus removed. Embryos older than 14.0 dpc were immediately removed from the uterus and decapitated. All embryos were dissected under a Nikon

A

Stage	11.0 dpc						11.5 dpc					
Tail somite number	9	10	11	12	13	14	15	16	17	18	19	20

Stage	12.0 dpc						12.5 dpc					
Tail somite number	21	22	23	24	25	26	27	28	29	30	31	32

B

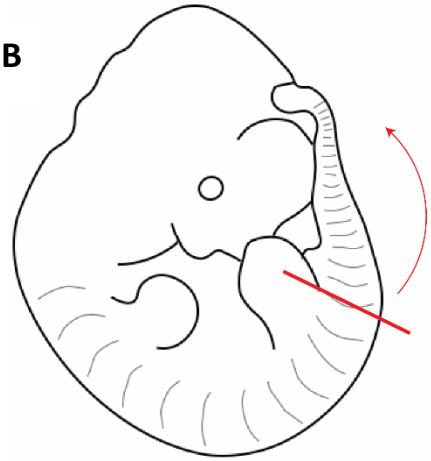

Figure 2.1 Tail somite staging of murine embryos
Table showing tail somite (ts) stage relative to dpc **(A)**. Diagram of embryo showing the section of the tail in which ts are counted, posterior to the hindlimb bud **(B)**.

MZ800 dissection microscope in ice cold PBS. Between 11.0 dpc and 12.5 dpc embryos were accurately staged by tail somite (ts) counting posterior to the hindlimb bud. A tail somite is formed approximately every two hours during murine development. Between 11.0 dpc and 12.5 dpc, somites are clearly visible and allow for more accurate staging of the embryo as shown in Fig. 2.1.

2.2.2 Wholemount *In Situ* Hybridisation (WMISH)

Dissected embryonic gonads were fixed overnight in a 4% PFA solution in PBS. The tissue was then washed in twice PBS and dehydrated using a series of ethanol (EtOH) washes: 1x 25% EtOH in PBS, 1x 50% EtOH in PBS, 1x 75% EtOH in PBS and 2x 100% EtOH. Gonads were then stored until use at -20°C in 100% EtOH.

2.2.3 qRT-PCR

Whole embryos were dissected from the uterus and snap frozen on dry ice. Tissue was then stored at -80°C until needed.

2.2.4 Immunohistochemistry

2.2.4.1 Wax sections

Embryonic gonads were fixed overnight at 4°C in 4% PFA solution in PBS. Gonads were processed into paraffin wax by the MRC Harwell histology Team (Adele Austin and Caroline Barker), cut in 8µm sections and placed on charged slides.

2.2.4.2 Wholemount gonadal tissue

See section 2.2.2

2.2.4.3 Wholemount blastocyst tissue

Uterine horns were harvested from dams and flushed with PBS to obtain blastocysts. Blastocysts were then fixed for 30mins at room temperature in 4% PFA in PBS, before being used immediately.

2.2.5 EdU (5-ethynyl-2´-deoxyuridine)

Dams had an intraperitoneal injection of 9mg/kg EdU 1hr before sacrifice. Embryonic gonads were dissected and fixed for 2 hours at room temperature in 4% PFA in PBS. Gonads were then dehydrated with an EtOH series (1x 25% EtOH in PBS, 1x 50% EtOH in PBS, 1x 75% EtOH in PBS and 2x 100% EtOH.) and stored at -20^{o}C in 100% EtOH for no longer than 1 week.

2.2.6 Protein extraction for Western Blot

2.2.6.1 Protein extraction from embryonic tissue

Tissues were homogenised in RIPA buffer supplemented with protease inhibitor, 1 tablet per 50ml (Complete EDTA-free protease inhibitor [Roche]). Samples were centrifuged for 15 minutes at 14000xg 4^{o}C, supernatant was transferred to a clean tube and placed on ice.A DC protein assay [BioRad] was carried out to determine the concentration of the samples. A standard set of concentrations was prepared using BSA [New England BioLabs] ranging from 0.15-10mg/ml. Samples were then plated out as per manufacturer's instructions and analysed using Epoch Biotek microplate spectrophotometer.

2.2.6.2 Protein extraction from cell lysates

Cells were washed in PBS and transferred to a pre-chilled Eppendorf. Cells were pelleted at 2000xg for 3 minutes at 4^{o}C. The pellet was suspended in RIPA buffer supplemented with protease inhibitor, 1 table per 50ml (Complete EDTA-free protease inhibitor [Roche]). Following a 30min incubation on ice the cell suspension was centrifuged at 14000xg for 15 minutes at 4^{o}C and the supernatant was transferred to a clean tube.

2.2.7 RNAseq

Embryonic UGRs were harvested, and sub-dissected to isolate the gonads. Gonads were then homogenised in RLT buffer by vortexing, as per the Qiagen RNeasy Plus Micro Kit [cat. no. 74034] instructions. RNA was extracted by following the kit instructions and was eluted in 14µl water. Once eluted RNA samples underwent quality control using the Agilent RNA 6000 Pico Kit [5067-1513], and

the Agilent bioanalyzer 2100. Only samples with a RNA integrity number (RIN) over 8 were shipped to the Oxford WTCHG facility for bulk RNA sequencing (RNAseq).

2.3 Expression analyses

2.3.1 Wholemount in-situ hybridisation (WMISH)

2.3.1.1 RNA probe synthesis

A 400-900 bp region of the gene of interest was amplified from cDNA via PCR (Table 2.2) and purified using a QIAquick PCR purification kit [Qiagen]. The product was then ligated into a pGEM-T vector [Promega] as per the manufacturer's instructions. This was then transformed into Subcloning Efficiency™ DH5α™ Competent E-coli cells [Life Technologies]. Cells were defrosted slowly on ice and 50µl of cells was added to 2µl ligation mixture. The tube was flicked gently to mix and incubated on ice for 20 minutes. Cells were then heat shocked for 20 seconds at 42°C before being incubated on ice for 2 minutes. 1ml of Lysogeny broth (LB) was then added to the cell mixture and incubated at 37°C with shaking for 1 hour. Varying amount of mixture were then spread on a LB/agar plate with 100µg/ml ampicillin and incubated overnight at 37°C. Colonies were then picked and cultured overnight in 3ml of LB at 37°C with shaking. This small culture was used to seed a larger 30ml culture which was grown overnight at 37°C with shaking. The plasmid was purified using the standard protocol with the QIAGEN Plasmid Midi Kit. Plasmid DNA was linearised using the appropriate restriction endonuclease and then transcribed with the appropriate RNA polymerase (T7 or SP6) to produce a digoxygenin (DIG)-labelled RNA probe complimentary to the endogenous mRNA of interest.

Tle3	F- AGTCTGAGAAGATGGGCGGG	R- TAGAAAAAGCCCAACAGCCCTTA	785bp
Ncor2	F- CTGCGCAGTGACCTTACACT	R- TAGAGACCAAAGCACAGCGG	577bp
Sec31a	F- AACAACAGGTACACCGCCTG	R- TGATGATGGTCGGGGAGAGT	626bp
Sox9	Wright et al 1995		
Stra8	Warr et al 2009		

Table 2.2 Primer sequences for generating WMISH probes
Table showing the primers used for creating WMISH probes. Final column shows product size in base pairs (bp).

2.3.1.2 WMISH protocol

Dissected gonads were transferred into Netwell inserts [Fisher] within a 12-well tissue culture plate, with no more than 5 pairs per well. Tissue was rehydrated with an Ethanol series and washed in PBT (PBS + 1% Tween). Tissue was then bleached in 6% H_2O_2 solution in PBT for 40min-1hr and washed again in PBT, before being digested with 10µg/ml proteinase K (Roche) in PBT for 15 minutes. This reaction was stopped with 2mg/ml glycine and followed with three more PBT washes. Tissue was then fixed in 2mg/ml glutaraldehyde in 4%PFA/PBT solution for 20 minutes. Following three more PBT washes the gonads were then placed in prehybridisation solution (50% formaldehyde, 5xSSC, 1% Tween 20, 50µl/ml Heparin) at 70°C for a minimum of 1 hour. The probes were denatured at 70°C for 10 minutes before being added (5µl/ml) to the hybridisation solution (prehybridisation solution + 5µl/ml salmon sperm DNA + 10µl/ml Yeast RNA). Tissue was then incubated at 70°C overnight in a hybridisation chamber.

After hybridisation gonads placed in wash solution (25% formamide, 2X SSC, 1% SDS) 2x 30 minutes at 70°C followed by 2x 30 minutes 65°C. Tissue was washed in 3x 5min TBST (25mM Tris pH 7.5, 0.1% Tween, 14mM NaCl, 0.02mM KCL) and pre-blocked in 10% Heat Inactivated Sheep Serum (HISS) in TBST for a minimum of 2.5 hours at room temperature. Embryo powder was added to 1ml TBST and heat inactivated for 30 minutes at 70°C, this was pulsed down and TBST was removed. Embryo powder was then resuspended in 1ml 1% HISS and 2.5µl/well anti-DIG-alkaline phosphatase conjugated fab fragments [Roche] and left on rotator at 4°C for a minimum of 1 hour. Embryo powder suspension was pulsed down and the supernatant was added to the remaining 1% HISS to make 1µl/ml antibody solution. Tissue was incubated in this overnight at 4°C.

Tissue then underwent at least 8 TBST washes over a 5 hour period before being washed in 3x 10min NTMT solution (100mM NaCl, 100mM Tris-HCL pH 9.5, 50mM $MgCl_2$, 0.1% Tween 20 in H_20). Gonads were then transferred to glass dishes treated with Repel-cote and incubated in alkaline phosphatase stain (20µl/ml NBT/BCIP [Roche] solution in NTMT) in the dark until the stain developed. Once stained, tissue was placed in PBT and left to whiten for a maximum of 3 days before being fixed in 4% PFA

solution in PBS for 1 hour at room temperature. Samples were then stored in PBT at 4°C before being imaged on 1% agarose in PBS with a dissection microscope with a digital camera attached [Leica MZ16].

2.4 qRT-PCR

2.4.1 RNA extraction for qRT-PCR

RNA was extracted from embryonic tissue using the RNeasy Midi kit [Qiagen] and following the manufacturer's instructions. RNA was eluted in 500µl RNase-free water, in 2X 250µl batches.

2.4.2 cDNA synthesis

cDNA was synthesised in a thermocycler at 37°C for 2 hours, using a High capacity Transcription kit [Applied biosystems] as per the manufacturer's instructions. The resulting solution was then diluted 1:6 RNase-free water.

2.4.2.1 qRT-PCR reaction

Mastermix solution (1x SYBR©Green Master Mix [ThermoFisher] , 0.2µM forward and reverse primer [Table 2.3]) was prepared and added to a Microamp fast optical reaction plate [Applied Biosystems] at 15µl/well. cDNA was then added to this plate at 5µl/well, with each sample plated in duplicate. The plate was loaded into the 7500 Fast real time PCR system [Applied biosystems] and ran according to machine's instructions.

Sec31a	F- CCTGTGTCGGGACAGGAATC	R- CCTGGAGGTGGGGGATTTTC	149bp

Table 2.3 Primers for qRT-PCR
Table showing the primers used for qRT-PCR.

2.5 2.3.3 Immunofluorescence

2.5.1 Wholemount embryonic gonads

Gonadal tissue was rehydrated in an Ethanol series, and washed in PBS. Tissue was then permeablised in 1% Triton-X-100 in PBS for 30 minutes on a shaker at 300rpm. Following a further PBS wash, tissue was then blocked for 1 hour in 4% Foetal Bovine Serum (FBS) in PBS at room temperature. Tissue was then incubated with primary antibody at the relevant dilution in 4% FBS/PBS either at room temperature for 1 hour or overnight at 4°C. Tissue was thoroughly washed again with PBS and incubated with the appropriate secondary antibody at a dilution of 1:200 for 1 hour at room temperature. Gonads were then washed for a final time in PBS before being mounted in Antifade Mounting Medium either with/without DAPI [Vectashield].

2.5.2 Wholemount blastocysts

Blastocysts were washed in PBT (0.1% Tween in PBS) before being permeablised in 0.5% Tween in PBS for 20min at room temperature. Blastocysts were then blocked in 10% donkey serum in PBS for 1 hour at room temperature before being incubated with primary antibody at the appropriate dilution overnight at 4°C. Blastocysts were then washed in PBT and incubated with the appropriate secondary antibody at a dilution of 1:200 for 1 hour at room temperature. Blastocysts were washed again with PBT before being incubated in a Vectashield DAPI solution (diluted 1:30 in PBS) overnight at 4°C prior to imaging.

2.5.3 Wax embedded sections

Slides were placed in Xylene for 20 minutes to remove the wax prior to a series of Ethanol washes. Slides were then steamed in Declere for 50 minutes for antigen retrival. Slides were washed in PBTriton (0.1% Triton-X-100 in PBS) and then blocked with 10% FBS in PBS. Primary antibody was then added to the slides at the appropriate dilution in blocking solution and incubated for either 1 hour at room temperature or overnight at 4°C. Slides were washed in PBS and incubated with secondary antibody at 1:200 in blocking solution for 1 hour at room temperature in the dark. Slides were washed

in PBS and incubated in 0.1% Sudan black in 70% EtOH for 10 minutes. Slides were washed with a mixture of PBtriton and PBS washes before being coverslipped with Antifade Mounting Medium with DAPI [Vectashield].

2.6 EdU protocol

Tissue was rehydrated in an EtOH series and washed with PBS followed by 3% BSA in PBS. Tissue was then permeablised with 1% Triton-X-100 in PBS for 30min at 300rpm and washed again in 3% BSA in PBS. Tissue was then incubated for 30 minutes at room temperature in reaction cocktail (made as per the manufacturer's instructions [ThermoFisher]) then washed again in 3% BSA in PBS. Tissue was then blocked for 1 hour in 3% BSA in PBtriton (0.1% Triton in PBS) and incubated at room temperature for 2 hours with conjugated GATA4 antibody [SantaCruz] at 1:50 in PBtriton at 300rpm. Tissue was mounted in Antifade Mounting Medium [Vecatshield] and imaged the next day.

2.7 Western Blot protocol

Samples were loaded onto a NuPage 4-12% gradient gel [ThermoFisher] and run for 50 minutes in MOPS buffer [Biorad]. Protein was transferred onto a nitrocellulose membrane using the iBlot dry electrotransfer system [ThermoFisher] as per the manufacturer's instructions. The membrane was then blocked (1xTBS [Biorad], 0.1% Tween, 5% Skimmed milk) for 1 hour at room temperature. Membrane was then incubated with primary antibodies at the appropriate dilution in block solution for either 1 hour at room temperature or overnight at 4^{o}C. The membrane was washed in TBST (1xTBS [Biorad], 0.1% Tween) and then incubated with secondary antibody at 1:10000 in block solution for 1 hour at room temperature in the dark. The membrane was the washed again in TBST and left to dry in the dark before being imaged on the Odyssey scanner.

3 Analysis of mouse lines lacking *Tle3* and *Sec31a*

3.1 INTRODUCTION

As previously discussed, potential candidate genes for DSDs are often discovered via exome sequencing of patients with a DSD of unknown cause. Clinicians then collaborate with other teams to study these candidate genes further. Both of the candidate genes discussed in this chapter were discovered this way, by a human geneticist collaborator; and both were studied using the mouse as a model organism with a view to supporting the claim that they play a role in human sex determination and identifying underlying mechanisms.

3.1.1 *TLE3*

Two cases of 46,XY gonadal dysgenesis of unknown cause were identified; the patients were related (sisters), and underwent exome sequencing to identify potential candidate genes. Both sisters were homozygous for a rare variant in *TLE3* (rs200508723) causing a T498M (threonine>498>methionine) substitution, which affects exon 15. SIFT analysis predicted damaging, and PolyPhen2 analysis predicted probably damaging. Both parents were heterozygous for the variant, and the case was located in Tunisia. The North African carrier frequency for this variant is 1:75, making the predicted homozygous frequency around 1:15,000, which is a reasonable rate for a DSD candidate gene considering the incidence of gonadal dysgenesis, the possibility of reduced penetrance and expressivity, and the possibility that 46,XX homozygotes do not present with a phenotype. This suggested that *TLE3* was a reasonable candidate gene in these individuals. No other similar candidates were identified.

The *TLE* genes encode a family of co-repressors, which cannot bind DNA directly but are recruited by transcription factors and other proteins to repress transcription; they are considered to mainly be involved with long-range repression (Agarwal, Kumar and Mathew 2015). In humans and mice, there are four full-length TLEs and two truncated forms. The truncated proteins are thought to repress *TLE1*-

4 function. TLE corepressors have known functions mediating NOTCH, EGF, TGFβ and WNT signalling, and have been shown to regulate many developmental and cell fate decision processes, both *in vitro* and *in vivo* (Gasperowicz et al. 2013).

More specifically, TLE3 is known to have many functions throughout development, including roles in osteogenesis, adipogenesis, pituitary development, pancreas development, kidney development and heart development. Many of these roles depend on TLE3's interaction with the WNT signalling pathway (Agarwal et al. 2015), suggesting that TLE3 is vital for regulating WNT signalling activity during development.

The known function of *TLE3* in regulating WNT signalling further highlighted it as a candidate gene for testis determination, as canonical WNT signals are known to be a major pro-ovarian factor. In addition, microarray data from mouse gonadal cells showed *Tle3* to be expressed in the supporting cell lineage at 11.5 dpc, around the time of sex determination, and sexually dimorphic by 12.5 dpc (Jameson et al. 2012b). Together with the patient data, these observations made *TLE3* a strong candidate gene and suitable for further investigation.

3.1.2 *SEC31A*

A familial case was identified with three affected children who had a combination of growth and endocrine abnormalities, DSD, mild cranio-facial abnormalities, and learning difficulties. Parents were unrelated and unaffected. More specifically, there was a 46,XY daughter with complete gonadal dysgenesis, a 46,XY son with partial gonadal dysgenesis and growth hormone deficiency, and a 46,XX daughter with growth hormone deficiency and pituitary deficiency. Exome sequencing of the children found a *de novo* nonsense mutation within *SEC31A* in the heterozygous state in all three children, Q929* (Glutamine>929>STOP), which affected exon 22. The corresponding region in the mouse was found to be located in exon 21.

SEC31A is a component of the outer layer of coat protein complex II (COPII), which is involved in anterograde transport from the endoplasmic reticulum (ER) to the Golgi apparatus (Jensen and

Schekman 2011). Further to the abnormalities listed above, the three affected children all presented with a marked dilation of the ER within the majority of their skin fibroblast cells. This observation supports the candidature of *SEC31A* as the gene responsible for their phenotypes; indeed, when other members of the COPII complex are mutated similar phenotypes can be seen. For example, Cranio-lenticulo-sutural dysplasia (CLSD) is caused by a mutation in *SEC23A* and results in craniofacial defects and learning difficulties similar to those seen in these three children. Further to this, CLSD patients also have gross dilation of the ER in their fibroblasts cells (Boyadjiev et al. 2006). SEC23 is a part of the inner layer of COPII along with SEC24, whilst SEC31 and SEC13 make up the outer layer. In addition to *SEC23*, *SEC24* mutants have also been associated with neural tube defects and craniofacial development abnormalities (Yang et al. 2013, Wansleeben et al. 2010). Depletion of *SEC13* by siRNA has been shown to cause craniofacial defects in zebrafish (Townley et al. 2008). In this latter study, Townley *et al.* suggested that it is not in fact the loss of *SEC13* or *SEC24* that is the cause of the craniofacial defects, but rather the loss of efficient coupling between SEC23-24 or SEC31-13, respectively. This hypothesis further corroborates the prediction that the phenotypes presented by all three patients are due to their nonsense mutation in *SEC31A*, since a truncated SEC31A protein would be predicted to lead to improper coupling between SEC31A-SEC13, which has already been shown to cause craniofacial defects in zebrafish.

SEC31 has two isoforms in humans, SEC31A and SEC31B, whilst SEC13 only has one. SEC31-SEC13 hetero-tetramers make up the outer layer of COPII and are thought to form a scaffold that enables curvature of vesicles. In yeast, mutation of *Sec31* results in lethality but loss of *Sec13* doesn't, as *Sec31p* is sufficient to generate COPII vesicles as long as the cargo is evenly distributed across the membrane (Copic et al. 2012). SEC31 is considered to drive assembly, whilst SEC13 helps maintain the structure of the budding vesicle, which is crucial for the transport of large molecules such as collagen (Townley et al. 2008).

Efficient transport from ER to Golgi involves many different components. Membrane-bound SEC12 catalyses SAR1-GDP to SAR1-GTP, which itself then becomes membrane bound. SAR1-GTP then recruits the heterodimer SEC23-SEC24, which enables the capture of cargo molecules; this then further recruits the hetero-tetramer SEC31-SEC13, which forms a structural cage around the vesicle, enabling budding and transport to the Golgi (Townley et al. 2008). Not only do some of the components have links to previously discussed phenotypes, but some components are also linked to known sex determining genes. *SEC12*, also known as PREB, is a membrane-localised guanine nucleotide-exchange (GEF) activator of SAR1-GTPase, which is recruited to ER exit sites by SEC1B and initiates COPII formation. Transient overexpression of *Sec12* has been shown to enhance WNT secretion by 40%, whereas knockdown of *Sec12* by 40% reduces WNT secretion by 24% (Sun et al. 2017). These data suggest that WNT is one of the many molecules transported by COPII from the ER to the Golgi, and as previously discussed, WNT is a known pro-ovarian factor and plays a key role in sex determination. Further to this, FGF signalling, a known pro-testis factor, has been shown to be necessary for proper COPII function by allowing for autophagy (Cinque et al. 2015). All of this further validates the selection of *SEC31A* as a candidate gene for the DSD observed in the patients and the decision to create a mouse model of this mutation for further study.

3.2 RESULTS

3.2.1 *Tle3* expression in the mouse embryonic gonad

Previous microarray analyses (Jameson et al. 2012b) show that *Tle3* is expressed in the developing gonad between 11.5 dpc-13.5 dpc, within the supporting, interstitial/stromal, germ and endothelial cell lineages. More specifically, within the supporting cell lineage, *Tle3* expression becomes sexually dimorphic between 11.5 dpc and 12.5 dpc, with higher levels of expression in XX cells (Fig 3.A)

To confirm this *Tle3* expression profile, wholemount in situ hybridisation (WMISH) studies were carried out on wildtype C57BL/6J (B6J) urogenital ridges (UGRs) at 11.5 dpc and 14.5 dpc. Signal in the gonad was found to be weak and the probe had to be left for two days for specific staining to be

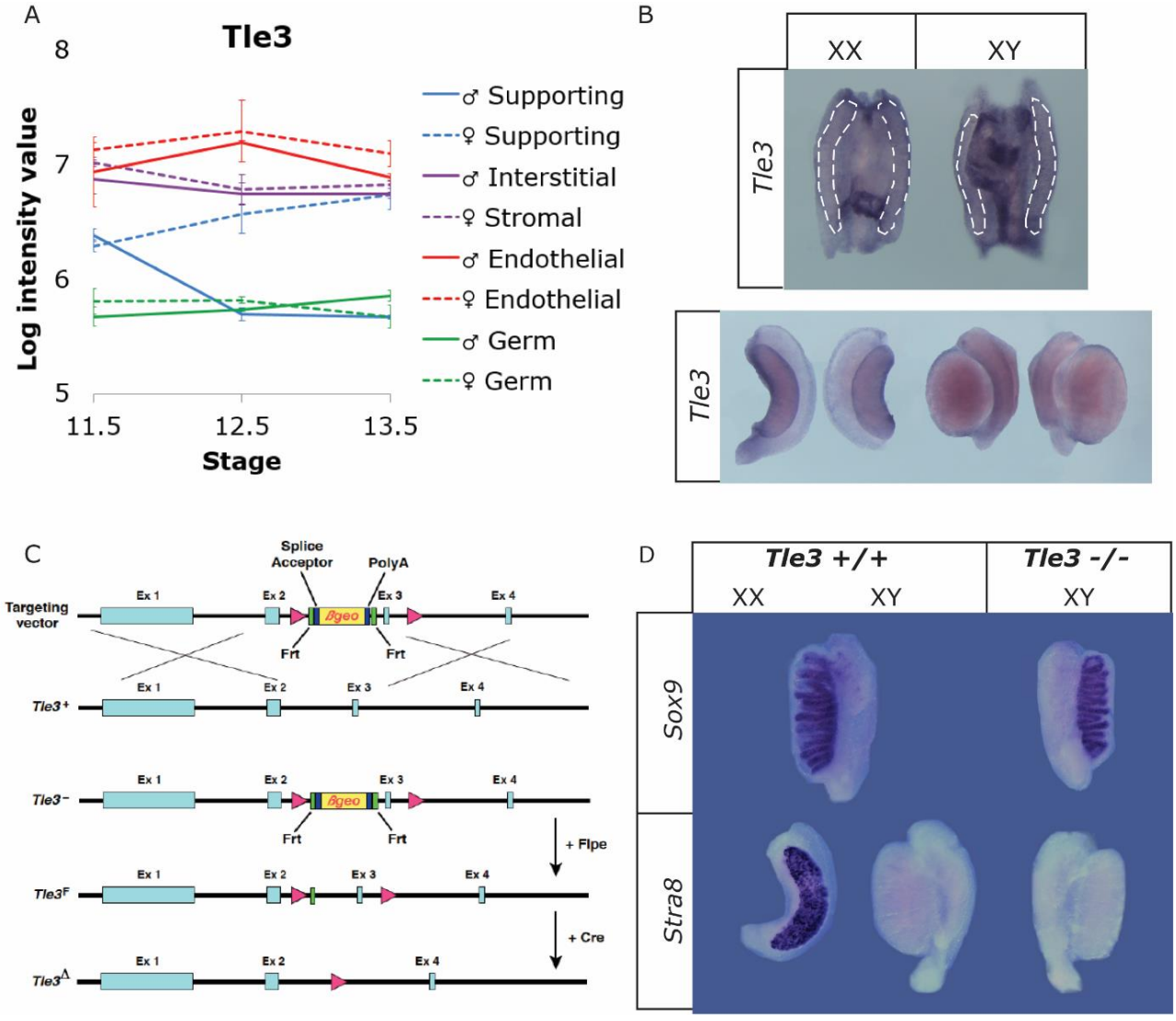

Figure 3.1 Study of *Tle3* as a potential sex-determining gene.
Microarray studies (Jameson et al. 2012b) show expression of *Tle3* in the supporting cell lineage (blue), interstitial/stromal cell lineage (purple), endothelial cell lineage (red) and germ cell lineage (green) between 11.5 dpc-13.5 dpc in XX and XY gonads **(A)**. WMISH study shows expression of *Tle3* in 11.5 dpc (top) and 14.5 dpc (bottom) XX (left) and XY (right) gonads **(B)**. Allele structure showing $Tle3^{Flox}$ ($Tle3^{F}$) has two loxP sites flanking exon 3; after exposure to soluble Cre these recombine to generate the *Tle3* null allele **(C)**. WMISH study shows the expression of *Sox9* (top) and *Stra8* (bottom) in 14.5 dpc *Tle3* wildtype (left) and *Tle3* homozygous null (right) gonads **(D)**.

observed. At 14.5 dpc staining was sexually dimorphic, with XX gonads staining more strongly; however, gonadal staining was not observed at 11.5 dpc (Fig. 3.1B). These data are consistent with reports in the literature on *Tle3* expression in the developing murine gonad.

3.2.2 Generation of *Tle3*-null embryos

The nature of the *TLE3* mutation found in the 46,XY individuals with complete gonadal dysgenesis is unclear. However, it was assumed in the first instance that it is likely to be disruptive, rather than a gain-of-function allele. The decision was made, therefore, to model the human mutation by analysing a knockout (null allele) of the mouse *Tle3* gene. Mice harbouring a floxed allele of *Tle3* were imported from Peter Tontonoz's lab (Fig 3.1C) (Villanueva et al. 2013). The male mice were sacrificed and sperm was collected for IVF using soluble Cre and oocytes from B6J wildtype females. Two founder males, heterozygous for the deletion allele, were then mated with B6J females to produce a colony of $Tle3^{-/+}$ mice. As figure 3.1C shows *Tle3* floxed mice possess one allele with a loxP site on either side of exon 3. So, when derived with soluble Cre, exon 3 is excised from this allele to produce the null allele in the heterozygous state. Removal of exon 3 results in a truncated form of the protein, 42 amino acids of protein followed by 7 amino acids of junk before a premature stop codon. As this protein is so highly truncated it is predicted non-functional and unstable. Genotyping was optimised and performed as described in Chapter 2. Inter-cross matings were then set up between $Tle3^{+/-}$ mice to produce embryos for WMISH. $Tle3^{-/-}$ embryos showed no gross morphological defects, and were present in the expected Mendelian ratios (data not shown).

3.2.3 Expression of sex determining genes in $Tle3^{-/-}$ embryonic gonads

WMISH studies were carried out on $Tle3^{+/+}$ and $Tle3^{-/-}$ gonads at 14.5 dpc using probes for sex-determining markers. As previously discussed, *Sox9* is routinely used as a marker for Sertoli cell specification, whereas *Stra8* is a marker of pre-meiotic germ cells and as such only marks ovarian germ cells in the embryonic gonad. In XY $Tle3^{+/+}$ gonads, *Sox9* expression is seen in the testis cords, but *Stra8* is not detected. However, in XX $Tle3^{+/+}$ gonads, *Stra8* is detected along the length of the gonad with

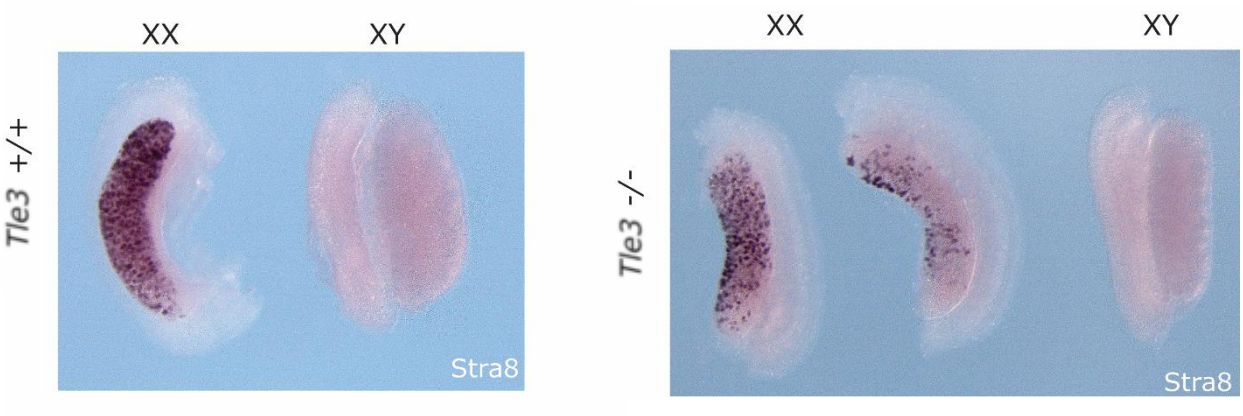

Figure 3.2 Study of *Tle3* as a potential ovarian factor.
WMISH study shows the expression of *Stra8* in 14.5 dpc *Tle3* wildtype (left) and *Tle3* homozygous null (right) XX and XY gonads.

no *Sox9* expression (Fig 3.1D). In XY *Tle3*$^{-/-}$ gonads, *Sox9* labels the testis cords as it does in wildtype gonads; furthermore, there is no ectopic expression of *Stra8* in these gonads (Fig 3.1D). From these data, it can be concluded that the loss of TLE3 does not disrupt testis determination in mice.

The known involvement of TLE3 in WNT signalling not only suggested a role in testicular development but also a role as an ovarian factor, as such *Tle3*$^{-/-}$ XX gonads were studied using *Stra8* (Fig 3.2). The data showed *Stra8* expression to be reduced in the homozygous mutant gonads, suggesting a lack of ovarian determination. However, the XY homozygous mutant gonads are noticeably smaller in size, something also seen in the XY WMISH study (Fig 3.1D). The small size of all the homozygous mutant testis suggests a developmental delay in the *Tle3*$^{-/-}$ gonads, this would affect *Stra8* expression. The literature had suggested that homozygosing this allele would result in lethality around 14.5 dpc, due to placental defects. Now the small testis size seen in the WMISH study was confirming this lethality, and confounding any associated results.

3.2.4 *Sec31a* expression in the embryonic gonad

Previous microarray studies (Jameson et al. 2012b) have shown *Sec31a* to be expressed in the developing gonad between 11.5 dpc-13.5 dpc within multiple lineages. Expression levels do not differ much between the supporting, interstitial/stromal, endothelial and germ cell lineages, and no sexually

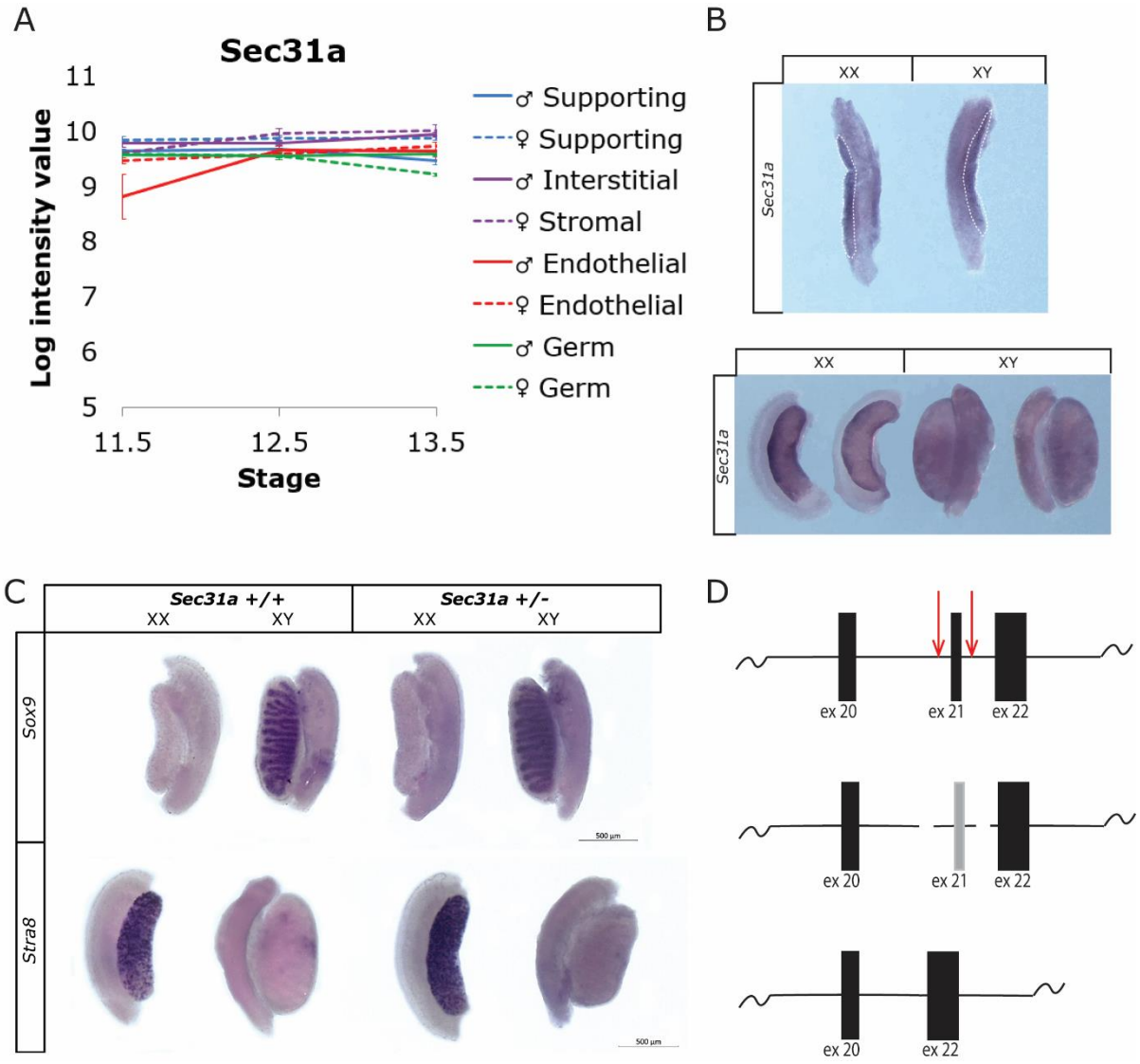

Figure 3.3 Study of *Sec31a* as a potential sex-determining gene.
Microarray studies (Jameson et al. 2012b) show expression of *Sec31a* in the supporting cell lineage (blue), interstitial/stromal cell lineage (purple), endothelial cell lineage (red) and germ cell lineage (green) between 11.5 dpc-13.5 dpc in XX and XY gonads **(A)**. WMISH study shows the expression of *Sec31a* in 11.5 dpc (top) and 14.5 dpc (bottom) XX (left) and XY (right) gonads **(B)**. WMISH study to examine expression of *Sox9* (top) and *Stra8* (bottom) in 14.5 dpc XX (left) and XY (right) *Sec31a* wildtype (left) and *Sec31a* heterozygous mutant (right) gonads **(C)**. Allele structure showing position of guide RNAs (red arrows) for excision of exon 21 of *Sec31a* via CRISPR/Cas9. Exon deletion is predicted to cause a frameshift followed by a premature termination codon **(D)**.

dimorphic expression is seen either (Fig 3.3A). It has, therefore, an expression profile reminiscent of a house-keeping gene. This, in itself, should not disqualify it as a candidate testis-determining gene: both *Map3k4* (Bogani et al. 2009) and *Dhx37* (McElreavey et al. 2020) are expressed in essentially a ubiquitous fashion, but loss of either results in gonadal sex reversal phenotypes in mice or humans, respectively.

WMISH studies were carried out on wildtype B6J UGRs at 11.5 dpc and 14.5 dpc to confirm the expression profile of *Sec31a* in the developing gonad. At 11.5 dpc, expression of *Sec31a* was clear in both XX and XY gonads; however, by 14.5 dpc, there is some evidence of sexually dimorphic expression, with XX gonads exhibiting higher levels of signal (Fig 3.3B). As WMISH is only semi-quantitative it cannot confirm higher levels of XX expression, but examination of the rotated gonad under the microscope from different angles and with varied lighting is indicative of this. Further, *Sec31a* expression in 14.5 dpc XX gonads appears to be more concentrated around the edge of the gonad whilst XY gonads show even levels of expression across the UGR.

3.2.5 Generation of *Sec31a*$^{-/-}$ embryos

A deletion allele of *Sec31a,* predicted to generate a similarly truncated form of the protein as predicted to exist in the patients, was generated using CRISPR/Cas9 genome editing technology, by the Molecular and Cellular Biology team at MRC Harwell using methodologies as previously described (Mianne et al. 2016, Mianne et al. 2017). Cas9 RNA and guide RNAs were injected into 1-cell B6J embryos, targeting exon 21 out of 28 (Fig 3.3D). Two founder males were identified; one contained a 423-nucleotide deletion with a 4-nucleotide insertion, and the other possessed a 1055-nucleotide deletion (Appendix 1). Both deletions removed the whole of exon 21. Both founders were mated with wildtype B6J females to produce colonies of *Sec31a*$^{+/1055del}$ and *Sec31a*$^{+/423del}$ mice. Heterozygotes were then inter-crossed to produce *Sec31a* 1055del and 423del homozygous embryos for further study. An initial study was performed to determine if the two colonies differed in phenotype, and they were

found to be the same (data not shown). All further work was performed on the colony with the 1055-nucleotide deletion, *Sec31a*^{1055del}, from here on this allele will be referred to as *Sec31a* $^{-}$.

3.2.6 Early lethality of *Sec31a*$^{-/-}$ embryos

Timed matings were set up between *Sec31a*$^{+/-}$ mice to produce *Sec31a*$^{-/-}$ embryos at 14.5 dpc for WMISH analyses. Litter sizes averaged seven embryos per litter and genotyping showed a complete absence of *Sec31a*$^{-/-}$ embryos. *Sec31a* wildtype and heterozygous embryos were present in the predicted Mendelian ration of 1:2, respectively, but there were no homozygous mutant embryos present, suggesting lethality (Fig 3.4A). To identify when lethality of homozygotes was occurring, further litters at various timepoints were harvested and genotyped. It was found that homozygous mutant embryos were dying between 3.5 dpc and 6.5 dpc, with no mutant homozygotes present at either 9.5 dpc or 6.5 dpc (Fig 3.4A), but some detectable at 3.5 dpc.

To determine if the early lethality was a strain-specific phenotype, *Sec31a*$^{+/-}$ B6J mice were outcrossed with wildtype 129X1/SvJ (129) to produce *Sec31a*$^{+/-}$ F1 B6J/129 mice. These were then intercrossed with *Sec31a*$^{+/-}$ B6J mice in the hope that a mixed background would at least partially rescue the early lethality and allow for an examination of sex determination. However, homozygous mutant mice on this mixed background were still absent at 14.5 dpc, 9.5 dpc and 6.5 dpc (data not shown), suggesting the early lethality phenotype is not strain-specific.

To identify a potential cause for the early lethality, 3.5 dpc (blastocyst) embryos derived from *Sec31a*$^{+/-}$ B6J intercross matings were studied using immunofluorescence. Blastocysts were labelled with antibodies against SEC31A and GATA3, a marker of the trophectoderm at this stage, as well as DAPI stained. Following immunostaining and imaging, blastocysts were then genotyped as normal.

The *Sec31a* homozygous mutant blastocysts showed a clear developmental delay, with one not progressing past the 4-cell state. Furthermore, several null blastocysts failed to develop the blastocoelic cavity seen in wildtype blastocysts at this stage. One blastocyst also exhibited aberrant GATA3 expression, suggesting a potential failure of trophectoderm specification (Fig 3.4C). These

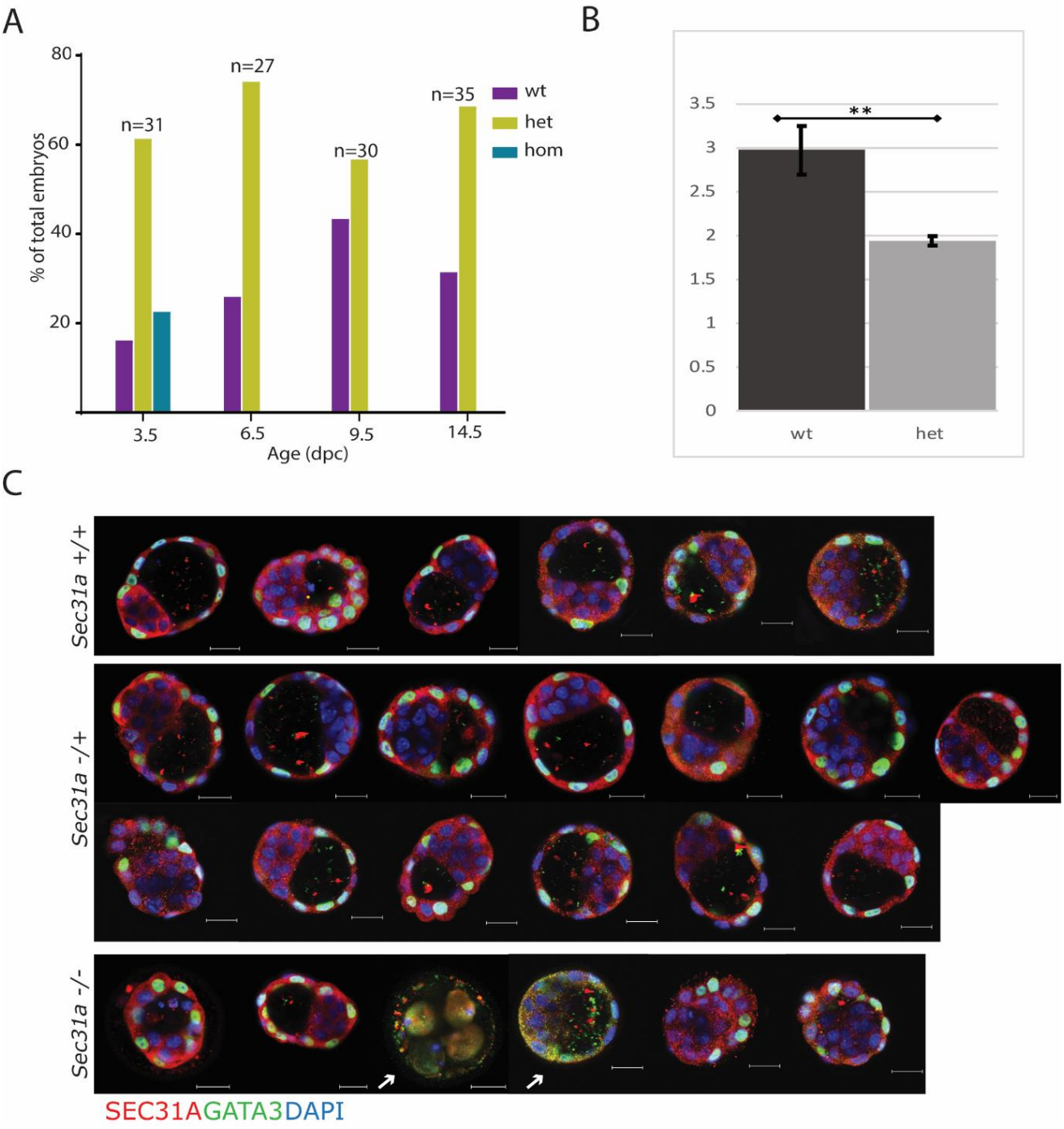

Figure 3.4 Studying the early lethality phenotype of *Sec31a*$^{-/-}$ embryos.
Graph depicting the ratio of *Sec31a*$^{+/+}$ (purple), *Sec31a*$^{+/-}$ (green), and *Sec31a*$^{-/-}$ (blue) embryos between 3.5 dpc and 14.5 dpc **(A)**; qPCR to determine the levels of nonsense-mediated decay (NMD) in *Sec31a*$^{+/+}$ (left) and *Sec31a*$^{+/-}$ (right) embryos at 11.5 dpc **(B)**; Wholemount immunofluorescence images to study the localisation of SEC31A (red), GATA3 (green) and DAPI (blue) in *Sec31a*$^{+/+}$ (top), *Sec31a*$^{+/-}$ (middle), and *Sec31a*$^{-/-}$ (bottom) embryos at 3.5 dpc **(C)**.

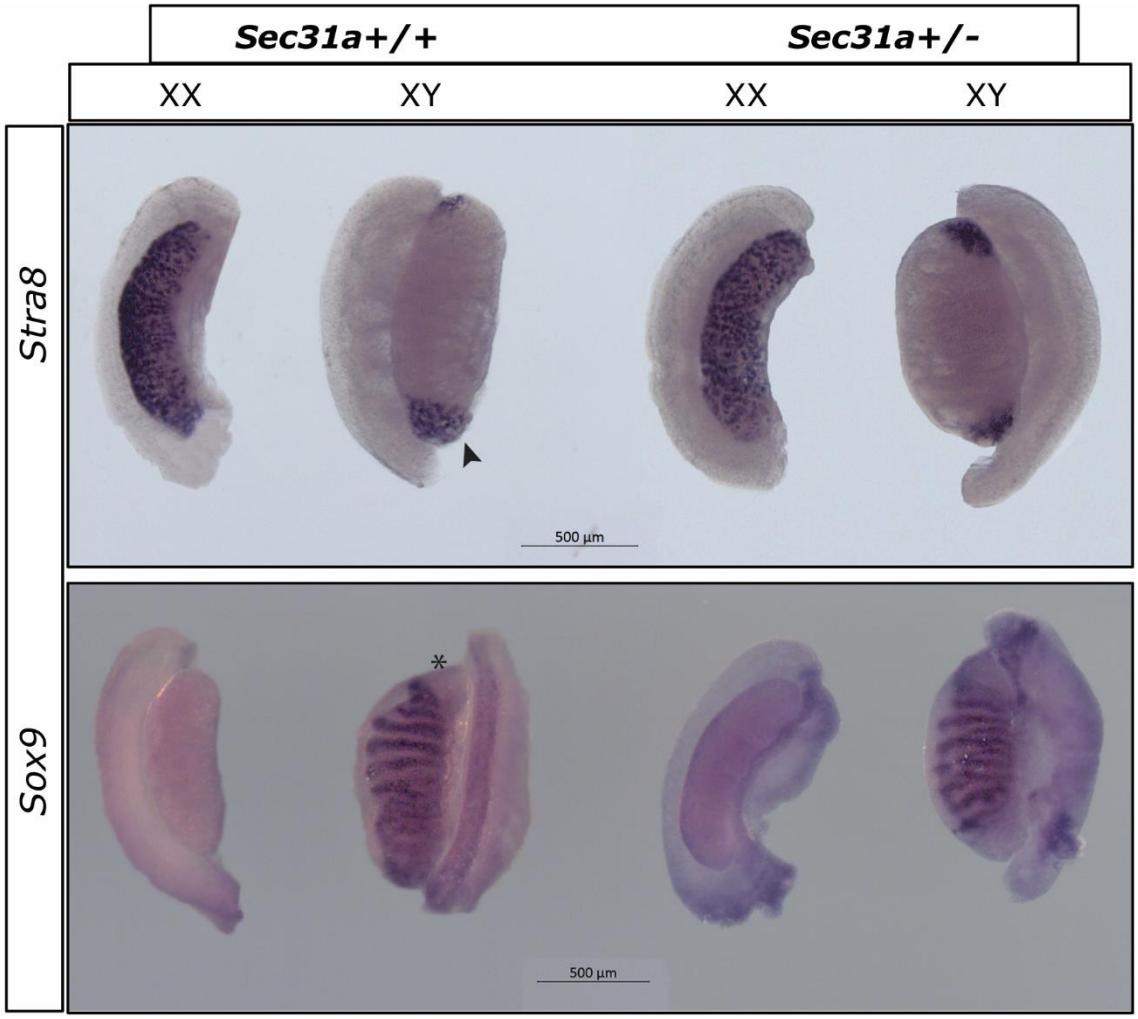

Figure 3.5 WMISH of sex-determining genes in B6J.Y^{AKR} *Sec31a*$^{+/-}$ gonads at 14.5 dpc.
WMISH study shows the expression of *Stra8* (top) and *Sox9* (bottom) in *Sec31a* wildtype (left) and *Sec31a* heterozygous (right) XX (left) and XY (right) gonads. The arrowhead shows the presence of *Stra8* and the star shows the lack of *Sox9* at the poles of a wildtype XY gonad.

immunolabelling data reveal clear differences between *Sec31a*$^{-/-}$ and *Sec31a*$^{+/+}$ blastocysts, suggesting that even at this early stage of development the homozygous mutant embryos are already dying.

The *Sec31a* mutant allele has a deletion of exon 21, causing a predicted frameshift and a premature stop codon (Fig 3.4D). To determine if this allele was targeted for nonsense mediated decay (NMD) (Hug, Longman and Caceres 2016, Lejeune 2017), qPCR was performed on 11.5 dpc *Sec31a*$^{+/+}$ and

Sec31a$^{+/-}$ whole embryos, using primers that could detect the truncated protein. The results show a significant decrease in *Sec31a* expression, suggesting that NMD of the truncated allele is occurring. However, expression is decreased by less than 50%, suggesting that NMD of the truncated protein is not complete.

3.2.7 Expression of sex-determining genes in *Sec31a*$^{+/-}$ embryonic gonads

Due to the inability to harvest *Sec31a* $^{-/-}$ gonads at 14.5 dpc for WMISH, these studies were instead carried out on heterozygous *Sec31a*$^{+/-}$ embryonic gonads. As previously discussed, *Sox9* and *Stra8* probes were used to mark testicular and ovarian fate, respectively. In wildtype XY gonads at 14.5 dpc, *Sox9* clearly labels the testis cords, whilst *Stra8* is absent. Conversely, in XX gonads at the same stage, *Stra8* marks cells along the length of the gonad, whilst *Sox9* is absent. In *Sec31a*$^{+/-}$ XY gonads at 14.5 dpc, *Sox9* is detected in the testis cords, as seen in the wildtype samples, and there is no ectopic expression of *Stra8*. Furthermore, in heterozygous XX gonads at the same stage, *Stra8* is expressed in cells along the length of the gonad with no *Sox9* present (Fig 3.3C). These results show that the *Sec31a*$^{+/-}$ embryos do not differ phenotypically from wildtype embryos.

Because only heterozygous embryos could be used for this WMISH study, the decision was made to study this line on a sub-strain of mouse that is highly sensitised to disruptions in testis determination. The B6J.Y^{AKR} mouse possesses the B6J genome (autosomes and X chromosome), but carries a Y chromosome derived from the *Mus domesticus* mouse strain. The B6J.Y^{AKR} background is so sensitised to disruptions to testis determination that sex reversal can occur when animals lack just one copy of a testis-determining gene (Bouma et al. 2007), (Bogani et al. 2009, Harris et al. 2018). At 14.5 dpc, even wildtype B6J.Y^{AKR} XY gonads exhibit transient ovotestis formation, due to this sensitisation. *Sox9* is present in the testis cords at the centre of the gonad, but absent at the poles. Moreover, *Stra8*, a known ovarian germ cell marker, is expressed at the poles of this XY gonad.

In B6J.Y^{AKR} *Sec31a*$^{+/-}$ XY gonads, *Sox9* labels the centre of the gonad but is absent from the poles, with *Stra8* marking these instead, making expression the same as seen in the wildtype (Fig. 3.5). The XX heterozygous gonads also do not differ from wildtype, with no *Sox9* expression, but rather *Stra8* expressed along the length (Fig 3.5). These results show that even on a highly sensitised genetic background, *Sec31a* heterozygous gonads do not exhibit any abnormalities of testis determination.

3.3 DISCUSSION

3.3.1 *Tle3* expression in the developing gonad

This chapter has described the study of two candidate testis-determining genes, *Tle3* and *Sec31a*. Both were identified in exome sequencing screens of patients with gonadal dysgenesis of unknown cause, and both had been shown to be present in the developing mouse gonad in previous microarray studies (Jameson et al. 2012b).

My own work using WMISH to examine *Tle3* expression in the developing gonad found expression levels to be very low, with the probe having to be hybridised for two days rather than a few hours. Although the WMISH process is not a quantitative one, and signal strength can depend on other factors such as probe design and synthesis, this long staining period is indicative of weak expression levels within the developing gonad. Early microarray data (Jameson et al. 2012b) suggested expression levels would be the same in XX and XY gonads at 11.5 dpc, and more recent RNA sequencing data has confirmed this (Stevant et al. 2019, Zhao et al. 2018). WMISH study found a lack of expression in both XX and XY gonads, indicative of equal expression levels. The lack of gonadal staining in either sex does not necessarily indicate that *Tle3* is not expressed; more likely, expression levels are too low to be detected.

At the later stages of 12.5 dpc and 13.5 dpc, the microarray data showed sexually dimorphic expression, with XX gonadal expression increasing from 11.5 dpc and XY expression decreasing. My WMISH study found the same sexual dimorphism present at 14.5 dpc, suggesting this expression

pattern is maintained from 12.5 dpc to at least 14.5 dpc, if not longer. The microarray study suggests that the sexually dimorphic pattern is only present in the supporting cells of the gonad and the WMISH expression reported here in the XX gonad supports this observation. The supporting cell lineage differentiates by 12.5 dpc, after sex determination occurs at 11.5 dpc. The expression of *Tle3* reported here suggests that it may function beyond the period of sex determination, particularly in the XX gonad where expression is most prominent. This raises the possibility that the *TLE3* mutations identified in the two 46,XY sisters might be gain-of-function (GOF), disrupting testis determination by the activation of an ovary-determining gene. However, the expression profile in the human embryonic gonad at this stage is not known, so this is mere speculation. Moreover, whatever the role of *Tle3* in the developing XX gonad, there appears to be no obvious loss-of-function phenotype in XY gonads.

Modelling the appropriate allele, loss-of-function (LOF) or GOF, is critical in assessing the candidature of a gene for a given phenotype. For example, GOF in the *FGFR1* gene causes craniosynostosis, whereas LOF causes Kallmann syndrome (Jung et al. 2015). All the candidate genes discussed in this thesis were discovered using forward genetic screens, when a specific candidate gene is identified due to association with a phenotype before being functionally studied. The most common approach for a functional study in the mouse is to use the null allele, because this is the simplest way to assess a gene's function. However, this focus on the null allele, or knockout, is not a true reflection of the potential complexity of many human mutations, and will result in any GOF phenotypes that might be in play being missed. It is possible to model GOF mutations, for example by over-expression of a gene, but this may not reflect the phenotypic consequences of an altered protein sequence. Perhaps the ultimate test of the consequence of an amino acid substitution in a human protein is to introduce the equivalent mutation into the mouse gene using CRISPR/Cas9 genome editing. However, whether such an approach phenocopies a human condition will depend on the biology of that protein: whether the amino acid substitution disrupts the mouse protein and whether the mouse protein's interactions are disrupted. It was not felt that such an approach was warranted for the study of *Tle3* due to these inherent risks and the absence of an overt LOF phenotype.

Instead it was decided to study any potential *TLE3* GOF in the 46,XY sisters using the KO model. By studying XX gonadal development using the KO model it is possible to determine if TLE3 may play a role as an ovarian factor. If this was indeed the case this could in turn suggest a GOF mutation in the sisters. WMISH study was performed on 14.5 dpc gonads using a *Stra8* riboprobe; unfortunately, the results were found to be inconclusive. *Stra8* has a specific spatiotemporal expression pattern, as previously discussed. Expression starts in the anterior pole around 12.5 dpc and moves towards the posterior pole, with peak expression at 14.5 dpc. At 13.5 dpc expression is just over 1/3 of that at 14.5 dpc (Soh et al. 2015); highlighting just how variable *Stra8* expression can be over a period of a few hours.

WMISH study showed a reduction of *Stra8* expression in *Tle3* KO XX gonads. However, this was deemed inconclusive due to confounding factors seen alongside this phenotype. All XY KO gonads collected for this study appeared smaller than their wildtype counterparts (data not shown), which can be seen in the XY control for the XX WMISH study (Fig 3.2). The images collected from the WMISH clearly show that the XY KO gonad is significantly underdeveloped compared to the wildtype XY gonad, and looks more on par with a 13.5 dpc testis. This suggests that the KO gonads are either developing at a slower rate than the wildtype gonads or aren't progressing past the 13.5-14.0 dpc timepoint; the latter option had been suggested prior (Villanueva et al. 2013). As *Stra8* expression is so varied between 13.5-14.5 dpc any delay in development greatly impacts the amount of expression visualised; both wildtype and KO gonads must be developmentally matched to be compared. This is the confounding factor mentioned as developmental timepoint cannot be ruled out as the cause for the reduction in *Stra8* expression. To study this further would require the KO model to be aged further, something that is not possible due to embryonic lethality; or to use younger wildtype controls and assume they are the right age, but these couldn't be littermates and thus are less comparable. Unfortunately using the KO model was unsuccessful due to embryonic lethality and a developmental delay, something that will be discussed further in this chapter; as mentioned earlier it was felt further

genetic manipulations were not warranted for the study of *Tle3*, and so I moved on to the study of my next candidate gene.

3.3.2 *Sec31a* expression in the developing gonad

Microarray studies had previously shown *Sec31a* to be expressed in the developing gonad between 11.5 dpc and 13.5 dpc (Jameson et al. 2012b). My WMISH study confirmed the expression at 11.5 dpc, with gonadal expression clearly visible in both XX and XY gonads at this stage. The signal is visible along the length of the gonad and appears weaker in the mesonephros. By 14.5 dpc, expression appears to be sexually dimorphic, with XX gonads showing higher expression levels than XY gonads. Although the microarray data did not show distinct sexual dimorphism by 13.5 dpc, there was a slight reduction in *Sec31a* expression in XY gonads, whilst XX gonads maintained the same expression levels seen at 12.5 dpc. This is indicative of the start of a change in expression levels between the sexes, and could support the sexual dimorphism seen in the WMISH study. In conclusion, the WMISH study is consistent the microarray data and confirms *Sec31a* expression in the developing gonad.

3.3.3 Embryos homozygous for the *Sec31a* 1055 deletion die early in development

As the human mutation discovered was predicted to be deleterious, the study discussed here was designed around a LOF allele that aimed to mimic the human mutation by truncating the protein relatively close to the C-terminus. The *Sec31a* 1055 allele has a deletion of exon 21, which results in a predicted frameshift, following splicing of exon 20 to 22, and a premature stop codon. The mRNA containing this premature stop codon was predicted to undergo nonsense mediated decay (NMD), which I confirmed using qPCR. The qPCR study suggested that NMD was not 100% efficient, and some of the truncated transcript remained. This contrasts to another study published whilst I was investigating this gene, which showed NMD of a mutated version of *SEC31A* to be 100% efficient in their human patients (Halperin et al. 2018).

The 2018 study by Halperin et al. reported two patients who were homozygous for *SEC31A* LOF mutations (p.A927fs*61), and two relatives who were heterozygous carriers. They did not discuss any

potential phenotypes in the carriers, but the homozygous siblings had cranial abnormalities that were similar but more extreme than our heterozygous patients. The 2018 study used *Drosophila* as a model organism, and found homozygotes for a *Sec31a* null allele to be lethal even at the larval/pupal stage, suggesting an early lethality phenotype (Halperin et al. 2018). This corroborates my work in the mouse model, which also showed loss of *Sec31a* to cause early embryonic lethal. Specifically, I found the homozygous mutant embryos to be lethal between 3.5 dpc and 6.5 dpc, which is around the time of implantation, suggesting a failure of to implant.

To investigate this lethality further, I used immunofluorescence to study the homozygous mutant embryos at 3.5 dpc, and found that whilst mutant embryos are still present at 3.5 dpc they show a clear developmental delay. Furthermore, some of the null embryos present with abnormal expression of trophectoderm (TE) marker, suggesting that the first lineage segregation expected around 3 dpc has failed in these (Jedrusik et al. 2015). Lethality around this time point is indicative of a failure in the pre-implantation stage, rather than the implantation stage as previously suggested. In the pre-implantation phase the vital process of zygotic genome activation (ZGA) occurs, allowing the developing embryo to produce gene products using its own genome. Prior to ZGA, development is dependent on maternal RNA and proteins (Jedrusik et al. 2015). Previous studies have shown that maternal factors can sustain the development of an embryo until the late morula stage, allowing for a delay in the expression of mutant phenotypes (Riethmacher, Brinkmann and Birchmeier 1995). This 1995 study presented many similarities to my own study in regards to lethality. The embryos they examined also failed to produce the cavitation expected in blastocysts, and failed to specify the TE, and as such were lethal at the morula stage of development. Due to the similarities in phenotype the same conclusion can be drawn, which is that maternal factors can delay the expression of a lethal phenotype, but by the time ZGA occurs at the morula stage maternal products are no longer a factor and the lack of functional protein results in immediate lethality.

This model of the early lethality phenotype associated with loss of *Sec31a* also explains why Halperin *et al.* observed lethality in their *Drosophila* model; however, they also reported two homozygous null allele patients, who survived until the age of four. So, whilst loss of *SEC31A* causes lethality in humans, it is not pre-natal lethality, as it was in our model systems. This disparity is most likely caused by differences between the human genome, including transcript complexity at a locus, and those of model organisms such as the mouse or *Drosophila*. Specifically, in regards to *SEC31A,* the human locus encodes 41 various transcripts for this gene, whereas the mouse only has 12.

From this study it is concluded that the *Sec31a* mutant phenotype reported here is early embryonic lethal due to the inability of the embryo to survive without maternal RNA. I hypothesise that *Sec31a* is vital for murine cell survival, and that human survival until 4 years of age (Halperin et al. 2018) was only possible due to the complexity of *SEC31A* when compared to the mouse orthologue. The lethality phenotype necessitated that for the rest of this study I used heterozygous embryos.

3.3.4 Studying sex determination in *Sec31a*$^{+/-}$ embryos

As previously discussed, the *Sec31a* homozygous mutant embryos were found to be early embryonic lethal, thus preventing the study of sex determination in them. Instead, I used gonads from *Sec31a* heterozygous mutant embryos for WMISH study with *Sox9* and *Stra8* probes. Both XX and XY heterozygous gonads expressed these probes as expected and in line with wildtype gonadal expression, suggesting that loss of one *Sec31a* allele does not affect murine sex determination.

To further test for the possibility of a heterozygous sex determination phenotype, I crossed the null allele onto the B6J.Y^{AKR} strain, which is highly sensitised to disruptions to testis determination. When outcrossed onto this sensitised background both XX and XY heterozygous gonads had the same *Sox9* and *Stra8* expression pattern as wildtype gonads, indicating the absence of gonadal XY sex reversal in *Sec31a*$^{+/-}$ embryos. However, this does not confirm that the gonadal dysgenesis observed in patients was not caused by their mutation in *SEC31A*; it may highlight a limitation of the mouse as a model.

Often phenotypes seen in the heterozygous state in humans are only seen when the equivalent mutation is homozygosed in the mouse. Heterozygous mutant phenotypes can be caused by haploinsufficiency of some human gene mutations, or possibly the presence of a different allele type to the null, such as a dominant negative mutation. However, just because a mutation is haploinsufficient in humans, this does not mean the same is true in the mouse. The absence of a heterozygous phenotype in the murine model, including in the B6J.Y^{AKR} background, is not enough to rule out a role for *SEC31A* in human sex determination. Previous studies of phenotypes associated with the heterozygous mutant state in humans have also found no phenotype in mice until the mutant allele was homozygosed (Harris et al. 2018), highlighting the inconclusiveness of studying heterozygotes in a murine model. However, some studies have revealed heterozygous sex determination phenotypes in the mouse when the B6J.Y^{AKR} background is used (Bouma et al. 2007, Bogani et al. 2009, Harris et al. 2018). This suggests that haploinsufficiency phenotypes, explained by genetic background effects (modifier genes) in humans, can be modelled in the mouse.

Due to the other phenotypes present in the three patients, and their similarities to phenotypes seen when other COPII components are mutated, I would argue that the DSD reported is most likely caused by their mutation in *SEC31A*. The clear expression of *Sec31a* in the developing gonad at 11.5 dpc, when sex determination occurs, suggests that it may play an important role which is further implied by the sexually dimorphic expression that is seen later in development. The heterozygous human phenotype is most likely due to the haploinsufficiency of *SEC31A*. This model is supported by Halperin et al. who showed nonsense mediated decay (NMD) of truncated SEC31A to be 100% efficient in humans highlighting that the allele is truly in the heterozygous state and that the truncated allele has no function. In contrast, I have shown that NMD of the mutant allele in the mouse reported here is not 100% efficient and that there is still some truncated protein present. This could provide some explanation as to why there is a heterozygous phenotype in humans but not in the mouse.

3.3.5 Limitations of the mouse as a model for human disease

In both the studies discussed in this chapter, the mouse model was unable to confirm if the candidate gene mutation was responsible for the DSD observed in the patients. However, this lack of confirmation does not amount to proof that they are not causative. For example, in the *Sec31a* study there was a clear expression of the gene in the developing gonad, and the patients' other phenotypes had strong links to COPII defects. This suggests that *SEC31A* is a strong candidate; the inability to establish a causal relationship between the gene and sex determination in the mouse does not weaken the human gene's candidature. In this case it merely highlights the difference in biology, if the homozygous mutants had been viable then the association could've been tested further to establish a causal relationship. However even if homozygous mutant gonads lacked dysgenesis it would not rule out the human gene's candidature due to the limitations of using the mouse to model human diseases.

About 25% of mouse knock-out (KO) models produced are embryonic lethal (Wu et al. 2019), showing the limitations of using a KO model system. The complete loss of an allele often has a much more drastic effect than many of the human mutations being modelled, but attempting to specifically recreate these mutations can be complicated and not guaranteed to cause a phenotype. For example, the recent study showing the involvement of *Znrf3* in murine testis development was modelled using a *Znrf3* null allele (Harris et al. 2018), but when an attempt was made to model one of the specific *ZNRF3* amino acid substitutions found in two human DSD patients, no phenotype was observed in heterozygous or homozygous mice (Harris & Greenfield, unpublished data). This is most likely because the amino acid substitution in question can be tolerated in the context of the mouse protein, although other explanations are possible. Nevertheless, this highlights one of the limitations of using mice to model human diseases: one cannot be certain if the lack of causal evidence is due to organism differences or a non-causal relationship in humans. For this reason, KO models are often used to model human disease in mice. By utilising null alleles, it is much easier to get an accurate representation of

a gene's specific role; however, there are downsides to this approach, one of which being the high levels of embryonic lethality previously mentioned.

There are other examples of limitations in using the mouse. For example, although 99% of mouse genes have an equivalent in the human, some of these genes will have undergone divergence in function. For example, *MAP3K1* mutations have been shown to be involved in human 46,XY gonadal dysgenesis (Pearlman et al. 2010), but *Map3k1* KO mice did not show a sex determination phenotype (Warr et al. 2011). However, *Map3k4* KO mice do exhibit XY gonadal sex reversal, suggesting that maybe this MAPK gene has taken over the role that *MAP3K1* plays in human sex determination. Alternatively, the human *MAP3K1* mutations associated with 46,XY GD may be gain-of-function (Pearlman et al. 2010, Chamberlin et al. 2019).

Furthermore, the expression of *SRY* has been shown to be different in humans and mice, with the latter showing transient expression, as previously discussed. Also, an additional *Sry* C-terminal CAG repeat domain, not present in humans, has been shown to be vital for testis determination in mice (Eggers and Sinclair 2012, Bowles et al. 1999, Zhao et al. 2014). These examples all highlight differences between humans and mice in regards to sex determination and its molecular underpinnings, and suggest that, whilst the mouse is an excellent mammalian model organism, it does have its limitations when modelling human disease.

4 Analysis of the role of ZNRF3 in testis determination

4.1 Introduction

I have previously discussed the importance of canonical (β-catenin) WNT signalling in sex determination, and how its activity can initiate ovarian development, even in XY gonads. *Znrf3* is a novel regulator of testis determination via its antagonism of WNT signalling. Zinc and ringer finger 3 (ZNRF3) is a membrane bound E3 ubiquitin ligase. Its extracellular domain acts as a receptor allowing for ZNRF3 degradation in the presence of certain proteins. This domain is more widely understood than other parts of the protein, with a crystal structure available. The intracellular domain is less characterised, but what is known is that it contains the RING-domain which allows ZNRF3 to function as a ubiquitin ligase (Zebisch and Jones 2015).

A 2012 study found that deletion of *Znrf3* and its homologue *Rnf43* in the intestinal epithelium of mice resulted in rapidly growing adenomas. Further, they found that growth of organoids derived from these adenomas was stopped when a WNT inhibitor was present, suggesting that *Znrf3/Rnf43* are required for correct control of WNT signalling (Koo et al. 2012). A model was then proposed for ZNRF3 function in which it ubiquitylates FRIZZLED to promote its clearance from the membrane, alongside LRP6, thereby inhibiting WNT signalling through increased turnover of its FRIZZLED receptor. The model further proposed that ZNRF3, in the presence of LGR4, can act as a receptor for R-SPONDIN, a key ovarian factor, to promote ZNRF3's clearance from the membrane and prevent its antagonistic action against WNT (Hao et al. 2012).

This model (Fig. 4.1) was further confirmed the following year in a study investigating R-SPONDIN signalling activity. They found that R-SPONDIN promotes WNT signalling by increasing membrane clearance of its antagonist, and that it does this by binding both LGR4 and ZNRF3 through distinct motifs. Their results supported a 'dual-receptor' model where LGR4 acted as the 'engagement receptor' and ZNRF3 the 'effector receptor' (Xie et al. 2013). However, since then, studies have found

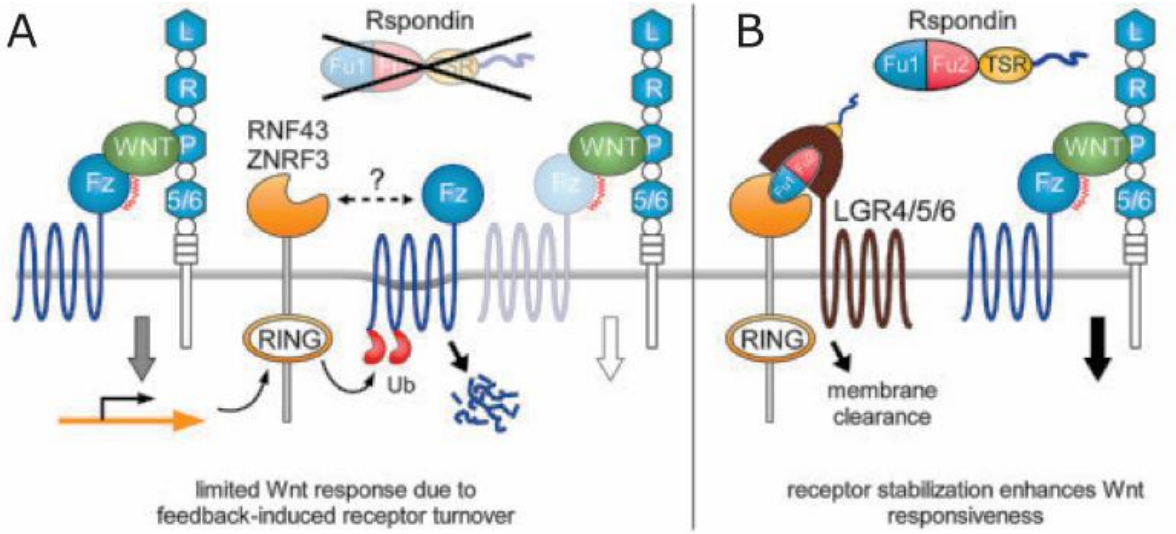

Figure 4.1 ZNRF3 regulates WNT signalling.
ZNRF3 works to clear FRIZZLED from the membrane, thus inhibiting WNT signalling **(A).** If R-SPONDIN is present this binds to ZNRF3 preventing FRIZZLED clearance **(B)** (Zebisch and Jones 2015).

that R-SPONDIN can act independently of LGR4 to antagonise ZNRF3 (Szenker-Ravi et al. 2018). Whilst the specific mechanism of R-SPONDIN's interaction is still unclear, it is clear that it does influence ZNRF3's antagonistic function against WNT signalling.

Studies by the McElreavey laboratory identified potentially disruptive variants in human *ZNRF3* through exome sequencing of patients with 46,XY DSD. Two mutations were identified, the first (S554N) was predicted deleterious by *Sift*. The second (R768G), was predicted deleterious by *Condel*. The known role for ZNRF3 in antagonising WNT signalling, and its interaction with R-SPONDIN, both key ovarian factors, certainly added support to its candidature as a human testis determining gene. At the beginning of my research, our studies in mice revealed that deletion of *Znrf3* caused XY gonadal sex reversal, with variable degrees of severity (Harris et al. 2018). These data indicated a novel testis-determining role for *Znrf3* in mice and suggested that RSPO1 potentiates WNT signalling in ovarian development via interactions with ZNRF3 (Harris et al. 2018). Further study showed that *Znrf3*-null XY embryonic gonads showed up-regulation of canonical WNT signalling components. *Znrf3* is not

sexually dimorphic in expression within the somatic cells of the gonad, making it an unlikely target of transcriptional upregulation by known testis factors such as SRY or SOX9.

The purpose of the research described in this chapter was to contribute further to our understanding of the role of ZNRF3 in mouse testis determination. My initial research, on cell proliferation in the *Znfr3*-null gonad, contributed directly to the initial report of a role for ZNRF3 in sex determination (Harris et al. 2018). Subsequent to this, I aimed to develop materials to allow detection of the ZNRF3 protein and also to use expression profiling to examine the consequences of ablation of *Znrf3*.

4.1.1 Cell proliferation in *Znrf3* $^{-/-}$ *gonads*

Cell proliferation has been shown to be vital for proper testis determination in mice. More specifically, in gonads where proliferation has been blocked at around 11.0 dpc, XY gonads do not develop testis cords and exhibit aberrant expression of known pro-testis factors *Sox9* and *Amh* (Schmahl and Capel 2003). In the developing murine XY gonad, *Sry* is expressed at around 18 ts and at the same time an increase in proliferation is seen in these gonads highlighting the central role that proliferation has in testis determination. Further studies found that proliferation was reduced in *Fgf9* null gonads; this was not only an overall reduction, but the sharp increased expected at 18 ts was also absent, suggesting that FGF9 induces proliferation in the developing gonad (Schmahl et al. 2004).

This suggests a model in which proliferation is enhanced in XY gonads at around the time of testis determination due to the presence of testis factors, and if these factors are absent then proliferation is reduced. Further to this, a 2012 study found that *Wnt4/Rspo1* double knockout XY gonads also have reduced proliferation, suggesting that ovarian factors may also play a role in regulating proliferation (Chassot et al. 2012). Specifically, they observed reduced proliferation in the coelomic epithelium of the gonad, the outer most layer of cells surrounding the gonad, leading to impaired testis development. However, on further investigation they found reduced *Fgf9* expression in these double null gonads, suggesting that this was the reason for reduced proliferation and corroborating the earlier work of proliferation in the developing gonad (Chassot et al. 2012).

Dye-labelling experiments have shown the coelomic epithelium to be a vital part of cell contribution to lineages of the developing gonad, with data showing that a single coelomic epithelial cell can give rise to both supporting and interstitial lineages. This work suggested a model in which proliferation occurs in the coelomic epithelium and then cells migrate into the body of the gonad (Karl and Capel 1998). Further to this work, *Numb* expression was found to be higher in coelomic epithelial cells when compared to the rest of the gonad. When *Numb*-null mice were studied they were found to have a loss of embryonic gonadal somatic cells as a result of a lack of polarity in coelomic epithelial cells (Lin et al. 2017), highlighting the importance of the coelomic epithelium in gonadal proliferation.

Due to the link between *Wnt4/Rspo1* and gonadal cell proliferation, and the smaller size of XY *Znrf3*-null gonads (Harris *et al*, 2018), I aimed to study proliferation in the developing *Znrf3*-null gonad using EdU as a detection method of proliferation (Salic and Mitchison 2008).

4.2 Results

4.2.1 A study of proliferation in the *Znrf3* $^{-/-}$ gonad

We had found that *Znrf3*-null XY gonads partially sex reverse, and that at 11.5 dpc they were smaller and less well-formed than their wild type counterparts. This raised the question of cell proliferation: specifically, was cell proliferation affected in these null gonads and what was its contribution to the gonadal sex reversal observed. As previously discussed, the role of cell proliferation in sex determination was well known and had been shown to be crucial for proper testis formation. In gonads where proliferation had been blocked within a critical time-frame around 11.0 dpc improper testis formation had occurred (Schmahl and Capel 2003), and further to this, *Fgf9*-null gonads had been shown to have a reduction in proliferation (Schmahl et al. 2004).

To determine whether cell proliferation was affected in *Znrf3*-null gonads, an EdU-based study of cell proliferation was performed on mutant and wildtype C57BL/6J (B6J) gonads at 11.0 dpc and 11.5 dpc gonads, between 15-18 ts, in XY and XX samples. EdU is a thymidine analogue with a terminal alkyne

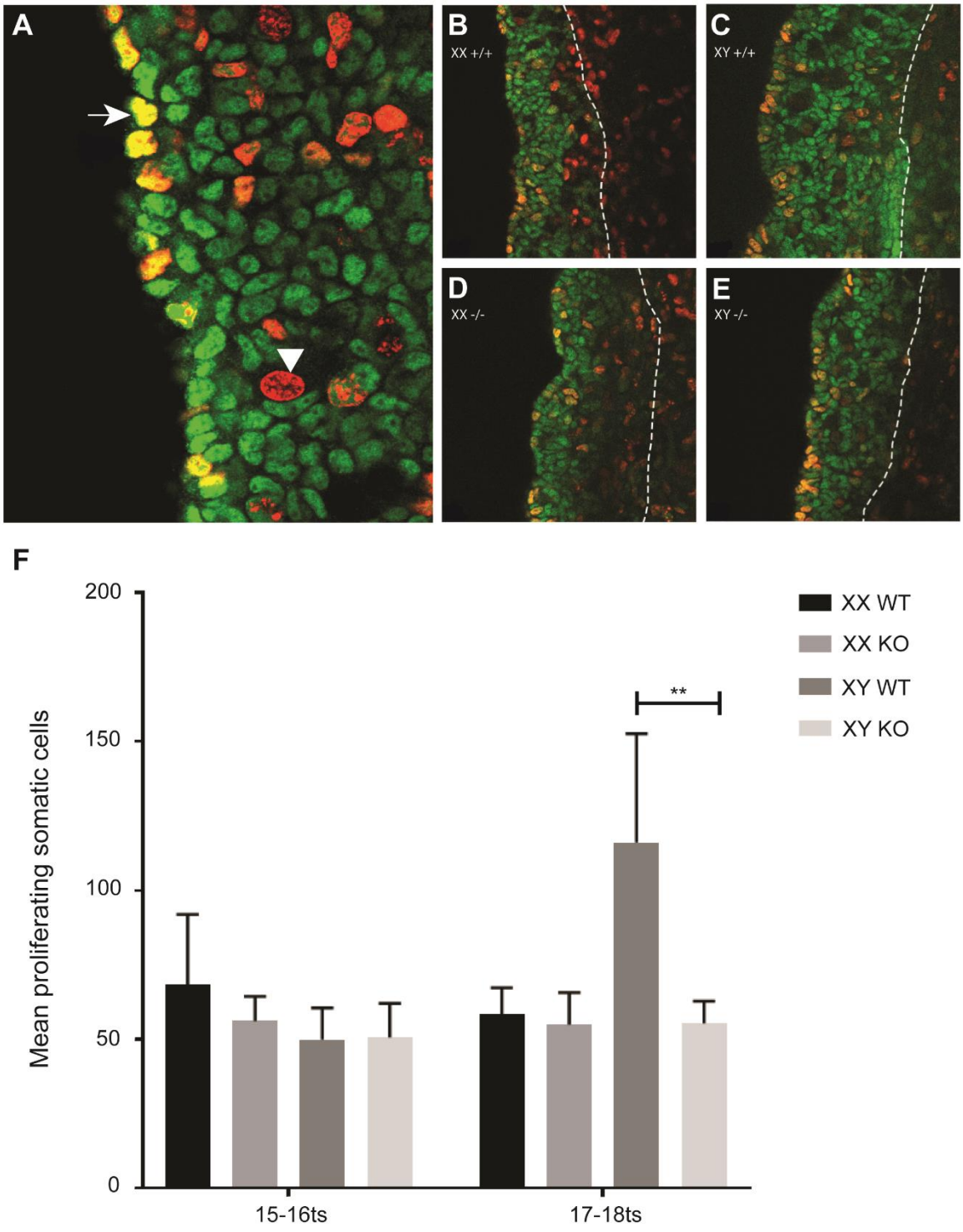

Figure 4.2 Analysis of cell proliferation in the *Znrf3*$^{-/-}$ gonad.

Gonads (11.0 dpc and 11.5 dpc) were stained for the presence of EdU (red) and GATA4 (green); arrowhead shows a proliferating germ cell and the arrow shows a proliferating somatic cell (x 40) **(A)**. Representative XX wildtype (17-18 ts) gonad (x20) **(B);** Representative XY wildtype (17-18 ts) gonad (x20) **(C);** Representative XX *Znrf3*$^{-/-}$ (17-18 ts) gonad (x20) **(D);** Representative XY *Znrf3*$^{-/-}$ (17-18 ts) gonad (x20) **(E);** Comparison of mean numbers of proliferating somatic cells in wild-type or *Znrf3*$^{-/-}$ gonads at 15-16 ts or 17-18 ts. **= p≤ 0.01 (n= 5-6) t-test **(F)**. ts= tail somites

group, instead of a methyl group. It is injected into the pregnant dam where it is incorporated into embryo cells during DNA replication, and the terminal alkyne then detected through a reaction with fluorescent azides (Salic and Mitchison 2008). The gonads were stained for the presence of EdU alongside GATA4, a marker of gonadal somatic cells, since only proliferation occurring in somatic cells was of interest at this stage. Only cells positive for both EdU and GATA4, detected using wholemount confocal microscopy, were counted for this study (Fig. 4.2A). The images shown indicate that *Znrf3*-null gonads are smaller when compared to wildtype controls (Fig 4.2B-E). Numbers of proliferating cells were then quantified from each image. A mean value for each sample was produced to allow for comparison across the genotypes. The 11.0 dpc time point was shown to have no significant differences in cell proliferation across all of the genotypes. However, at the 11.5 dpc time point, XY *Znrf3*-null gonads failed to undergo the massive upregulation in proliferation expected at this age due to the expression of *Sry* (Fig 4.2F). Instead, cell proliferation levels remained the same as in XX control gonads, suggesting that the null XY gonads are in fact behaving more like XX gonads.

4.2.2 Detecting ZNRF3 protein *in vivo*

Previous studies have relied on detecting *Znrf3* mRNA as a way of examining its expression and inferring function. There have been no reports of detecting ZNRF3 protein using a robust, highly specific antibody, and this means that a number of aspects of its function – sub-cellular trafficking, protein interactions etc. – have only been possible using cell transfection of tagged constructs. This certainly limits the sorts of study that can be performed, especially in terms of ZNRF3's *in vivo* function in sex determination. The lack of good commercially available antibodies to ZNRF3 led to my attempt to overcome this in two ways. Firstly, I attempted to generate an antibody, designed to detect the C-terminal domain of ZNRF3. By designing the antibody to the C-terminal it will be unable to detect the protein product of the null allele, which has been predicted to lack this domain, thus providing a method of validating the antibody. Secondly, I designed a tagged allele of *Znrf3* for *in vitro* experiments and attempted to generate an endogenous tagged allele using CRISPR/Cas9 genome editing.

4.2.2.1 Generating an anti-ZNRF3 poly-clonal antibody

Once the antigenic region of the protein had been selected, peptide sequences were sent off to Proteintech® for synthesis and used to raise antibodies in rabbits and guinea pigs. Following inoculation, blood was harvested and the serum purified to produce the antibodies. In total, 2 rabbits and 2 guinea pigs were inoculated, producing 4 final antibody samples.

Initial tests of the antibodies were performed using immunofluorescence (Fig 4.3) to determine if ZNRF3 could be detected in 11.5 dpc gonadal sections from wildtype and *Znrf3*-null mice, using any of the 4 antibodies. An anti-rabbit (ThermoFisher A32790) and anti-Guinea pig (ThermoFisher A-11073) secondary antibody was used, and both were confirmed to show no signal when tested without a primary (data not shown). The results of this initial screen showed neither of the rabbit antibodies to be specific, with both resulting in signal in samples from the null gonads. Further, guinea pig 1 antibody also resulted in non-specific staining. Guinea pig 2, however, appeared to have reduced staining in the null samples, suggesting that this antibody might be specifically detecting ZNRF3.

To address this, further immunofluorescence tests were performed using this antibody, but this time longitudinal sections were used to get a better picture of staining across the gonad (Fig 4.4B). However, further testing confirmed that guinea pig 2 was also unable to detect ZNRF3 specifically, with both XX and XY null gonads showing equal levels of protein expression to their wild type counterparts. The staining in the XY null gonad appeared to have a slightly different cellular localisation to that seen in the XY wt. However, this difference was slight, and the appearance of any staining, when the antibody should only detect the C-terminal, suggested non-specific signal. This suggested that all four antibodies were unable to specifically detect ZNRF3 using immunofluorescence. Further tests were then performed to determine if the antibodies produced worked on Western blots, and to confirm if their failure to be specific was limited to immunofluorescence. The results of Western blot confirmed that none of the four antibodies were able to specifically detect ZNRF3, with any band present at the expected 100kDa weight also present in the homozygous null samples (Fig 4.4A). The inability to detect ZNRF3 specifically with all four

antibodies ties in with the inability of commercial antibodies to do the same, a problem which has been linked to low levels and potentially high turnover of ZNRF3.

4.2.2.2 Generating a ZNRF3-MYC-6XHIS tagged allele

To overcome the previously discussed problems of antibody failure and an inability to study ZNRF3 protein, a tagged allele was designed that would allow CRISPR-Cas9 to introduce a MYC tag followed by a 6XHIS tag after the last codon of the open reading frame, before the 3 prime untranslated region (3'-UTR). Before generating an *in vivo* line containing this tagged allele, I wanted to confirm its efficacy *in vitro* by generating a plasmid containing *Znrf3* followed by the MYC/6XHIS tag sequence. *Znrf3* was cloned into a pcDNA3.1 expression vector by GENEWIZ®. This plasmid (Fig 4.5B) was transfected into NIH3T3 cells and cells were co-stained with anti-MYC antibody and antibodies to various proteins that mark sub-cellular compartments, in order to identify the sub-cellular region to which it localises (Fig 4.5A). The results highlighted that protein derived from this ZNRF3 construct could be visualised when tagged with MYC, and suggested that it co-localises with LAMP2, a known lysosomal marker within the cell.

Following the success of this in vitro study, a novel mouse line was generated that would tag the endogenous *Znrf3* gene in the same way, in an attempt to study ZNRF3 protein and its localisation in vivo (see Materials and Methods for details). Based on the results of the *in vitro* work, the ZNRF3-MYC-HIS-B6J line (called ZTAG here) was studied initially using immunofluorescence. 11.5 dpc wholemount gonads were co-stained with GATA4 and anti-MYC to allow protein detection in the somatic cells of the gonad. However, heterozygous ZTAG samples did not differ in staining to the wildtype samples, suggesting any staining was not specific and tagged ZNRF3 protein could not be visualised (Fig 4.6C). In an attempt to confirm the efficacy of this ZTAG line *in vivo,* I next performed Western blot analysis on 11.5 dpc embryo lysate from both wildtype and ZTAG heterozygous samples (Fig 4.6A-B). Unfortunately, as the results show, neither the MYC nor the HIS tag could be detected at

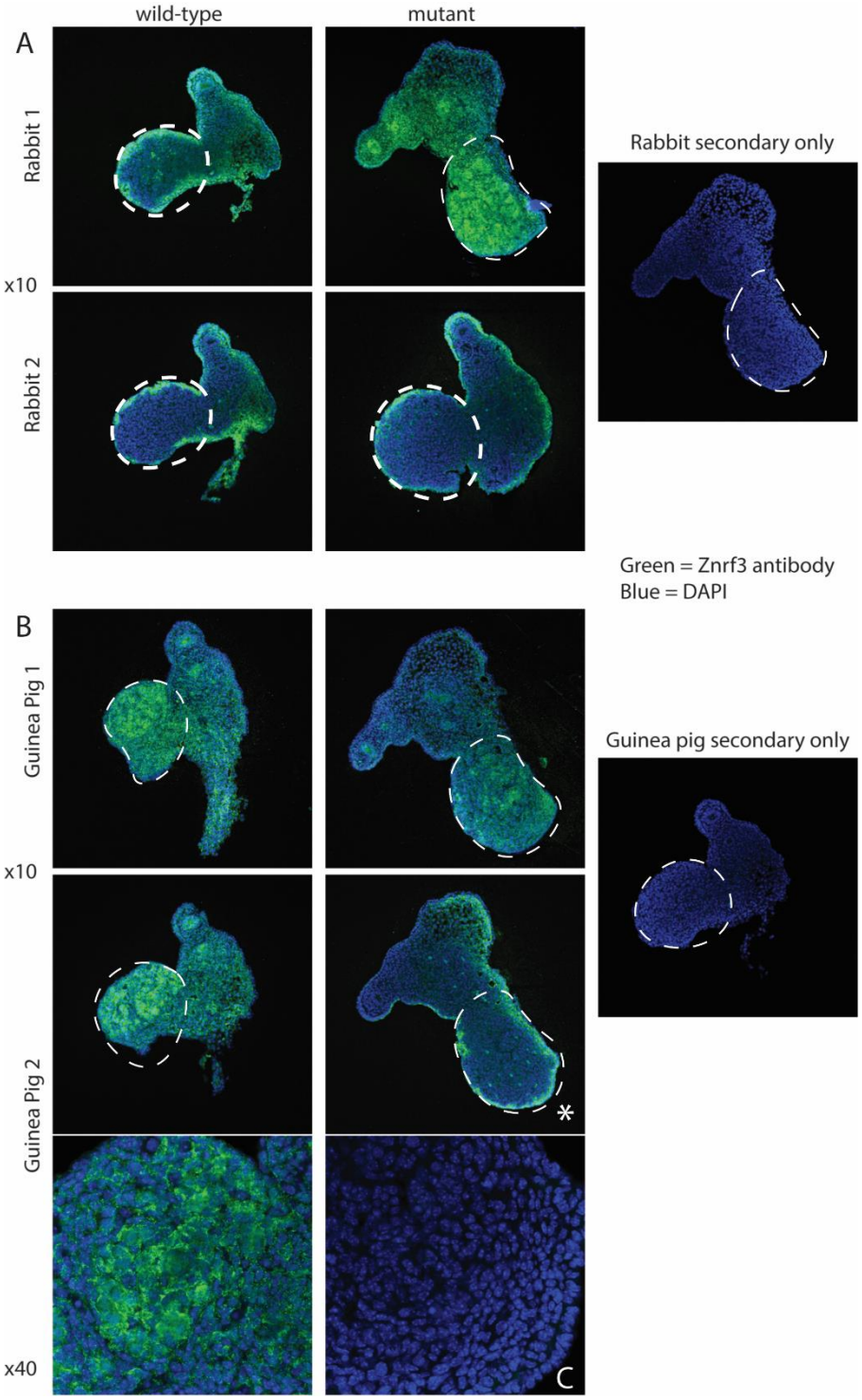

Figure 4.3 Testing potential ZNRF3 antibodies with immunofluorescence.
Antibodies designed to detect the C-terminal domain of ZNRF3 were tested on transverse gonadal sections from both wildtype and *Znrf3*$^{-/-}$ 11.5 dpc murine embryos. *Znrf3*$^{-/-}$ mice are predicted to lack the C-terminal domain; ZNRF3 staining (green) should thus be absent from these samples. Sections were counterstained with DAPI (blue). Two antibodies were derived from immunisation of rabbits **(A)** and two from guinea pigs **(B)**. White dashed line highlights the gonad. * highlights the only sample where a loss of signal was seen compared to the wildtype; this is further exemplified with a higher magnification image (x40) of the same sample stained using guinea Pig 2 antibody **(C)**.

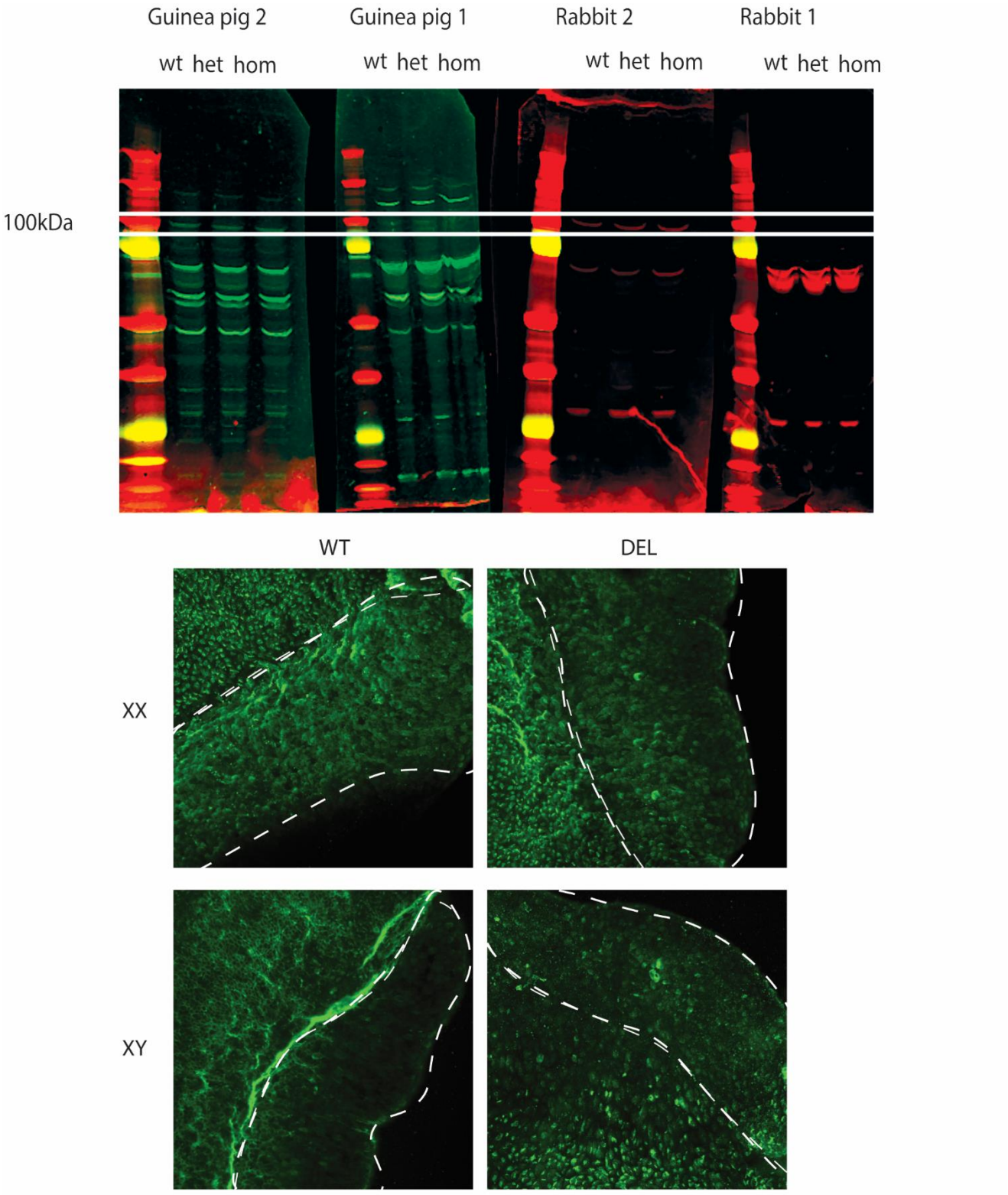

Figure 4.4 Testing potential ZNRF3 antibodies with Western blot and further study with immunofluorescence.
Antibodies designed to detect the C-terminal domain of ZNRF3 were tested on protein lysate from both wildtype (wt), *Znrf3*$^{+/-}$ (het) and *Znrf3*$^{-/-}$ (hom) 11.5 dpc whole embryos **(A)**. *Znrf3*$^{-/-}$ mice are predicted to lack the C-terminal domain; a ZNRF3 band (100kDa) should thus be absent from these samples. Guinea Pig 2 antibody was further tested on 11.5 dpc coronal gonadal sections in wildtype and *Znrf3*$^{-/-}$ **(B)**. Both XX and XY gonads were studied and neither showed a loss of ZNRF3 staining (green) in the mutant. White dashed line highlights the gonad.

the expected protein size of 105kDa, corroborating the immunofluorescence assay and suggesting an inability to detect a protein product of the appropriate size from the MYC-6XHIS protein tagged allele.

4.2.3 RNAseq study of XX and XY *Znrf3*$^{-/-}$ embryonic gonads

Earlier studies in our lab examined the expression of particular sex-determining genes in the *Znrf3*-null gonads from 11.5 to 14.5 dpc. In particular, it was demonstrated that *Wnt4* and other markers of active canonical WNT signalling were ectopically expressed in the XY null gonad at around 11.5 dpc i.e. the sex-determining stage of gonadogenesis (Harris et al 2018 and unpublished data). As anticipated, *Sox9* levels were also reduced in the mutant. However, consistent with variability in the mutant phenotype that is observed at 14.5 dpc, there was also variability in the degree of sex reversal, evidenced by gene expression, at 11.5 dpc. The aim of the experiments performed in this section was to survey gene expression in the mutant gonads on a genome-wide scale, as part of an ongoing study to understand the molecular basis of the sex reversal observed and shed light on the phenotypic consequences of losing this key WNT antagonist. I collected samples (see Material & Methods for details) from carefully staged and dissected embryos (Table 4.1) and following RNA extraction submitted these to the Oxford WTCHG facility for bulk RNA sequencing (RNAseq). Data analysis was performed by the MRC Harwell bioinformatics team before being returned to me for final analysis.

The heatmap (Fig. 4.7) shows all significant differentially expressed genes from an RNAseq analysis of 11.dpc gonads including both wildtype (wt) and *Znrf3*$^{-/-}$ (DEL) samples, it was generated using the research software Q. The heatmap has then been divided into groups based on the type of differential expression seen. Group A gene expression is low in all XY samples and high in XX samples. XY DEL samples have slightly higher expression levels compared to their wt counterparts, whilst XX DEL samples have lower expression compared to theirs. This group contains the pro-ovarian gene, *Wnt4,* and the non-coding X-linked gene required for X chromosome inactivation, *Xist*. The overexpression of *Wnt4*, as seen in XY DEL, is a feature of granulosa cell specification seen during ovarian development. In particular, *Wnt4* is expressed at almost equal levels in the DEL samples, suggesting

that these samples are more similar to each other than to either of their wt counterparts. Their similarity also indicates abnormal gonad development, with the resulting phenotype expected to be somewhere between a testis and an ovary based on the *Wnt4* levels observed.

Expression of genes within group B is much higher within both DEL samples, with a particularly strong difference seen between XY wt and XY DEL. Further, this group of genes appear to have stronger expression XY DEL compared to XX DEL. This contrasts the wildtype expression levels where XX have higher expression of the genes in this group. This group contains further ovarian-determining genes (*Axin2, Foxl2* and *Fst*), so higher expression of this group would be predicted to push gonad development towards the ovarian pathway. In particular, the overexpression of *Axin2* within the DEL samples suggests activation of the WNT/β-catenin pathway. These data, explained by the absence of anti-WNT *Znrf3* expression, confirm prior observations with individual gene probes (Harris et al). Group B also contains many key developmental genes eg. *Fgfr2*, suggesting that development could be severely compromised in DEL embryos; such transcriptional changes may underlie the fact that DEL individuals are post-natally non-viable. Further, group B contains genes involved in hormonal regulation and growth. These genes, *Ndrg1* and *Igfbp2*, are both expressed much more in XY DEL than XX DEL. This suggests the loss of *Znrf3* on an XY background has a strong impact on hormonal regulation and growth. This correlates with the earlier proliferation study which also showed a lack of cell division and growth, and suggests a hormonal role for *Znrf3.* Overall, the ectopic expression of the WNT pathway and the granulosa cell marker *Foxl2* seen in XY DEL samples validates the RNAseq data and suggest this dataset is an excellent resource for ongoing scrutiny of the transcriptomic consequences of deleting *Znrf3* in the developing gonad. Genes within group B should be of particular interest for future study, as they are particularly affected by *Znrf3* deletion on an XY background.

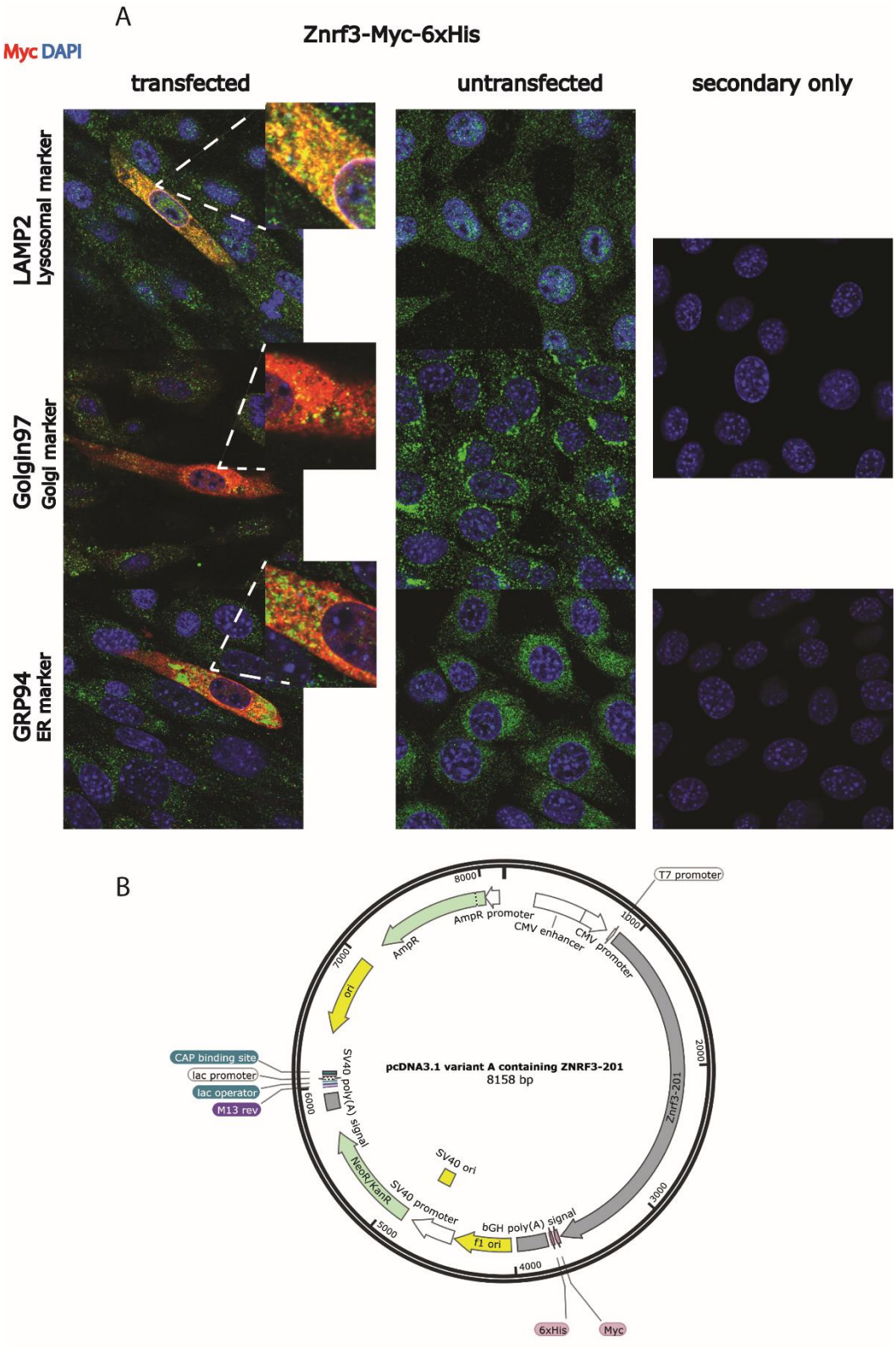

Figure 4.5 *In Vitro* study of *Znrf3-Myc-6xHIS* tagged allele in NIH 3T3 cells.
Cells were transfected with a *Znrf3-Myc-6xHis* plasmid and then co-stained with MYC antibody (red) alongside various cell markers (red) and DAPI (blue). Un-transfected and secondary only images are shown for comparison. All images were taken using an oil immersion lens (x63). Co-localisation is shown with a yellow stain (green + red) **(A)**. Plasmid map displaying the pcDNA3.1 expression vector containing *Znrf3* **(B).**

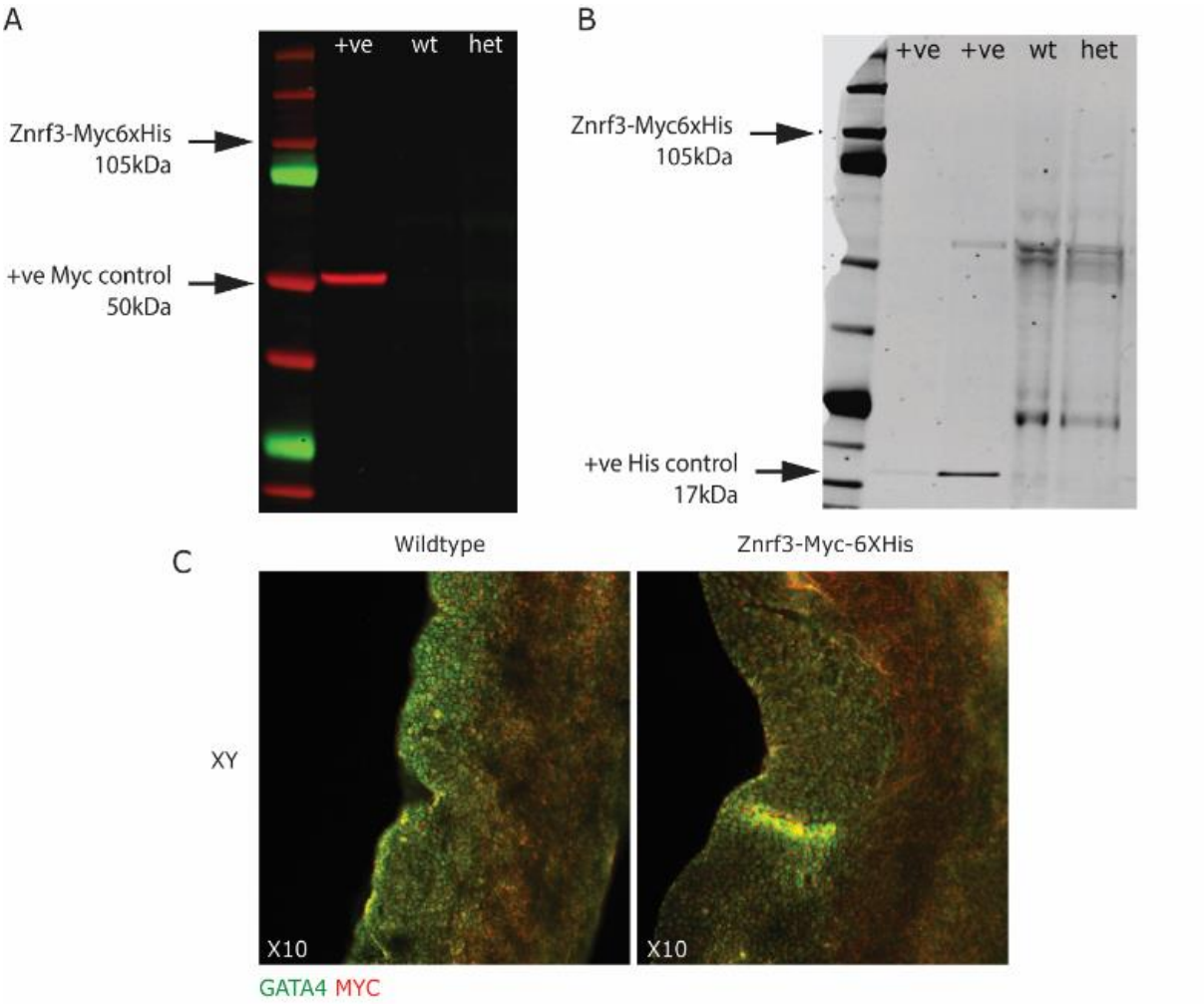

Figure 4.6 *In vivo* study of *Znrf3-Myc-6xHis* tagged allele using western blot and immunofluorescence.
Protein lysate from 11.5 dpc whole embryo wildtype and *Znrf3*$^{-/tag}$ was analysed on western blot using both MYC **(A)** and HIS **(B)** antibodies. Neither antibody produced a band at the expected 105kDa weight. Wholemount 11.5 dpc gonads from both wildtype and *Znrf3*$^{-/tag}$ embryos were co-stained with somatic cell marker GATA4 (green) and MYC (red) (x10) **(C)**. No loss of stain was seen in the wildtype samples.

Sex	Genotype	Age	No. of samples
XX	*Znrf3*$^{+/+}$	18-19ts	5
XY	*Znrf3*$^{+/+}$	18-19ts	5
XX	*Znrf3*$^{-/-}$	18-19ts	3
XY	*Znrf3*$^{-/-}$	18-19ts	5

Table 4.1 Samples collected for RNAseq analysis.
A table showing the number of samples collected for each genotype (n) for RNAseq analysis

Within group C, XY DEL samples have lower gene expression than XY wt samples. This group contains the testis-determining genes *Sry, Sox9* and *Fgf9*. So, a reduction of expression within this group correlates with the sex-reversal phenotype described above i.e. more ovarian-like. It is interesting to note that the expression levels are more affected further downstream in the testis-determining pathway. *Sry* expression, which initiates the pathway, is affected less than the downstream components *Sox9* and *Fgf9*. Nevertheless, it is interesting to note this impact on *Sry* expression, which was previously reported to be reduced in the XY null, but to a statistically non-significant degree (Harris et al). In contrast to group C, group D expression levels are increased in XY DEL compared to XY wt. Within this group is *Lars2,* a mitochondrial tRNA which has been shown to be involved in ovarian development, particularly in the development of oocytes (Pierce et al. 2013). Expression within Group E is unaffected; all of these genes are located on the Y chromosome, suggesting that the Y chromosome is functioning normally, despite the gonadal sex reversal phenotype. Due to the use of Cohen's D during primary analysis, these XY genes present as beige rather than white in XX samples on the heatmap. This is due to the method of analysis and does not represent expression.

Group F expression is varied, with XY DEL expression being greatly reduced compared to wt, and XX DEL being greatly increased compared to wt. The genes within this group are related to blood. This group highlights genes that are the most differentially expressed between the two DEL groups. Across the rest of the heatmap, the two DEL groups are reasonably similar, suggesting their phenotype is more like each other than either of their wt counterparts. However, that is not the case within group F, suggesting XX DEL embryos differ in phenotype to XY DEL embryos. It is unclear why there is such a large difference in expression of these genes between XX DEL and XY DEL, but it could be due to the different biological structures of the testis and the ovary. The testis is highly vascularised, correlating with high expression of these genes in the XY wt. The XY DEL is undergoing sex reversal, and as such is less vascularised, explaining the reduction of expression in these genes. However the XX del gonads have increased expression of these genes, and they are not highly vascularised, suggesting another role for these genes within the gonad. Some of the genes in this group are involved in gene regulation

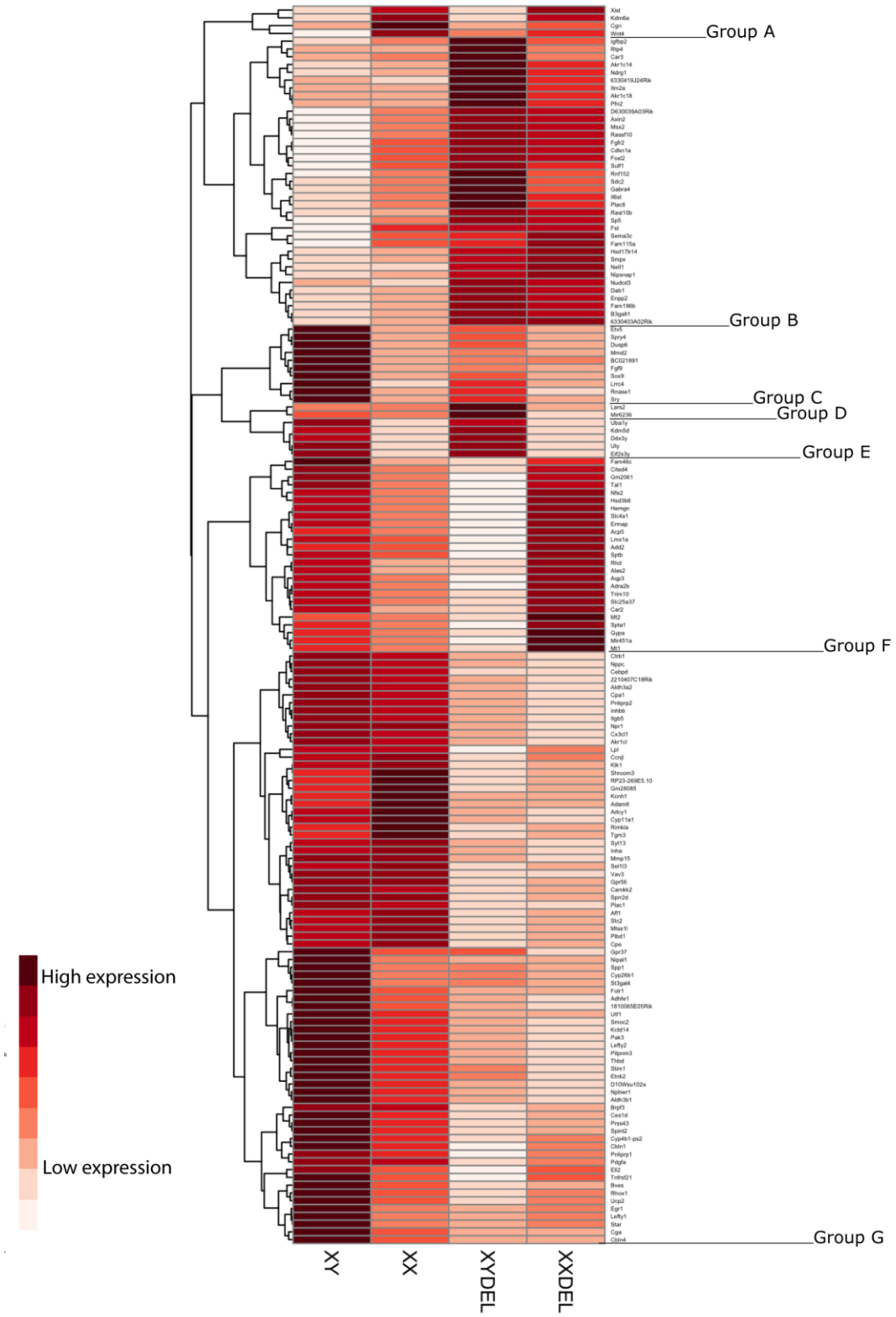

Figure 4.7 Heatmap depicting differentially expressed RNA in *Znrf3*$^{-/-}$ 11.5 dpc gonads.
RNA was extracted 18-19 ts gonads and then sequenced to enable comparison between samples. The heatmap shows the differences between the samples for those genes with statistically significant differences. Heatmap generated using Q. All replicate samples were averaged and significance determined by Q. Only Q-filtered genes with extremely high and extremely low read counts are shown. All values are converted to a Cohen's D. n=5 (except XX DEL n=3). Cohen's D = the mean is subtracted from the value(x) and then divided by the standard deviation (x-mean)/SD.

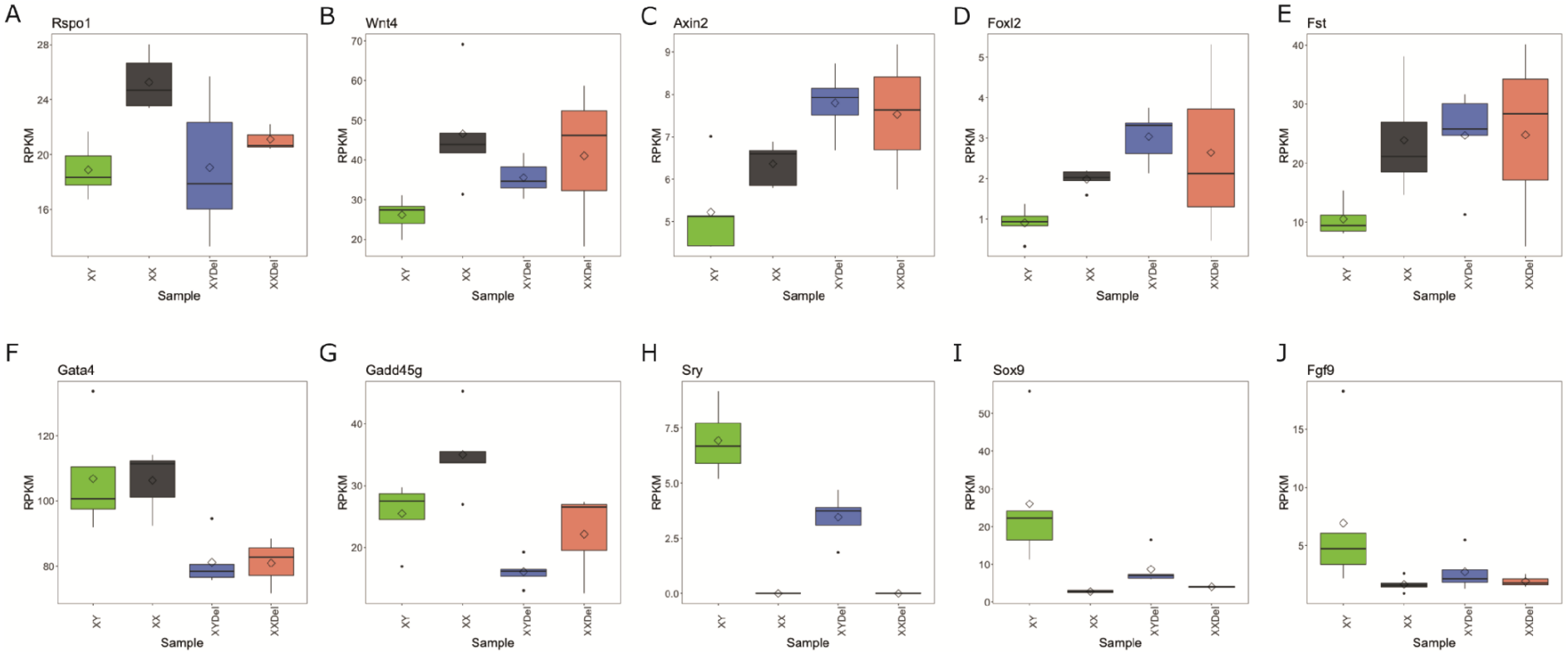

Figure 4.8 Graphs depicting the RPKM of genes of interest in XX and XY *Znrf3*$^{+/+}$ and *Znrf3*$^{-/-}$ 11.5 dpc gonadal samples.
Rspo1 **(A),** *Wnt4* **(B),** *Axin2* **(C),** *Foxl2* **(D),** *Fst* **(E),** *Gata4* **(F),** *Gadd45g* **(G),** *Sry* **(H),** *Sox9* **(I),** *Fgf9* **(J).** RPKM = reads per kilobase of transcript per million mapped reads, it is a normalised unit for transcript expression which compensates for longer RNA molecules producing more sequencing reads.

and cell differentiation of blood cells, eg. *Trim10*, *Tal1*, and *Cited4*. They could be playing a similar molecular role within gonadal cells. Expression within group G is reduced in both DEL groups compared to their wt counterparts. Some genes within this group relate to germ cell development (*Inha, Inhbb* and *Nppc*), suggesting that both XY and XX DELS are unable to undergo appropriate germ cell development. The majority of genes within this group, however, are related to cardiac functions. The ontology table (Appendix 2) also highlights multiple cardiac functions, suggesting a role for *Znrf3*-dependent pathways on gene expression pathways that function in the heart. This has already been observed with *Lgr4*, a known partner of *Znrf3*, which has been shown to have a role in the heart (Van Schoore et al. 2005). Further, both *Wt1* and canonical WNT signalling have also been shown to have roles within heart development (Hastie 2017, Zhang, Gui and Wang 2015) alongside their known roles in gonadal sex determination.

The graphs shown in Fig. 4.8 highlight some genes of interest from the heatmap in regards to gonadal development. *Rspo1* is expressed at higher levels in XX gonads and is involved in ovarian development; it is also known to functionally oppose *Znrf3* activity. The graph shown in Fig 4.8A shows that expression is not reduced in the XY DEL when compared to wt; however, expression is slightly reduced in the XX DEL. RSPO1 expression promotes WNT signalling, which can be determined using *Wnt4* and *Axin2* expression as a readout. Fig. 4.8B shows that *Wnt4* is expressed more in XX than XY gonads, and this expression is unchanged in XX DEL. However, XY DEL gonads express higher levels of *Wnt4* than the wt. This suggests that WNT/β-catenin signalling has been activated in XY DEL gonads, which is further corroborated by data shown in Fig. 4.8C. This graph shows that *Axin2*, a known readout for WNT/ β -catenin signalling, is greatly over-expressed in XY DEL gonads. Furthermore, XX DEL gonads also over-express *Axin2,* suggesting that WNT/ β -catenin signalling is increased in these also. The WNT/ β -catenin pathway is central to ovarian development, so any increase in its activity would push development towards ovarian determination, although the consequences of over-activation are unclear.

Other proteins which are key to ovarian development are FOXL2 and FST. Fig. 4.8D shows that *Foxl2* is expressed higher in XX gonads compared to XY, as predicted for a granulosa cell marker. However, XY DEL gonads have greatly increased levels of *Foxl2* compared to XY wt levels, and even slightly higher expression levels than XX wt, showing that this pathway is overexpressed in the XY DEL gonads. This is further corroborated by data shown in Fig. 4.8E, which reveals that *Fst* expression is also greatly increased in XY DEL gonads. Also, expression levels are raised in XX DEL gonads when compared to wildtype. *Axin2* and *Fst* are both markers of ovarian development, and in both of these graphs expression is most similar between the two DEL samples than either of their wt counterparts. This trend was also shown in the heatmap (Fig. 4.7). This suggests that DEL gonads will be more similar in phenotype to each other than to other wt gonads. Previous studies (Harris et al. 2018) in the lab suggested that XX DEL gonads also undergo abnormal development (fail to initiate meiosis); this works confirms this and proposes XY DEL and XX DEL could develop more like each other than either testis or ovary.

GATA4 is expressed in the somatic cells of the developing gonad. Fig. 4.8F shows that it is equally expressed in both XX and XY gonads and that expression is reduced in both DELS, suggesting that the phenotype seen is affecting the appropriate development of the somatic cell lineage. Figs. 4.8G-J highlight some genes that are known to be central to the testis determination pathway. *Gadd45g* is known to influence testis determination by aiding the timely expression of *Sry* (Warr et al. 2012). Fig. 4.8G shows that *Gadd45g* expression is greatly reduced in XY DEL samples when compared to wt, which would suggest that testis determination in the XY DEL gonads could be impacted due to loss of *Gadd45g*. Corroborating this further is Fig. 4.8H, which confirms that *Sry* expression is greatly reduced in XY DEL when compared to wt. These two factors, GADD45g and SRY, provide early readouts of the testis determination pathway. Further downstream, SOX9 and FGF9 can be used to measure commitment to the testis pathway. Figs. 4.8I-J show *Sox9* and *Fgf9* expression, respectively. In both of these graphs, expression levels have been greatly reduced in the XY DEL samples, with almost zero levels of expression. This lack of downstream pro-testis gene expression in the XY DEL gonads makes

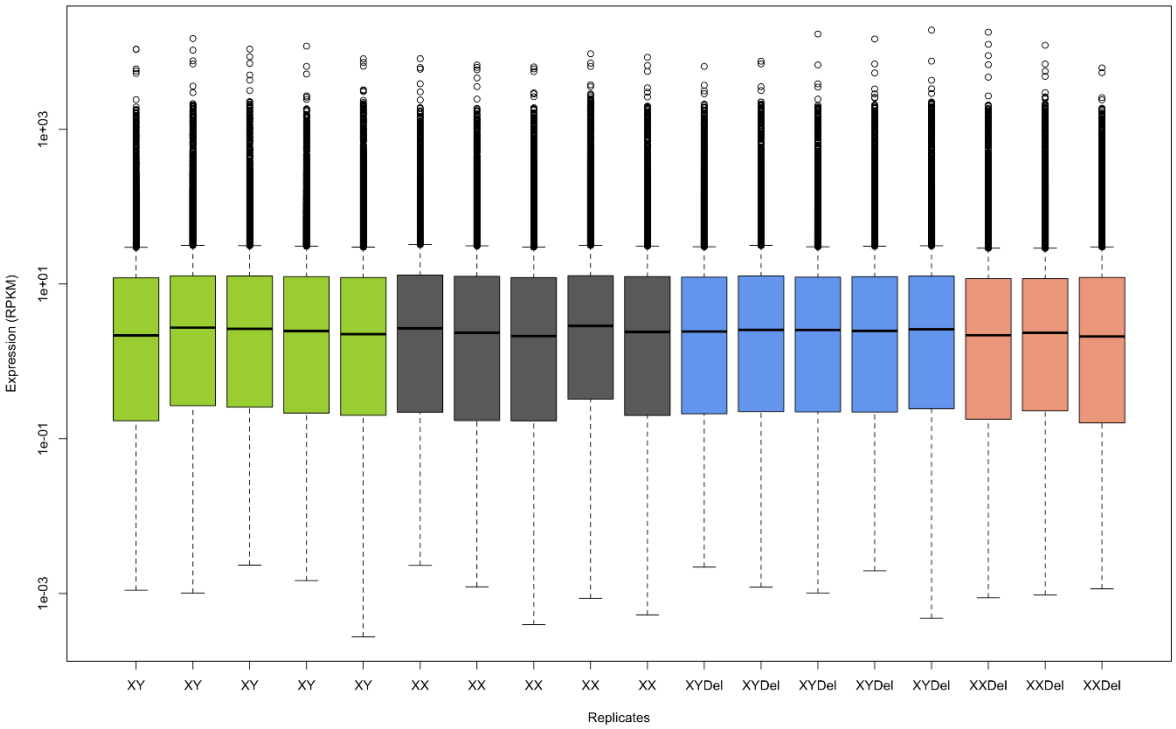

Figure 4.9 Variance of RNA expression levels in *Znrf3*$^{-/-}$ 11.5 dpc gonads.
RNA was extracted at 18-19 ts gonads and then sequenced to enable comparison between samples. Variance was measured using Fligner-Killeen test. XY: p-value = 1, XX: p-value = 1, XYDel: p-value = 1, XXDel: p-value = 0.02923. RPKM = reads per kilobase of transcript per million mapped reads, it is a normalised unit for transcript expression which compensates for longer RNA molecules producing more sequencing reads.

them more similar to XX gonads than XY gonads. This corroborates Figs. 4.8A-E, which showed that known pro-ovarian genes were overexpressed in these XY DEL samples. This increase, alongside the decrease in testis gene expression, likely accounts for the more ovarian phenotype seen in these gonads. However, we know the XY DEL gonads exhibit a variable phenotype, with varying degrees of sex reversal, not always associated with complete sex reversal. Whilst the pro-testis genes shown (Figs. 4.8G-J) suggest the DEL gonads are both similar to XX wt gonads in expression levels, the ovarian genes shown (Figs. 4.8A-E) suggest the DEL gonads are most similar to each other in expression levels, but both differ to either wt samples. To determine the similarity of RNA expression between the four genotypes, a PCA analysis was performed.

Fig 4.9 shows the variance of total RNA expression across all samples. It concludes that there is no significant variation between any of the genotypes when all RNA is compared. The test for homogeneity used is the Fligner-Kileen test (Conover, Johnson and Johnson 1981), which shows complete homogeneity (p-value 1) between all samples except the XX Del samples, although the result seen for XX Del is most likely a statistical error due to low sample size (n=3) for this genotype. This verifies the data presented in Fig 4.9, and confirms no variance between samples in total RNA expression. This shows that whilst individual RNA expression might suggest the two DEL samples to be different to their wt counterparts and more similar to each other, this is not supported when looking at overall RNA expression.

4.3 Discussion

This chapter describes experiments aimed at examining the role of ZNRF3 in mouse sex determination using different but complementary approaches.

4.3.1 Proliferation in the XY *Znrf3*$^{-/-}$ embryonic gonad

Previous studies on proliferation in XY gonads had suggested that it initially occurs within the coelomic epithelium (Schmahl et al. 2000). The coelomic epithelium is the outer layer of cells along the outer edge of the gonad. However, my work was unable to confirm this. I found no difference in proliferation between the coelomic cells of XX and XY gonads at 17-18 ts (Appendix 4), but a significant difference when all somatic cells were compared, suggesting that proliferation differences are occurring within the inner body of the gonad rather than the coelomic epithelium. This difference in the results of my study compared to the earlier study could be due to the advancements in scientific techniques. The earlier study used BrdU, the older version of the EdU technology, which was a bulkier compound requiring DNA denaturation to allow visualisation (Smith 2016). This could have affected the results of the earlier study and resulted in differences being confined to the coelomic epithelium, but this would warrant further study to confirm.

The results presented here show a reduction in cell proliferation between 17-18 ts (11.5 dpc) in XY del samples when compared to XY wt samples. This was suggested to be having a potential impact on testis determination in these samples, as it had earlier been shown (Schmahl and Capel 2003) that blocking proliferation *in vitro* can prevent correct testis formation, as previously discussed. However, the earlier study specifically showed that cell proliferation needed to be impacted at around 11.0 dpc (15-16 ts) for it to prevent proper testis formation; when blocked earlier or later, for example at the time point of 11.5 dpc, testis determination continued as normal. This indicates a temporal 'window' during which cell proliferation is key for testis determination. So, my data showing a reduction in cell proliferation in *Znrf3*$^{-/-}$ gonads at 17-18 ts (11.5 dpc) are not enough to confirm that any phenotype seen is due to such a lack of cell proliferation. As such, proliferation was studied at the earlier time point of 15-16 ts (11.dpc). At this age there was no significant difference in proliferation between samples. Assuming that the method of detection of cell proliferation (EdU labelling) is sufficiently efficient and sensitive to detect the small differences that might exist between genotypes at this stage, this suggests that the impact on testis determination seen is not due to a lack of cell proliferation. Accordingly, the reduction in cell proliferation in XY mutants at 17-18 ts is likely to be a consequence of XY del gonads developing like XX gonads. The causal explanation for XY del gonads undergoing partial sex reversal, and proliferating at XX levels, was not confirmed by these experiments, but is likely due to impacts of elevated canonical WNT signalling on *Sry* and *Sox9* expression, as revealed by RNAseq (see below).

4.3.2 Examining ZNRF3 protein *in vivo*

To shed further light on the role of ZNRF3 in testis determination and the sex reversal phenotype, I decided to create a murine custom ZNRF3 antibody. This was required because there were no commercially available one. (I tested several of these, but with no success data not shown). Such an antibody would also be immensely useful to any labs studying the role of ZNRF3 in WNT signalling more broadly. I designed the antibody to the C-terminal region of ZNRF3 as this region is missing in the null, thus creating a way of testing antibody specificity. Unfortunately, none of the antibodies

produced were able to specifically bind to ZNRF3, with all giving signals in wildtype and null samples. I further tested the antibodies on cells overexpressing *Znrf3* but this was also unsuccessful (data not shown). It is well known that antibodies may not work equally well on all applications, so I tested each antibody both on immunofluorescence and Western blot applications as these would be of the most use to me. The lack of specificity to ZNRF3 – evidenced by failure to detect an appropriate protein only in the wildtype samples - was seen in both applications. This phenomenon was also seen with all the commercially available antibodies tested: all were unable to specifically detect ZNRF3.

The inability to produce a working ZNRF3 antibody makes studying the protein's function within gonadal development incredibly challenging and also means that many of the protein's properties are still currently inferred from *in vitro* studies in potentially irrelevant biological contexts. To try and overcome, this I attempted to generate a new *Znrf3-Myc-6xHis* tagged mouse line. Initial work was performed *in vitro* using NIH3T3 cells into which a *Znrf3-Myc-6xHis* tagged plasmid was transfected. Transfection of the plasmid into the cells successfully enabled the visualisation of the tagged ZNRF3 protein. The results of this work found that ZNRF3 was co-localising with the lysosomal marker LAMP2.

ZNRF3 is known to be a trans-membrane protein, with its functional activity occurring whilst in its membrane bound state. It interacts physically with other proteins at the membrane to then clear these proteins. For example, membrane-bound ZNRF3 binds FRIZZLED protein and clears it from the membrane to prevent WNT signalling (Zebisch and Jones 2015). The presence of ZNRF3 in the lysosome of these transfected NIH3T3 cells is most likely linked to the ability of this protein to clear other proteins from the membrane, as the lysosome functions to degrade proteins and clear them from the cell (Saftig and Haas 2016). The lack of staining on the membrane of the NIH3T3 cells suggests that ZNRF3's localisation to the membrane of the cell is far more transient than its time in the lysosome. It also suggests that the concentration of ZNRF3 on the membrane at any one time may be quite low, with most of the ZNRF3 being concentrated in the lysosome. This high membrane turnover

of ZNRF3 might also account for the difficulty in detecting a band on a Western blot of the predicted size – much of the lysosomal ZNRF3 may not itself be intact and full-length.

The success of using this tagged *Znrf3* plasmid *in vitro* led me to design an identically tagged allele of the endogenous *Znrf3* gene. The allele contained a *Myc* tag followed by a *6xHis* tag, just as the *in vitro* plasmid had contained. The allele was generated using CRISPR/Cas9 genome editing in mouse embryos. Following derivation of a line with the confirmed genotype, heterozygous mouse embryos were harvested for study. Whole embryos were used to generate protein lysate due to the yield of protein available from a whole embryo when compared to a gonad and given that *Znrf3* is relatively widely expressed. This lysate was examined using Western blots, and 11.5 dpc gonadal samples were tested using immunofluorescence, both with a MYC antibody. As with the custom antibody, this was also unsuccessful. The immunofluorescence staining was no different to the negative controls, and the Western blots showed no bands at the predicted ZNRF3 size of 105k Da. Sequencing of the *Znrf3* tagged allele, done as part of allele generation and quality control, confirmed that the tag was definitely present. So, it appears that the results are due to an inability to detect the tag rather than a failure to produce the tag. This may suggest again that ZNRF3 protein levels are too low to be detected. The success of the *in vitro* work was due to the nature of the experiment. As the tagged gene was transfected into the cells, there was then an effective overexpression of ZNRF3 within the cells. This overexpression enabled detection using the MYC antibody. When ZNRF3 is at endogenous levels it may be undetectable in the developing mouse embryo using an antibody.

In the course of writing this thesis, an attempt was made to generate embryos that carried both the *Znrf3* tagged allele and the null allele (*Znrf3* $^{-/tag}$). It was predicted that these would be normal, since the tagged allele was predicted to be functional, and one functional copy of *Znrf3* is sufficient for viability and fertility. However, it was observed that these animals are non-viable. This was a surprise and suggests that the tagged allele is not just a simple tag and there may be another CRISPR-based indel event in the vicinity of the tag that has somehow disrupted function of the gene. Lack of time

prevented me from exploring this further. This might also be the basis for an explanation for why the tag could not be detected *in vivo*. It is also a reminder of the requirement to carefully analyse the products of CRISPR/Cas9 genome editing over some considerable distance from the target site (Burgio and Teboul 2020).

Finally, it is worth noting that the use of a tagged allele has some limitations when compared to a high quality antibody. The tag itself may have an impact on the function or stability of the protein in question, although the *in vitro s*tudies described here suggest this is not the case with the tagged ZNRF3 protein. One other drawback is the inability to examine the protein in the context of the homozygous null phenotype, since if the tagged allele is functional (as it should be) it will not be possible to generate such a phenotype. In the case of sex determination, however, it may still be possible to analyse the tagged protein's behaviour in a *Znrf3* $^{tag/-}$ B6J.Y^{AKR} gonad, which would still be predicted to undergo some degree of sex reversal (Harris et al 2018).

4.3.3 The transcriptomic consequences of *Znrf3* ablation in developing gonads

The inability to study ZNRF3 protein using antibodies made functional analysis of its role within gonadal development difficult. As an alternative, I decided to undertake an RNA sequencing project on 11.5 dpc *Znrf3*$^{-/-}$ gonads. The results of the RNAseq project highlighted various genes of interest, over which *Znrf3* could be having an influence.

It is well known that primary sex determination comprises two mutually antagonistic pathways, pro-testis and pro-ovary, with each pathway working to repress the other. So it is not surprising that when testis determination is disrupted, as it is in XY *Znrf3*$^{-/-}$ null gonads, we see an effect on both testicular and ovarian pathways. Within the testicular pathway, *Sry*, *Gadd45g, Sox9* and *Fgf9* expression are all reduced in XY del gonadal samples, with the downstream factors *Sox9* and *Fgf9* being the most affected. This suggests that the impacts are amplified throughout the testis pathway. The reduced expression of testis-determining genes links to the known phenotype of these gonads, which undergo partial (or variable) gonadal sex reversal. Further to these effects on the testicular pathway, known

ovarian factors are also shown to be affected. *Wnt4* expression appears to be upregulated in XY del samples when compared to wildtype. This is confirmed using the downstream readout of canonical WNT-signalling *Axin2*, which is highly upregulated in XY del gonads. Other ovarian factors, including *Foxl2* and *Fst,* are also upregulated in XY del gonads. This suggests that not only is the testicular pathway being repressed but the ovarian pathway is being overexpressed in these samples. As the two pathways are so intrinsically linked, any change to one of the pathways is likely to have a knock on effect on the other pathway. So there is the potential that all the changes we are seeing are due to one change to one of the pathways, rather than separate impacts to both of the pathways. This one change is caused by loss of ZNRF3.

Further to the analysis on specific RNA expression changes, homogeneity between gonadal samples was compared. It was found that, on the whole, none of the samples are significantly different to the others. However, this does not then mean that the previous expression changes discussed are not significant. The homogeneity between samples suggests that there are very few differences between

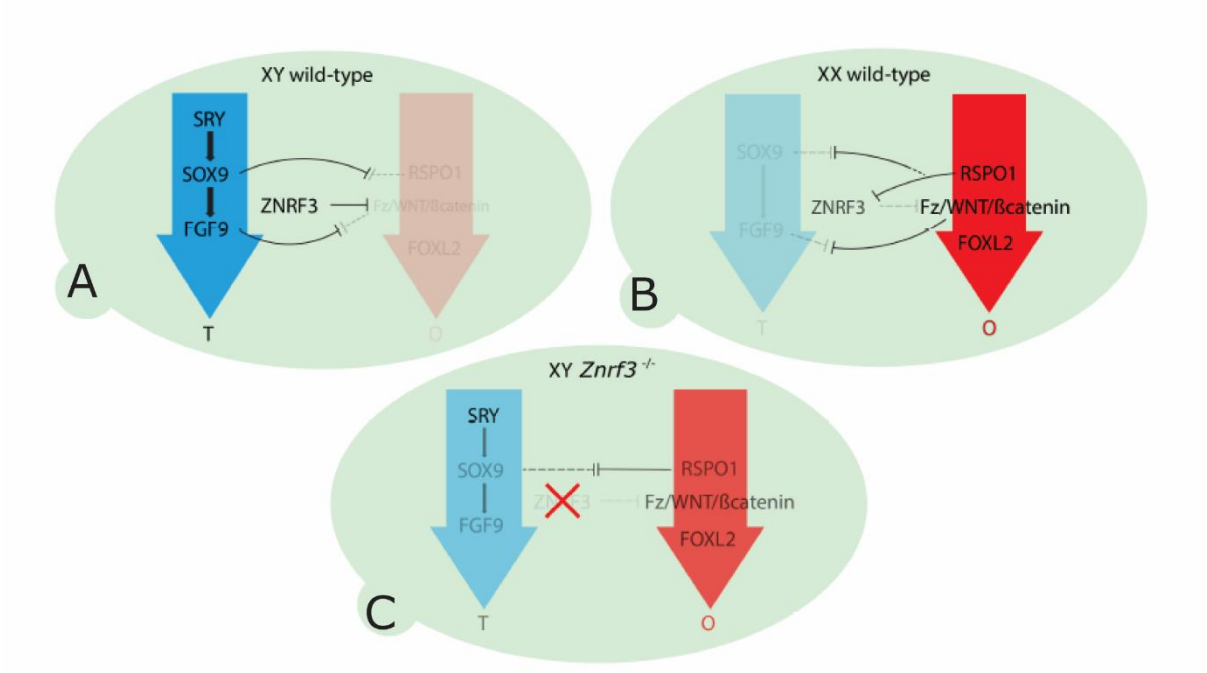

Figure 4.10 Potential role of ZNRF3 in developing gonad.
In the XY wildtype gonad ZNRF3 represses WNT signalling allowing testis development **(A)**, in the XX wildtype gonad RSPO1 represses ZNRF3 enabling WNT signalling and ovarian development **(B)**, in the XY *Znrf3*$^{-/-}$ gonad repression of WNT signalling cannot occur resulting in ovo-testis development **(C)** (Harris et al. 2018).

the DEL samples and the wildtype samples at this age. This could be due to a few reasons. One could be that as this early time point the variation is still very small; over time this variation would increase, resulting in the varied phenotype observed in 14.5 dpc samples. Another explanation could be the small sampling size. As the sex reversal phenotype of *Znrf3*$^{-/-}$ gonads is highly variable, there is a chance that an n=5 sample size is simply not large enough to capture the true picture of variation between samples, resulting in a form of sampling error. Finally, another explanation could be that the changes leading to aberrant testis development are very small and insignificant in the wider field of total RNA expression. This does not mean they have an insignificant impact, as we know they are impacting on testis determination. It merely suggests that the impact on testis development is due to a very small change in the RNA expression landscape, which is not visible when studying the landscape as a whole.

This suggests that the impact on the testis determination in *Znrf3*$^{-/-}$ samples is due to the expression changes in the known sex-determining factors discussed above, rather than a novel factor. The most likely scenario, since ZNRF3 has already been shown to repress WNT signalling in other organs, is that the impact on testis determination is due to ectopic activation of pro-WNT/pro-ovarian pathway and a consequential impact on *Sry* and *Sox9* (Fig 4.10). Nevertheless, this dataset has highlighted some potential genes of interest that warrant further study. In particular, the genes in Group B and Group F are of particular interest due to their sexually differential expression in both wildtype and DEL samples. Both of these groups undergo reversal of sexually differential expression when *Znrf3* is deleted. These groups both possess genes which are involved in regulation of gene expression and cell differentiation, and both will continue to be analysed in an attempt to identify any genes implicated in ZNRF3-mediated testis-determining events. This will be done alongside transcriptomic studies at the single-cell level, which are also being performed in the lab at this time.

5 Analysis of mouse lines lacking *Ncor2*

5.1 Introduction

As previously discussed, candidate DSD genes are often discovered via exome sequencing of patients; *NCOR2* was another candidate gene discovered in this way. The mouse model was used to study its potential role in sex determination.

5.1.1 Patient information

DSD patients presenting with *NCOR2* mutations were located across three different continents, and displayed a range of DSD phenotypes (Table 5.1). The patients presented with mutations located across the length of the gene, mutation location having no apparent correlation with patient phenotype (Appendix 3). Patient phenotypes ranged from 46,XX male to 46,XY complete gonadal dysgenesis (CGD), alongside other forms of DSD as well. This suggested that *NCOR2* could have a dual role, in both testicular and ovarian development. This potential dual role, in gonadal development, required a different approach for study.

Current literature highlights the importance of the mouse strain used, and how it impacts on phenotypic studies (Coleman and Hummel 1973, Linder 2001, Yoshiki and Moriwaki 2006), something that is also well documented in regards to testicular development studies (Yokoyama et al. 2019, Livermore et al. 2020, Munger et al. 2009, Correa et al. 2012). Throughout most of the research described in this thesis, studies have been performed on C57BL/6J (B6J) mice. This strain is known to be sensitive to disruptions to testis development, as previously discussed; and the work presented here thus far has investigated potential pro-testicular factors. However, as *NCOR2* mutations were identified in patients presenting at the clinic with both testicular and ovarian disorders, it was not appropriate to study any mouse phenotype solely on B6J. Throughout this chapter, *Ncor2*'s testicular role was studied on B6J and a further sub-strain of B6J (B6J.Y^{AKR}), but its potential role as an ovarian factor was studied using the strain 129X1/SvJ (129).

Origin	Phenotype	Mutation	Zygosity	Population: Minor Allele Frequency
Belgium	46,XY CGD	p.His1862Leu	heterozygous	Novel
North Africa	46,XY DSD, cardiac anomalies, dysmorphia	p.Gly1166Arg	homozygous	East Asian: 0.0007096
North Africa	46,XY CGD	p.Thr1586Met	heterozygous	Latino: 0.00002921
North Africa	46,XY syndromic DSD	p.Asp2075Asn	heterozygous	East Asian: 0.0001542
North Africa	46,XY CGD	p.Arg1947Gln	heterozygous	Novel: inherited from Father
India	46,XX male	p.Ile1099Phe	heterozygous	de novo, novel
Tunisia	46,XX male	p.Asn1665His	heterozygous	Novel
Egypt	46,XX male	p.Arg1905Cys	heterozygous	East Asian: 0.00007980: inherited from father
UK	46,XY CGD	p.Arg224Cys	heterozygous	South Asian: 0.00006571
Egypt	46,XX male	p.Arg1352His	heterozygous	European non-Finnish: 0.008008
Ukraine	46,XY DSD	p.Arg2234Gln	heterozygous	Novel

Table 5.1 Patients presenting with DSD and *NCOR2* mutation.
Patient data showing patient origin, their DSD phenotype, the specific mutation they possess, and the allele frequency of this mutation. Data are courtesy of Ken McElreavey, Pasteur Institute.

5.1.2 NCOR2 protein structure and function

Nuclear receptor co-repressor 2 (NCOR2) is a transcriptional coregulatory protein, which works to assist nuclear receptors in down-regulation of target gene expression. It further facilitates transcriptional repression by acting as a scaffold protein to recruit histone deacetylases (HDAC) and other chromatin remodelling factors. NCOR2 can form a large co-repressor complex with many components including NCOR1, HDAC3, TBLX1, TBL1R, CORO2A and GPS2 (Li et al. 2000, Guenther et al. 2000, Zhang et al. 2002, Cheng and Kao 2009, Oberoi et al. 2011). It is a 1495 amino acid protein with a molecular mass of around 170kDA. It has a proline rich N-terminal domain and a C-terminus that is highly conserved with its paralog NCOR1 (Chen and Evans 1995).

NCOR2 can recruit various deacetylases, such as HDAC4, HDAC5, HDAC7, HDAC1 and SIRT1; but HDAC3 appears to be the main deacetylase used by both NCOR1 and NCOR2 (Perissi et al. 2010). HDAC3 is part of the core NCOR2 repression complex alongside GPS2, TBL1 and TBLR1 (Oberoi et al. 2011). Further to this chromatin repression, NCOR2 can also recruit SMRT/HDAC1-associated repressor protein (SHARP), a repressor protein that can bind RNA. Human SHARP is thought to be involved in NOTCH signalling (Mikami et al. 2013).

NCOR2 and its homologue NCOR1 are highly conserved, around 40% identity at the amino-acid level, and share a similar overall structure with conserved functional domains (Ordentlich et al. 1999, Park et al. 1999). These functional domains are the repression domains, the SANT-like domains, and the nuclear receptor interaction domain (RID). The three repression domains are the most highly conserved, and are responsible for repressive activity (Li et al. 1997). The two SANT-like domains promote deacetylation. The first is part of the deacetylation activation domain (DAD), and is responsible for HDAC3 recruitment and activation (Guenther, Barak and Lazar 2001). The second is the histone interaction domain (HID), which binds histone tails and enhances repression (Yu et al. 2003).

5.1.3 NCOR2 physiological roles

Whilst homology between NCOR1 and NCOR2 is high, they appear to have non-redundant functions in mammals; deletion of either gene in mice is embryonic lethal. *Ncor2*$^{-/-}$ mice are lethal before 16.5 dpc due to heart defects. This role in heart growth is mediated by interaction with FOXP1 (Jepsen et al. 2008). NCOR2 has also been shown to be involved in forebrain development via its regulation of Retinoic acid receptor (RAR)-dependent differentiation of neural stem cells (Jepsen et al. 2007). Further, NCOR2 is crucial for development in non-mammalian organisms, with embryonic lethality even in organisms such as *X. laevis* and *D. rerio*. This suggests a role in early- as well as mid-embryogenesis (Koide et al. 2001, Xu et al. 2009, Mottis, Mouchiroud and Auwerx 2013).

Many different *Ncor2* mouse models, in addition to the KO, have been made, each exhibiting different phenotypes. Mouse models with mutations in RID1, or RID1 and RID2, have been shown to have various metabolic phenotypes, which ultimately lead to premature death postnatally (Nofsinger et al. 2008, Pei et al. 2011, Reilly et al. 2010). Another model, which contains a single amino acid mutation in the DAD domains of both NCOR1 and NCOR2 (NS-DADm), confirms the requirement of these two proteins for HDAC3 deacetylase function (You et al. 2013). In this model, histone acetylation in the liver is elevated to similar levels as seen in liver-specific HDAC3 KO models (Knutson et al. 2008).

However, lethality in the HDAC3 global KO is more severe than in the NS-DADm model, suggesting HDAC3 has other roles outside of deacetylation (Bhaskara et al. 2008).

5.1.4 Potential NCOR2 links to sex determination

A number of potential links exist between NCOR2 and genes or signalling pathways known to function in sex determination. Here, I offer some examples:

5.1.4.1 FGF signalling

As previously discussed, FGF9 is crucial for normal testis development (Colvin et al. 2001). In addition to this, FGF8 has been highlighted to be involved in the maintenance of primordial germ cell (PGC) proliferation upon colonisation of the gonad, between 10.0 and 13.0 dpc (Kawase, Hashimoto and Pedersen 2004). After 13.5 dpc, expression of *Stra8* causes germ cells in XX gonads to enter meiotic arrest (Menke, Koubova and Page 2003). Expression of *Stra8* is thus vital for one key aspect of ovarian development. *Stra8* expression in the developing XX gonad is induced by Retinoic Acid (RA), an active derivative of vitamin A (Koubova et al. 2006). As RA expression increases, FGF8 expression decreases; this correlation suggests that RA could act to repress FGF8 expression in the developing gonad. This relationship between RA and FGF8 would not be a novel one, and is seen during somitogenesis, where NCOR1/2 have been shown to redundantly mediate the ability of RA to repress FGF8 (Kumar, Cunningham and Duester 2016).

Regardless of its repression of FGF8, NCOR2's known interaction with RA (Kumar et al. 2016) could impact gonadogenesis in other ways. RA is known to induce *Stra8*, and this is considered to be achieved through epigenetic modifications. Unbound RARs can repress gene transcription by recruiting HDACs through co-repressors such as NCOR2, a process that is reversed in the presence of high levels of RA (Minucci and Ozato 1996, Wang and Tilly 2010). This might be a mechanism that explains how RA activates *Stra8* expression, by inducing a relaxed chromatin state free from HDACs and NCOR2. Further, as it is known that RA and NCOR2 can interact, RA might interact with NCOR2 competitively, thus preventing it from binding STRA8. This possibility could be highlighted by

examining gonadal *Stra8* expression in an *Ncor2*-null mutant and determining whether this is aberrant. However, any impact seen in the germ cells of an *Ncor2*-null gonad may be a secondary impact of a somatic cell phenotype, which must be kept in mind.

5.1.4.2 NOTCH/WNT signalling

NOTCH signalling is crucial for development. For example, in the developing heart, NOTCH and BMP2 are required for cardiac valve formation (Luna-Zurita et al. 2010). NOTCH signalling is also known to be controlled by NCOR2. CBF1 has been shown to bind NCOR2 and SKIP, allowing it to enter the nucleus and repress NOTCH (Zhou and Hayward 2001). If NCOR2 is non-functional, NOTCH may be unable to be repressed, resulting in constitutively active NOTCH signalling.

It is already known that loss of NOTCH signalling causes aberrant testis cord formation, as seen in *Hes1*$^{-/-}$ testes (Tang et al. 2008). Interestingly, the same study also showed that constitutively active NOTCH also causes aberrant testis cord formation, to a lesser degree. This suggests that an *Ncor2*$^{-/-}$ model might exhibit aberrant testis cord formation due to constitutively active NOTCH.

Another vital signalling pathway for gonadogenesis is WNT signalling. It is well documented that NOTCH and WNT interact on many levels (Ann et al. 2012, Jin et al. 2009, Hayward et al. 2005, Axelrod et al. 1996). Most recently it was shown that WNT5a can enhance NOTCH1 signalling via the down-regulation of SMRT (Ann et al. 2012). Thus, further to potential NCOR2 impacts on NOTCH signalling, it could impact on WNT signalling. As has previously been discussed, WNT signalling is vital to the ovarian development pathway. So, any impact on WNT signalling could result in ovarian defects. Both WNT and NOTCH signalling have known impacts on gonadal development. As NCOR2 has been suggested as a mediator between the two signalling pathways, it may have influence over both and thus has the potential to impact both testis and ovarian development.

5.1.4.3 Sry/Oct4

As previously discussed, HDAC3 is part of NCOR2's core repression complex (Oberoi et al. 2011). HDAC3 has been shown to be responsible for SRY deacetylation in HeLa cells (Thevenet et al. 2004). If this is also the case *in vivo,* then SRY could be deacetylated via an NCOR2 repression complex. NCOR2

LOF mutants might then have reduced SRY deacetylation, which could impact negatively on testis formation. Further to this, NCOR2 is known to deacetylate p300/CBP-associated factor (PCAF) (Gregoire et al. 2007). PCAF is structurally related to p300/CBP (CREB-binding protein), and has been shown to interact with p300/CBP (Yang et al. 1996). Interestingly, p300/CBP has been shown to be vital for SRY promotion and correct testis development (Gregoire et al. 2007, Carre et al. 2018). So, NCOR2 could theoretically impact negatively on SRY expression, and thus testis determination, in two ways. First via HDAC3, or secondly through PCAF/CREB-binding protein. However, these links are more theoretical to those previously discussed, as they are based on *in vitro* studies and have not been replicated *in vivo*.

In ovarian cells, *Oct4* expression is confined to the germline, and is expressed until germ cells enter meiosis (Pesce et al. 1998). This repression of *Oct4* at the start of oogenesis can be facilitated via germ cell nuclear factor (GCNF), which has been shown to recruit NCOR2 to repress *Oct4* (Fuhrmann et al. 2001). This might mean *Ncor2*$^{-/-}$ mutants are unable to repress *Oct4* and enter oogenesis.

All of these potential mechanisms discussed, concerning how NCOR2 might impact XY or XX gonadogenesis, alongside the patient data previously presented, highlighted NCOR2 as a strong candidate gene for involvement in human DSDs. Further proof of concept was shown by Mikolas *et al.* who found that mutants for an orthologue of NCOR2 have impaired gonadogenesis. Mutation of G*ei-8*, the *C. elegans* orthologue for *NCOR1/2*, caused fewer meiotic nuclei and germ cells in the gonads as well as no spermathecae (site of sperm storage and fertilisation), sperm or embryos (Mikolas et al. 2013). This study further emphasised *NCOR2* as an excellent candidate gene for a role in human gonadal dysgenesis.

5.2 Results

5.2.1 *Ncor2* expression in the mouse embryonic gonad

Previous microarray data (Jameson et al. 2012b) show *Ncor2* is expressed in the developing mouse gonad between 11.5-13.5 dpc. Expression is greatest within the supporting cell lineage, but is also present within the interstitial, stromal, endothelial and germ cell lineages. There is sexually dimorphic expression in the supporting lineage, with higher expression in XY cells from 12.5 dpc onwards (see (Fig 5.1A). Single-cell RNAseq (Stevant et al. 2019) data shows *Ncor2* is expressed in both Sertoli and granulosa cells (Fig 5.1B), suggesting that it could be involved in both testis and ovary development. To confirm this expression profile, wholemount *in situ* hybridisation (WMISH) studies were performed on wildtype B6J urogenital ridges (UGRs) at 11.5 dpc and 14.5 dpc. In 11.5 dpc gonads, staining was observed within gonads in both XX and XY samples, with stronger signal levels present in XY gonads in particular (Fig 5.1C). In 14.5 dpc samples, staining was less prominent than in 11.5 dpc samples, but still present in a sexually dimorphic fashion, with no staining in XX gonads and lesser staining in XY gonads (Fig 5.1D). These WMISH data confirm the sexually dimorphic expression pattern seen in the microarray dataset, with higher expression levels seen in XY gonads at both 11.5 dpc and 14.5 dpc. The WMISH data also reveal higher expression levels of *Ncor2* within the gonad at earlier time points, which could suggest a role in the early stages of sex determination.

5.2.2 Generating *Ncor2*-null embryos

As mentioned earlier, there is a range of patient phenotypes that highlight *NCOR2* as a potential candidate gene for sex determination in XY and XX individuals. It was decided to use a null allele to model the human mutations. Mice harbouring a floxed allele of *Ncor2* were imported on a 129 background (Shimizu et al. 2015) (see details in Fig. 5.2). This line had previously been used to study the impact of *Ncor2* deletion both in liver-only and global post-natal models. This specific line had not been used to study *Ncor2* deletion within development, but loss of *Ncor2* was already known to be lethal at 16.5 dpc in other models (Jepsen et al. 2008). Embryonic lethality was confirmed in this

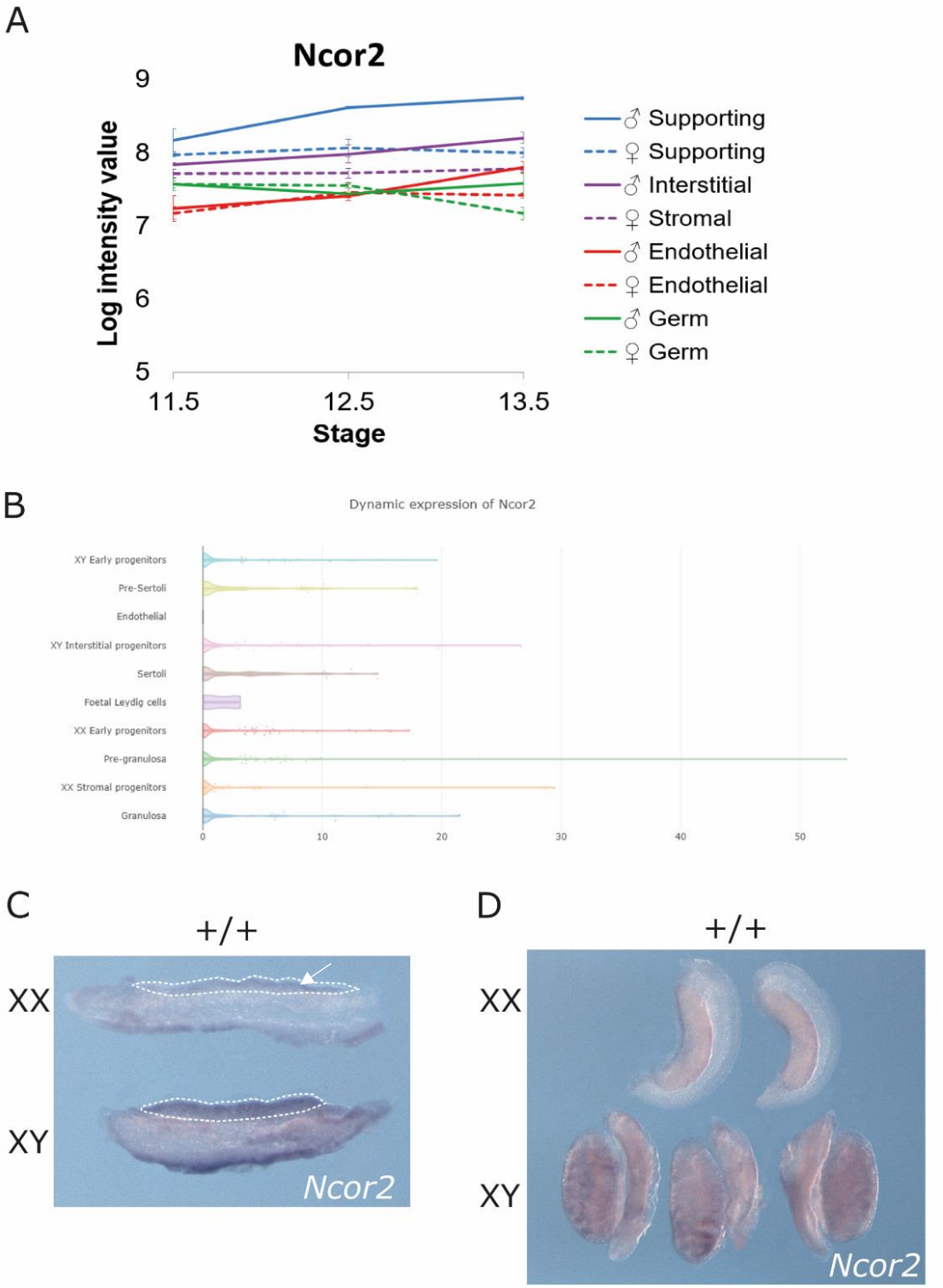

Figure 5.1 Expression of *Ncor2* in the developing gonad.

Microarray studies (Jameson et al. 2012) show expression of *Ncor2* in the supporting cell lineage (blue), interstitial/stromal cell lineage (purple), endothelial cell lineage (red) and germ cell lineage (green) between 11.5-13.5 dpc in XX and XY gonads **(A)**. Single-cell RNA sequencing data (Stévant et al. 2019), a violin plot highlighting *Ncor2* expression intensity within the various cell clusters of the developing gonad. Highlighting the range of cells expressing *Ncor2*, and suggesting a potential early role due to the large number of progenitor clusters present **(B)**. WMISH study shows expression of *Ncor2* in 11.5 dpc **(C)** and 14.5 dpc **(D)** XX (top) and XY (bottom) gonads. Dotted line marks the outline of the gonad. Arrow shows XX 11.5 dpc stain in coelomic epithelium **(C)**.

model at 16.5 dpc also (data not shown). Imported male mice (129) harbouring the floxed allele were sacrificed and sperm was collected for IVF with oocytes from B6J wildtype females, in the presence of soluble Cre recombinase (Kim, Kim and Lee 2009). Heterozygous founder males were then mated with B6J females to produce a colony of *Ncor2*$^{+/-}$ mice. The floxed allele possesses loxp sites on either side of exon 11. Therefore, when derived using IVF with soluble Cre, a deletion allele is generated that lacks exon 11. This is predicted to result in a truncated form of the protein being produced, due to the presence of an early stop codon following splicing of exon 10 onto exon 12, consisting of 383 aa instead of 2,473 aa. This truncated protein is also targeted for degradation (Fig. 5.2) (Shimizu et al. 2015). Intercross timed-matings were then set up between *Ncor2* $^{+/-}$ mice to produce null embryos; these were present in the expected Mendelian ratios at 14.5 dpc, with lethality not observed until 16.5 dpc (data not shown).

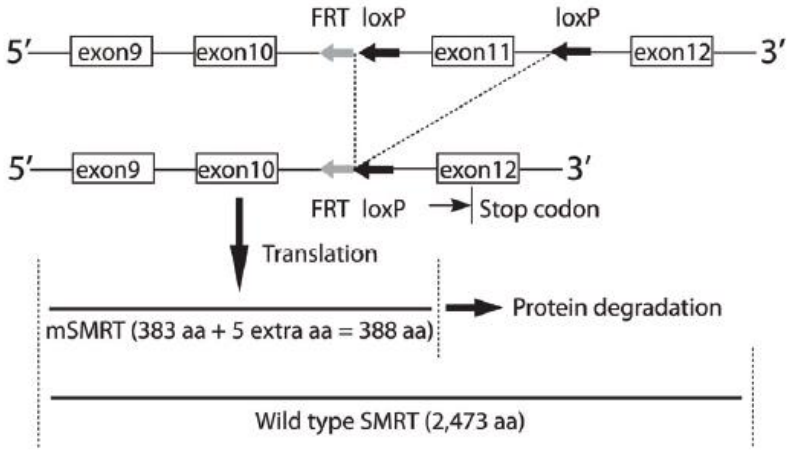

Figure 5.2 Generating *Ncor2*-null mice.
Mice harbouring the floxed allele were imported (Shimizu et al. 2015) (top). A new line was established with the use of soluble Cre during IVF derivation, resulting in the loss of exon 11 (bottom). *SMRT* is another name for *NCOR2.*

5.2.3 Expression of sex determining genes in *Ncor2*$^{-/-}$ embryonic gonads

WMISH studies were performed on 14.5 dpc *Ncor2*$^{+/-}$ and *Ncor2*$^{-/-}$ (also called *Ncor2*-null) gonads using the known sex-specific markers, *Sox9* and *Stra8*. As previously discussed, *Sox9* is a marker of pre-Sertoli and Sertoli cell differentiation during testis determination and *Stra8* is a marker of germ cell meiotic entry in ovaries at this time point. This initial WMISH study, on a mixed B6J and 129 background, found *Stra8* expression to be greatly reduced in the XX *Ncor2*-null gonads (Fig. 5.3A), with even some heterozygous gonads showing a slight reduction in *Stra8* as well. Further to this, XX null gonads also appeared to have an aberrant shape when compared to wildtype gonads, as they were less crescent shaped and more straight. These XX phenotypes suggested a disruption to ovarian determination in the null gonads, which is interesting given the patient data discussed earlier. Further to this, XX null gonads appeared to be expressing low levels of *Sox9* along the mesonephric edge of the gonad (see arrow Fig 5.2B).

XY *Ncor2*-null gonads showed no expression of *Stra8*, and were therefore comparable with their wildtype counterparts (Fig 5.3A). However, in the initial *Sox9* WMISH study, XY null gonads appeared to show a very slight testis cord phenotype (see star Fig. 5.3B), as their testis cords were less uniformly structured when compared to wildtype. This suggested a potential XY phenotype that would need to be studied further. It was decided to cross this line to B6J.Y^{AKR}, a mouse line highly sensitised to disruptions to testis determination, to enable a closer examination of *Ncor2*'s potential XY role (see later work).

Since there was a clear XX gonadal phenotype and a potential XY phenotype revealed by this initial WMISH study, it was decided to continue work on this line. Therefore, the colony size was increased to allow for further study by crossing *Ncor2*$^{+/-}$ males to B6J females. This enabled a quick increase in colony size without depleting *Ncor2*$^{+/-}$ females, which were needed for timed-matings. However, this also results in a less genetically diverse line than initially studied, with a higher contribution from B6J. Once a larger colony was established, the WMISH experiment was repeated to confirm the phenotype. The second WMISH study did not reveal a significant *Stra8*-related phenotype, with

Ncor2-null XX gonads only showing a slight loss of *Stra8* when compared with wildtype (Fig 5.3C). Further, these gonads did not have the aberrant shape seen in the initial study (Fig 5.3A), nor did they have *Sox9* expression along their mesonephric edge. All of this suggested that the increase of the B6J genome in this second cohort of animals might be affecting the XX phenotype originally observed and it was decided to outcross this line onto the 129 strain (the line it was imported in on), by breeding B6J *Ncor2*$^{+/-}$ males with 129 females, in an attempt to rescue the XX phenotype (see later work).

Further to this loss of the XX phenotype, the second WMISH study of *Ncor2*-null gonads found an additional XY phenotype. The XY null gonads had poor testis cord morphology and a 'twisted' shape when compared to the wildtype gonads; they also appeared to have a slight developmental delay as they were narrower and smaller in size (Fig 5.3D). These observations built on the very subtle phenotype seen in the initial WMISH study and suggested a potential role for *Ncor2* in mouse XY gonad development that might be relevant to the XY patient data.

These WMISH studies resulted in the generation and maintenance of three different *Ncor2* colonies: B6J-*Ncor2*$^{+/-}$, B6J.Y.AKR- *Ncor2*$^{+/-}$ and 129- *Ncor2*$^{+/-}$. It was decided that all three lines would be studied to allow insight into how *Ncor2* might be influencing both ovarian and testis development, with both B6J lines being used to study testis determination and the 129 line being used to study ovary development.

5.2.4 Expression of sex determining genes in B6J.Y^{AKR} *Ncor2* $^{-/-}$ embryonic gonads

WMISH studies were carried out on 14.5 dpc *Ncor2*$^{-/-}$ gonads using the known sex-specific markers *Sox9* and *Stra8*, as before. The B6J.Y^{AKR} line possesses the Y chromosome from the *Mus domesticus* AKR mouse strain, with the rest of its genome being derived from the B6J strain; this combination makes this strain extremely sensitised to disruptions to testis development, with even wildtype B6J Y.AKR gonads showing a transient sex reversal (ovotestis) phenotype at 14.5 dpc (Fig. 5.4A).

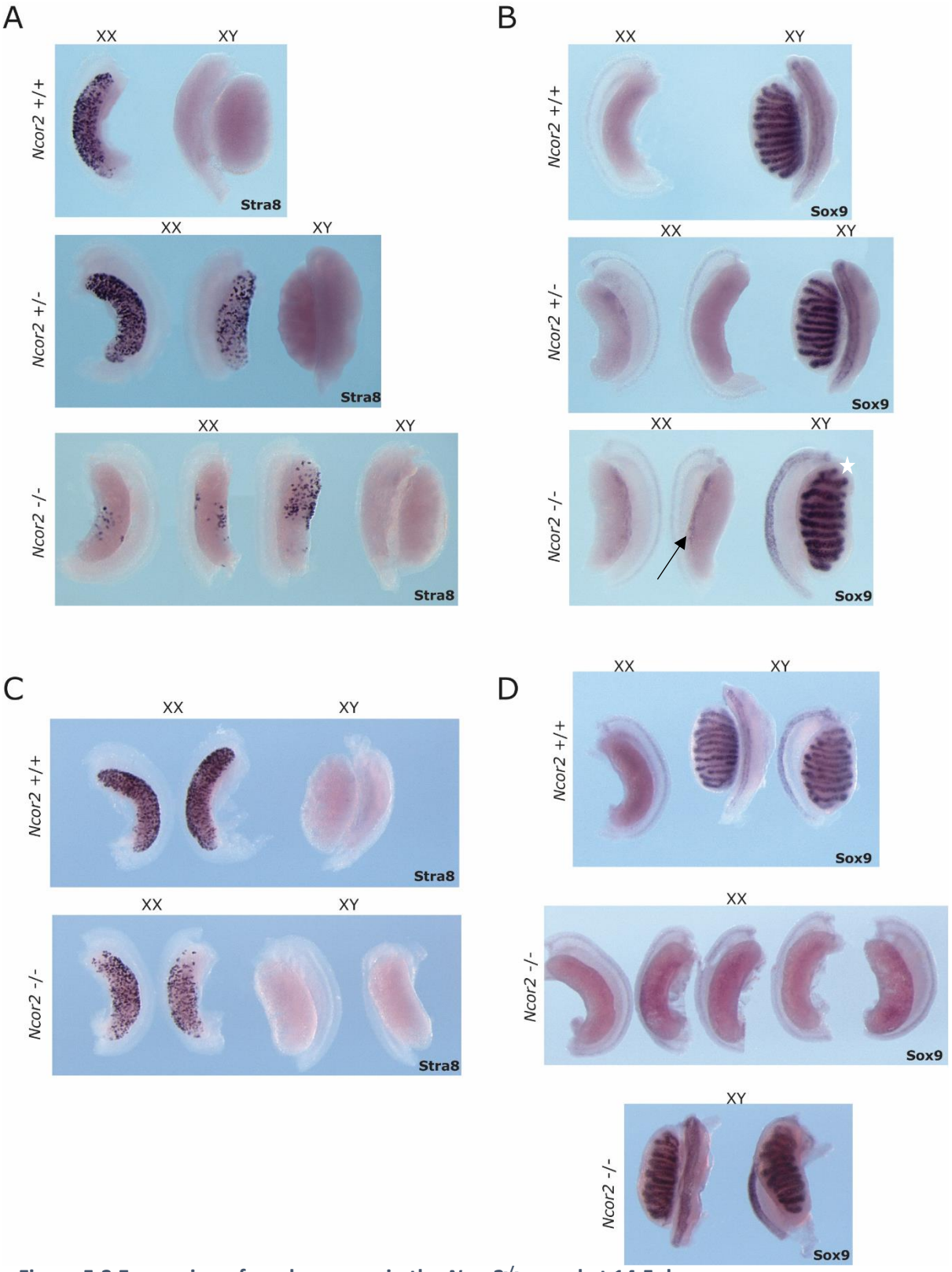

Figure 5.3 Expression of marker genes in the *Ncor2*$^{-/-}$ gonad at 14.5 dpc.
Stra8 expression marks ovarian meiotic germ cells **(A,C)** and *Sox9* marks testicular Sertoli cells **(B,D).** Two rounds of WMISH were performed. **(A,B)** was the initial study done on a mixed 129 and B6J background; **(C,D)** was performed on a more B6J background. Arrow shows *Sox9* expression along the mesonephric edge of XX gonads. Star shows a region of testicular disorganisation, suggestive of a slight testis phenotype.

The *Stra8* WMISH study found that XY *Ncor2*$^{-/-}$ gonads did not express significantly more *Stra8* than the wildtype controls: *Stra8*-positive germ cells were mainly detected at the poles of the gonad in both genotypes, indicating ovotestis development. However, the XX null gonads exhibited reduced numbers of *Stra8*-positive cells compared to the wildtype XX gonads (Fig 5.4A).

The *Sox9* WMISH study showed that some XY *Ncor2*$^{-/-}$ gonads had more severe disruptions to testis determination when compared to the wildtype controls. Whilst the controls lacked *Sox9* expression at the poles of the gonad, as expected for an ovotestis, they still had clearly organised testis cords and a round testis shape. The null gonads, by contrast, were lacking *Sox9* expression (and thus testis cords) in a much larger region than the controls. They also had very disorganised testis cords and an aberrant testis shape that was twisted and crescent-like (Fig 5.4B).

This phenotype was then confirmed using 14.5 dpc gonadal sections and examination using immunofluorescence (IF). XY *Ncor2*-null gonads were studied using antibodies to SOX9 and DDX4, in order to detect the presence of Sertoli cells and germ cells, respectively. DDX4 is expressed in all germ cells from the colonisation of the gonad until the post-meiotic stage (Toyooka et al. 2000). The SOX9 IF study found that the *Ncor2*-null gonads have significantly reduced SOX9 expression compared to the wildtype control; again, SOX9-positive cells was more disorganised, reflecting the impacts on testis cord morphology of loss of NCOR2 in this genetic background. In the wildtype samples, SOX9 is expressed along the edge of the testis cords in a uniform way; however, the null gonads showed a range of expression levels: the null gonad with the most SOX9 had the most uniform testis cord formation, whilst the gonad with the least SOX9 showed little to no cord formation (Fig 5.4C). All the null gonads were also smaller in size than controls and did not have the classic round testis shape that the wildtype gonad possessed, all of which further confirmed the results seen in the WMISH study.

The DDX4 IF study also showed that the null gonads exhibit a range of phenotypes; however, the germ cell phenotype is more pronounced. The null gonad that was the most similar to the wildtype

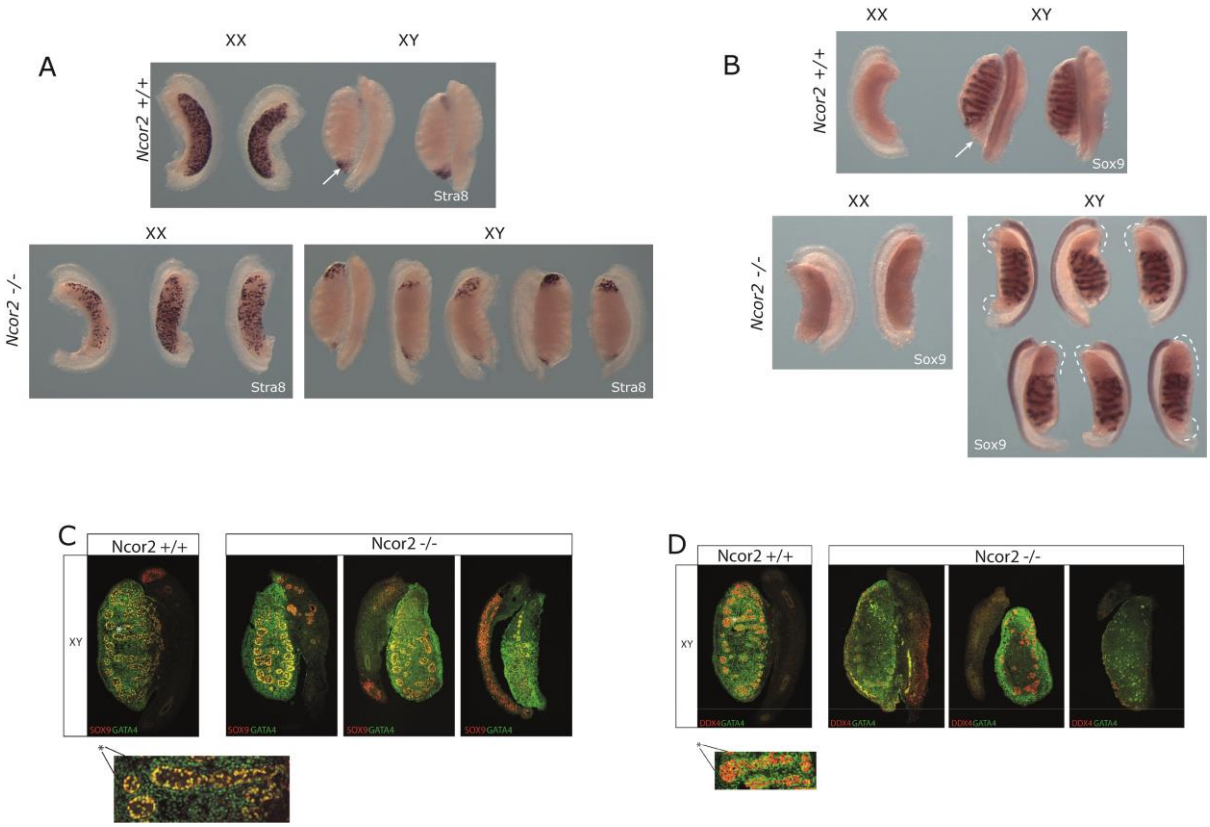

Figure 5.4 Expression of marker genes in *Ncor2*$^{-/-}$ gonads on a B6J.Y^{AKR} background.
WMISH study using *Stra8* as a marker of ovarian germ cells **(A)**, and *Sox9* as a marker of Sertoli cells **(B)**. Arrows highlight the ovarian portion of the B6J.Y^{AKR} wildtype ovotestis **(A,B)**. White dashed line highlights the large *Sox9* lacking region in *Ncor2*$^{-/-}$ testis **(B)**. Immunofluorescence study on 14.5 dpc gonadal wax sections using SOX9 (red) and GATA4 (green) to mark Sertoli cells/somatic cells **(C)**, and DDX4 (red) and GATA44 (green) to depict germ cells/somatic cells, respectively **(D).** Asterisk shows an in-depth view of somatic and germ cell clustering **(C,D)**. Sertoli cells stain with both SOX9 and GATA4 (yellow) and arrange themselves around the edge of the testis cords, with a black space where the germ cells are situated **(C)**. DDX4 marks germ cells (red) within the testis cords, which are surrounded by somatic cells (green) **(D)**. *Ncor2*$^{-/-}$ n=3 **(C,D)**

control, and had shown the strongest SOX9 expression previously, showed an almost complete lack of DDX4 expression. In the wildtype control, DDX4 is expressed inside the testis cords, as it marks the germ cells. None of the *Ncor2*-null gonads showed proper DDX4 staining in the testis cords, with any DDX4 staining present being completely disorganised and mislocalised (Fig 5.4D). When taken together, the data presented in Figure 5.4 suggest an inability of *Ncor2*$^{-/-}$ gonads on the B6J Y.AKR genetic background to undergo proper testis development, with both a somatic and germ cell phenotype observable.

5.2.5 Expression of sex determining genes in *Ncor2*$^{-/-}$ 14.5 dpc gonads in other genetic backgrounds: C57BL/6J and 129X1/SvJ

WMISH studies were performed on the *Ncor2*-null line following further backcrossing to B6J and 129 to study the effect of *Ncor2* deletion on testis and ovarian development, respectively. *Stra8* and *Sox9* probes were used as sex-specific markers, as before. The B6J line, which is sensitive to disruptions of testis development, showed impaired testis development (Fig. 5.5A). In particular, the testes in the null were smaller and had improper cord development. However, the phenotype was not as strong as that shown earlier in the null B6J.Y^{AKR} gonads. This is to be expected since B6J.Y^{AKR} is the most sensitised strain available for the study of testis determination. Ovarian determination was also slightly impacted in the B6J XX gonads, with slightly less *Stra8* expression when compared to the wildtype controls (Fig 5.5A); however, this phenotype was minimal.

In contrast, the 129 line showed a massive loss of *Stra8* expression in the XX null gonads when compared to wildtype controls (Fig. 5.5B). This suggests that the XX null gonadal germ cells are unable to enter meiosis, or there are fewer XX gonadal germ cells present. Further, the XY null 129 gonads also showed aberrant development. The null testes were smaller than their wildtype counterparts, with fewer but larger testis cords that were improperly organised throughout the gonad.

5.2.6 *Sox9* expression in *Ncor2* $^{-/-}$ 11.5 dpc gonads in different genetic backgrounds

Ncor2-null gonads at 11.5 dpc were harvested from the B6J, 129 and B6J.Y^{AKR} lines for WMISH study with a *Sox9* probe. Previous WMISH and IF study at 14.5 dpc had shown abnormal *Sox9* expression and distribution, and this study aimed to confirm if these changes were present at the sex-determining stage of 11.5 dpc.

None of the lines showed *Sox9* expression in XX null gonads, with all XX null gonads matching that of their wildtype counterpart. However, all lines showed aberrant *Sox9* expression in the XY null gonads. In the B6J line, there was a reduction in *Sox9* expression compared to wildtype. There was still some expression of *Sox9* and the change was only minimal. This aligns with the phenotypic changes seen

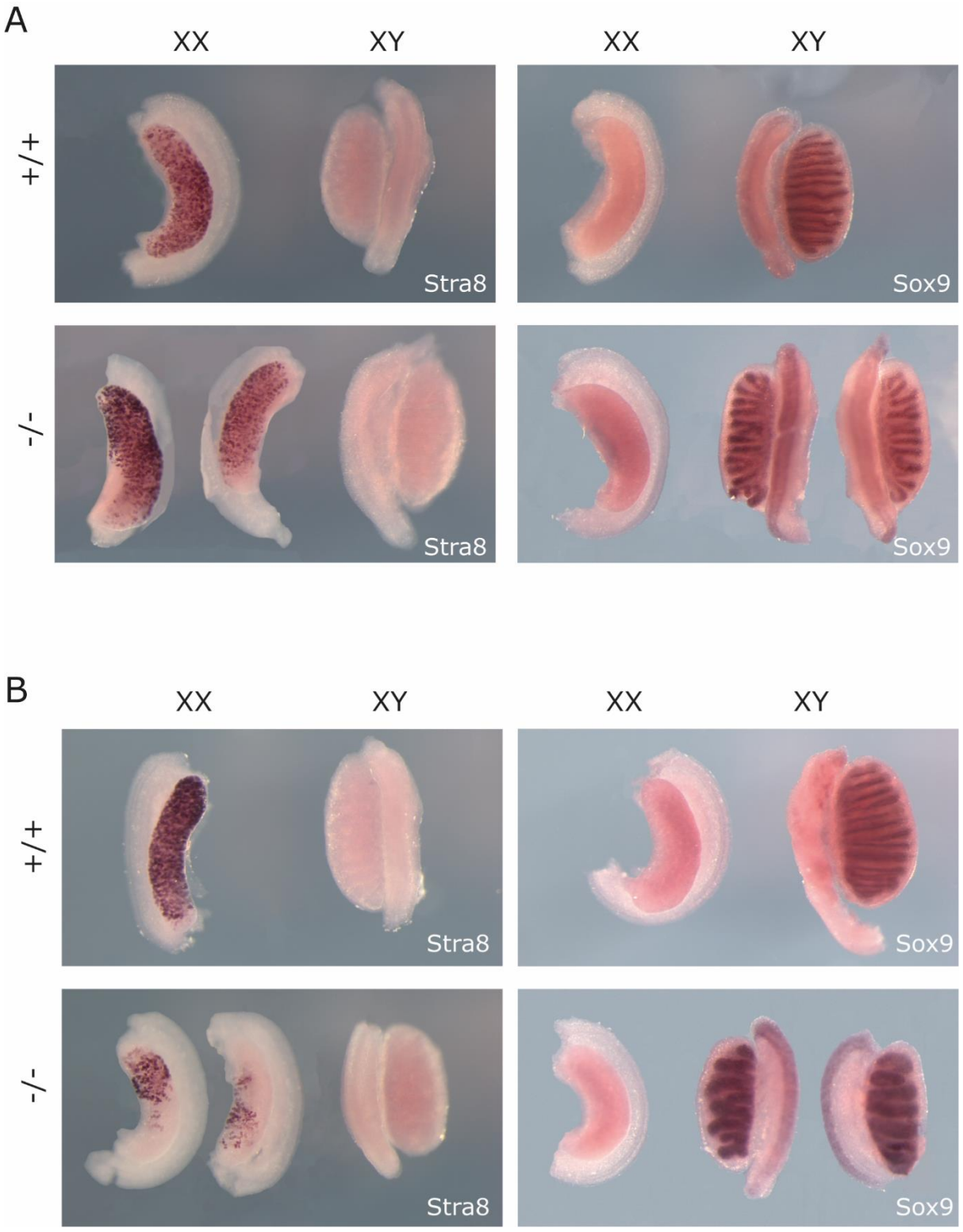

Figure 5.5 Expression of sex determining markers in *Ncor2*$^{-/-}$ gonads on further congenic strains. WMISH study of *Stra8* (left) and *Sox9* (right) as markers of ovarian and testicular development, respectively, in further backcrossed lines of B6J **(A)** and 129 **(B)**.

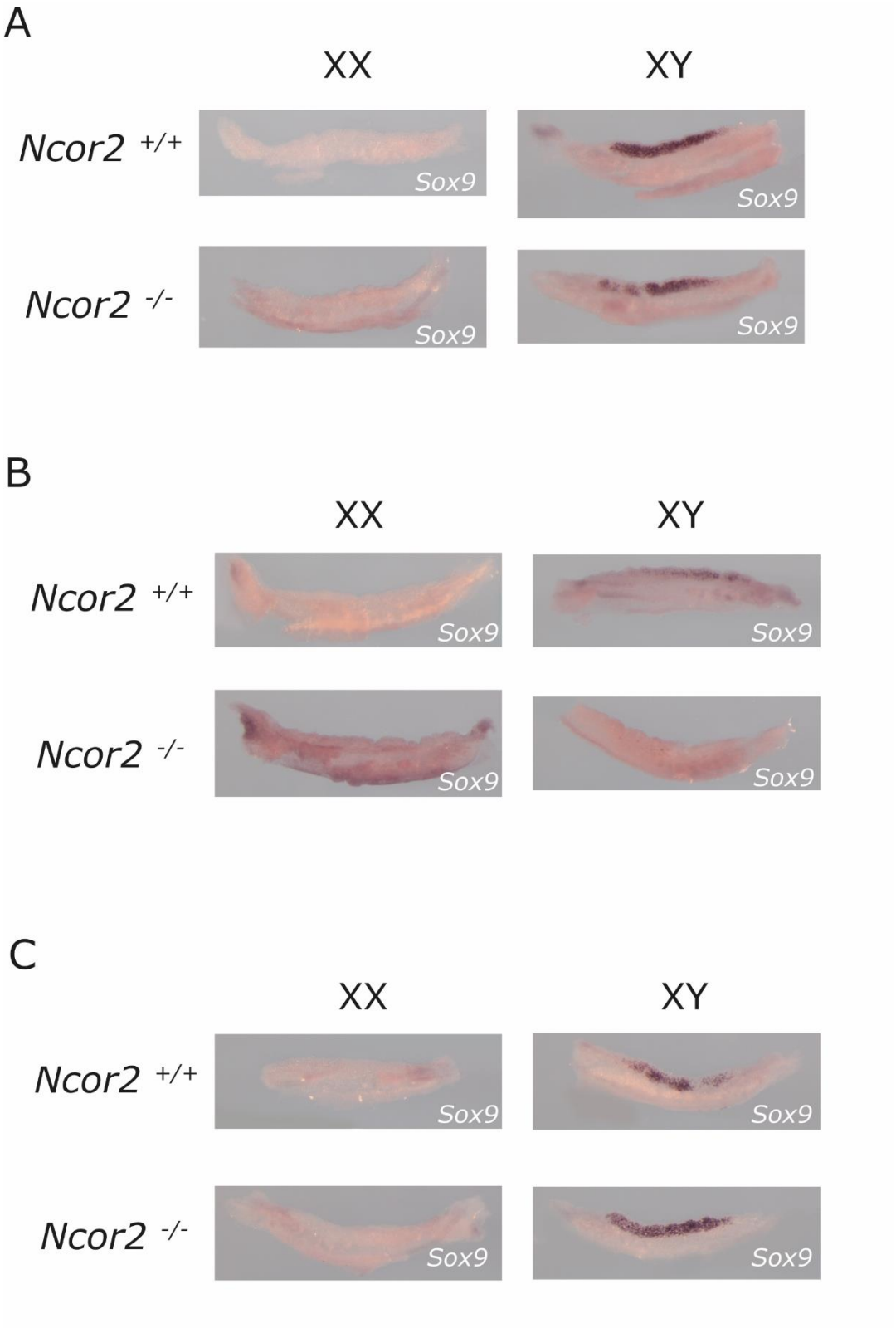

Figure 5.6 Expression of *Sox9* in *Ncor2* $^{-/-}$ 11.5 dpc gonads following further backcrossing.
WMISH study of *Sox9* as a marker of testicular development in further inbred lines of B6J **(A)**, B6J.Y^{AKR} **(B)**, and 129 **(C)**. Wildtype (top) 18 ts gonads are compared to *Ncor2*-null (bottom) 18 ts gonads, in both XX (left) and XY (right). n=4; representative samples shown.

in this line at 14.5 dpc. In the B6J.Y^{AKR} line, the change was more striking. This line is already highly sensitised to disruptions to testis determination. As such, expression of *Sox9* in B6J.Y^{AKR} is much reduced when compared to a B6J XY gonad at the same stage. The *Ncor2*-null XY B6J.Y^{AKR} gonads had almost no detectable expression of *Sox9*, with only a few dots of signal seen throughout the entire gonad. This lack of *Sox9* expression aligns with the 14.5 dpc phenotype for this line, which is much more feminised.

Finally, in contrast to the B6J and B6J.Y^{AKR} lines, the 129 line exhibited an increase in *Sox9* expression when compared to the wildtype. At 18 ts, the 129 wildtype XY gonad does not yet have complete *Sox9* expression throughout the gonad. However, the *Ncor2*-null gonad has *Sox9* expression across the length of the entire gonad and the expression is also more pronounced than that seen in the wildtype. This phenotype was consistent across all XY null gonads within the assay (data not shown). This suggests that the 129 *Ncor2*-null gonad may be more primed towards testis determination than the wildtype.

5.3 Discussion

5.3.1 Expression of *Ncor2* in the developing gonad

This chapter has described experiments aimed at determining whether there is a role for *Ncor2* in mouse gonad development. *NCOR2* had previously been highlighted as a candidate human sex-determining gene because of sequence variants identified by exome sequencing of patients with 46,XX and 46,XY gonadal dysgenesis of unknown cause. Further to this, it had also been shown to be expressed in somatic cells of the developing mouse gonad in previous microarray studies (Jameson et al. 2012b). This study had suggested that, in the supporting cell lineage, expression of *Ncor2* was sexually dimorphic, with higher expression in the XY embryonic gonad. My WMISH study reported in this chapter, whilst only semi-quantitative in nature, confirmed this expression profile. I showed that at 11.5 dpc, *Ncor2* was expressed in both XX and XY gonads, with higher expression in XY. In the XY gonad at 11.5 dpc, *Ncor2* was clearly expressed throughout the gonad, with expression in XX being

limited to the coelomic epithelium. The coelomic epithelium provides supporting cell precursors to the gonad proper, and is therefore an important site of expression (Karl and Capel 1998). The presence of *Ncor2* in the gonad at this stage suggests that it could play a role in sex determination, as we know that 11.5 dpc is a critical time for sex determination in the developing mouse gonad. Furthermore, the sexually dimorphic expression pattern could suggest that it is playing a different role within each sex. This final point is of particular interest due to the patient data (Table 5.1), which shows *NCOR2* variants associated with both XX and XY DSD. This suggests that *Ncor2* could play vital and varied roles in both testicular and ovarian development.

The microarray data previously discussed suggested that *Ncor2* expression increased in XY gonads from 11.5 dpc to 13.5 dpc, whilst expression in XX gonads remained virtually unchanged, making the sexual dimorphism even greater at 13.5 dpc than at 11.5 dpc. My WMISH study did show that the XY 14.5 dpc gonads clearly have more staining than the XX gonads at the same age. However, the staining was relatively weak, suggesting that expression is possibly reduced after 13.5 dpc in both sexes. The strong staining seen at 11.5 dpc, when compared to the later stage of 14.5 dpc, suggests that *Ncor2*'s role in the developing gonad could be an early one. As previously discussed, 11.5 dpc is a crucial time for somatic cell sex determination within the gonad. The expression of *Ncor2* in the coelomic epithelial cells of both XX and XY 11.5 dpc embryonic gonads, with expression limited to only this region in XX, could suggest a role in the provision of supporting cell precursors, as the these are generated in the coelomic epithelium before migrating to the gonad proper (Karl and Capel 1998). All of this suggests *Ncor2* could be influencing the supporting cell lineage, and as such, sex determination. However, its role may not be limited to influence of the somatic cells, and there could be potential for a germ cell phenotype also.

5.3.2 Aberrant expression of sex determining genes in *Ncor2*$^{-/-}$ gonads on a mixed genetic background

When we received the *Ncor2* line it was on a 129 background, although the precise contribution of this was unknown. As with all stock we receive, we crossed it onto a B6J background. B6J is our

standard stock for gonadal studies as it is sensitised to disruptions to testis development, making it easier to discover XY gonadal phenotypes than using other mouse inbred lines. The initial WMISH study was performed using embryos from an early cross, meaning the genetic background of these embryos was still fairly mixed, between 129 and B6J. The WMISH study at 14.5 dpc showed that XX null gonads had a clear loss of *Stra8* expression, a known marker of ovarian germ cell development. The XX null gonads were also more bulbous in shape, lacking the crescent ovary shape expected in XX gonads at this stage. Further to this phenotype in the null, some of the *Ncor2*$^{+/-}$ gonads were even lacking a normal *Stra8* expression profile. This suggested that deletion of *Ncor2* was impacting on ovarian development, and preventing XX gonads from developing germ cells correctly and/or preventing them from undergoing correct ovarian germ cell sex determination.

Further to the *Stra8* WMISH study, *Sox9* expression was also investigated in this mixed background line. It was discovered that XY null gonads had abnormal testis cord formation, although this phenotype was rather minimal when compared to the stark contrast seen in *Stra8* expression in XX gonads. To study this minimal XY phenotype further, I crossed this line further on B6J and also on B6J.Y^{AKR}. These two lines are sensitised to testis determination disruptions, making them more suitable for studying a subtle phenotype such as this. However, the most interesting phenotype observed in this initial *Sox9* WMISH study was in the XX null gonads. As I have previously discussed, these gonads were not undergoing correct ovarian development, as seen in the S*tra8* study. In this *Sox9* WMISH study, they also had the bulbous and non-crescent like shape seen in the *Stra8* study, but further to this they also appeared to be expressing *Sox9*. There was low-level *Sox9* staining on the mesonephric side of the XX *Ncor2*$^{-/-}$ gonad. Further, there was even a small amount of *Sox9* staining in one of the *Ncor2*$^{+/-}$ gonads, although this was very low. This WMISH suggested that the XX gonads might be expressing testis-determining genes, in addition to lacking expression of pro-ovarian genes. These data could indicate that the XX gonads were exhibiting a degree of masculinisation, as was observed in some of the patients. This WMISH also hinted at the potential impact *Ncor2* deletion may have on testis cord formation, although this was only small compared to the impact on ovarian

development. This would suggest that *Ncor2* might play separate roles in both ovarian and testis determination. This point would also align with the patient data, in which both XX and XY individuals with *NCOR2* mutations exhibit gonadal dysgenesis.

5.3.3 Impacted testis development on a more B6J background

This second WMISH was performed on a more B6J background. This *Sox9* repeat on a more B6J background showed a more significant phenotype in XY null gonads. In the initial WMISH, only a slight deformation was seen in the testis cords of the XY null; but in the repeat, the XY null gonads had much greater testis cord deformation, in addition to a twisted, almost crescent-like shape. This suggested that crossing further onto B6J was increasing the severity of any XY phenotype. The increase in the XY phenotype on a more congenic B6J background was expected, as we know this line is more sensitive to disruptions in testis determination. This confirmed *Ncor2*'s role in testis determination.

5.3.4 Loss of *Ncor2*-null ovarian phenotype when bred onto a more B6J background

The second WMISH study, with a greater contribution from B6J, was expected to confirm the results of the first study. However, it yielded a different result in regard to XX gonads. The phenotype seen in the first study, loss of *Stra8* expression in XX null gonads, was no longer observed. XX null gonads had slightly reduced *Stra8* expression when compared to their wildtype counterparts, but this phenotype was nowhere near as clear as in the first WMISH study. Further, the bulbous shape seen in the XX null gonads of the first WMISH study was not seen in the repeat. XX null gonads were more crescent-shaped, although not as perfectly crescent-shaped as wildtype XX gonads. This suggested that on a more B6J-derived background the ovarian phenotype was being lost. In the *Sox9* WMISH repeat, no expression was seen in XX null gonads, confirming the loss of phenotype.

5.3.5 Aberrant testis development in *Ncor2*$^{-/-}$ gonads on a B6J background

To further study the role of *Ncor2* in testis determination, WMISH studies were performed on 14.5 dpc and 11.5 dpc gonads on a further B6J congenic background backcross level (BC) 3. As expected,

the *Stra8* phenotype observed on the more mixed background was further lost, with XX null gonads displaying almost wildtype levels of *Stra8* expression. Furthermore, these XX null gonads were far more crescent shape than the XX null gonads on a mixed background, although not quite as crescent shaped as the wildtype gonads. This confirmed the loss of the ovarian phenotype on a B6J background.

The *Sox9* WMISH study showed that the development of testes was significantly impaired, confirming that the use of the B6J background was increasing the phenotype. The XY null gonads were much smaller than the wildtype gonads, with a more elongated ovarian-like shape. Further the testis cords in the XY null were unorganised compared to their wildtype counterparts. This confirmed that the loss of *Ncor2* in the developing gonad was impacting testis determination. Whilst testes were able to develop, they were malformed both in overall shape and cellular organisation.

To investigate this phenotype further, I performed a *Sox9* WMISH study at 11.5 dpc. This showed that XY null gonads were expressing less *Sox9* at 18 ts than their wildtype counterparts. This reduced expression of *Sox9* at such a critical time period in testis determination aligns with the improper testis development seen at 14.5 dpc and confirms the role of *Ncor2* in testis determination.

5.3.6 Aberrant testis development in *Ncor2*$^{-/-}$ gonads on a B6J.Y^{AKR} background

To investigate this role of *Ncor2* in testis determination further the null was studied on a B6J.Y^{AKR} background. This strain has the Y chromosome from the *Mus domesticus* mouse strain and the rest of the genome from the B6J mouse strain. This strain is extremely sensitised to disruptions in testis development, with even the wildtype XY gonads showing partial sex reversal. The backcross level (BC) onto the B6J background is 2, but the line has the added advantage of being extra sensitised to testis disruptions due to the presence of the 'weaker' Y.^{AKR} *Sry* allele. As such, it shows a stronger phenotype than the B6J line at BC 3.

WMISH studies were performed which showed the XY null gonads clearly unable to undergo testis determination. The *Sox9* WMISH study showed the testis cords produced in XY null gonads were

unorganised and did not stretch the length of the gonad, with cords only visible in the central part of the gonad. Further to this, the gonads were lacking the round shape seen in wildtypes, and were instead more crescent like and twisted. All of this confirmed the role of *Ncor2* in testis determination, as seen on the B6J background also.

The *Stra8* WMISH study once again showed a slight reduction in expression in XX null gonads, although not as much of a reduction as seen on a mixed background, confirming that the XX phenotype was being lost on a more B6J background.

The sex reversal seen in the *Sox9* WMISH study showed that testis determination was only occurring in the central part of the gonad. As such, we would expect to see *Stra8* expression in the large regions at the poles that aren't expressing *Sox9*. However, this was not the case, whist slightly more *Stra8* was expressed at the poles than in the wildtype XY gonads the difference was minimal.

To confirm the results seen in the 14.5 dpc WMISH study, that showed *Ncor2* loss to impact on testis determination, I also performed *Sox9* WMISH study at 11.5 dpc. *Sox9* expression at 11.5 dpc is critical to testis determination, and any delay or loss of expression can severely impact. My WMISH study showed a significant loss of *Sox9* expression in XY null gonads when compared to the wildtype. The levels of *Sox9* expression are already quite low in the B6J.Y^{AKR} wildtype wen compared to a B6J wildtype, as previously discussed the B6J.Y^{AKR} line has weak testis determination, and *Ncor2* knockout almost removed *Sox9* expression altogether. Only a few spots of *Sox9* expression were seen in the WMISH. This suggests that the XY phenotype is more severe at the 11.5 dpc time point and then recovers somewhat by 14.5 dpc, allowing the 14.5 dpc gonad to have a central portion of testis develop.

Further to the WMISH studies, IF studies were also performed on 14.5 dpc gonadal sections, using SOX9 and DDX4 antibodies. At 14.5 dpc, SOX9 is expressed in the somatic cells that line the testis cord structure. The IF study showed that XY null gonads still express SOX9 around the edge of the cords but are unable to properly form testis cords to varying degrees. The range of phenotypes seen

across the XY null samples was broad, with one completely unable to form any testis cords and with almost no SOX9 expression as a result. The results of the IF align with that of the WMISH, in highlighting the inability of XY null gonads to form correct testes. They also show that SOX9 is not being aberrantly expressed at this time point; rather, the structures aren't present for it to be expressed in. This further suggests the impacts that *Ncor2* knockout is having on testis determination are happening earlier in development.

IF studies were also performed using DDX4 antibody. DDX4 is a germ cell marker, and stains the germs cells which are located within the testis cords at 14.5 dpc. A lack of *Stra8* expression can sometimes be linked to a reduction in germ cells, as *Stra8* is expressed when cells are entering meiosis and this only occurs within the gem cell lineage. As we had seen a lack of *Stra8* expression at the tips of the XY null and within the XX null in the 14.5 dpc WMISH study I decided to investigate the presence of germ cells within the gonad at this stage as well. I found the germ cell phenotype to be stronger than that of the somatic cells. Even in the XY gonad that produced the best attempt at a testis, the level of germ cell was drastically reduced compared to wildtype. This suggests that loss of *Ncor2* affects both the somatic and germ cell lineages, which further corroborates the indication that *Ncor2*'s role in gonadal development is an early one.

Overall, the work performed in the B6J.Y^{AKR} alongside the B6J line confirmed *Ncor2*'s role in testis determination. However, the studies discussed are highly preliminary and more mechanistic studies are needed. Further, the phenotype described is quite subtle. Even homozygosing the null allele on B6J.Y^{AKR} doesn't produce a complete sex reversal phenotype, as is often expected. This may be rectified by breeding onto a congenic B6J background, or it could be that *Ncor2* has less of an impact on testis determination in mouse when compared to human. Even the nature of the human *NCOR2* mutations is unclear: are they all loss of function or might there be other allele types? Studies aimed at how *Ncor2* is interacting with the testis development pathway would be an initial next step, alongside breeding it onto a congenic B6J background.

5.3.7 Aberrant ovarian and testis development in *Ncor2*$^{-/-}$ gonads on a 129 background

To further study the role of *Ncor2* in ovarian development, a more congenic 129 line was used: BC 3. WMISH studies were performed on both 14.5 dpc and 11.5 dpc gonads, using both ovarian and testicular markers. The 14.5 dpc WMISH study showed that XX null gonads express far lower levels of *Stra8* than their wildtype counterparts, confirming the rescue of the ovarian phenotype on a 129 background. Further there was still a clear XY phenotype on this background also, although this phenotype was slightly different to the one seen on the B6J/ B6J.Y^{AKR} backgrounds. The XY null gonads expressed *Sox9* throughout the gonad but the testis cords appeared enlarged and the gonads slightly smaller in shape. Further to this 14.5 dpc phenotype, the 11.5 dpc WMISH study showed that XY null gonads on this background express more *Sox9* than their wildtype counterparts. In 129 wildtype gonads, *Sox9* is not yet spread throughout the entire gonad, and expression levels aren't particularly strong. However, in the XY null gonad, *Sox9* expression is present across the length of the gonad and is far stronger. This suggests that *Ncor2* knockout on this background is not only reducing *Stra8* expression in XX gonads but increasing S*ox9* expression in XY. Most likely this is due to the mutual antagonism discussed previously. *Ncor2* is either repressing the ovarian pathway and as such the testis pathway, and *Sox9,* are being overexpressed. Or it is overexpressing *Sox9,* and as such the ovarian pathway (and *Stra8*) are being repressed. From the studies performed thus far, I am unable to confirm which mechanism is at play. The work performed in the B6J and B6J.Y^{AKR} line confirm that loss of *Ncor2* can alter *Sox9* expression. However, in the case of those lines, it was a reduction in *Sox9* expression. If *Ncor2*'s only impact was on *Sox9* expression then it would be having opposite effects in the B6 and 129 lines. The alternative is that *Ncor2* is separately involved in both ovarian and testicular determination. These data are highly preliminary and further mechanistic work is required but it suggests, that alongside a congenic B6J line, the congenic 129 line should also be studied for the null allele in regards to testis development.

In regards to an XX phenotype, the data presented are even more preliminary, as only a germ cell marker has been examined. There appears to be a germ cell phenotype, but as no ovarian somatic

cell markers have been studied (due to a lack of time) it is unclear whether this is a consequence of disruption to somatic cell sex determination (i.e. the formation of granulosa cells) that has a knock-on effect on germ cell sex, or whether it is a direct effect on germ cell development. Further, in regards to the germ cell phenotype, studies are needed to confirm whether the *Stra8* phenotype is due to a failure of meiotic entry within germ cells or due to a reduction in germ cell numbers. The patient data suggested there would be a masculinisation phenotype, however, there was no strong *Sox9* expression or formation of a coelomic vessel seen in XX null gonads. However, these XX masculinisation phenotypes are very rare in murine studies. For example, loss of *Foxl2* during development leads to early XX sex reversal in goats but not in mice. However, LOF of *Foxl2* in an adult murine ovary does induce XX gonadal sex reversal (Pannetier et al. 2016, Uhlenhaut et al. 2009). Further to this, the masculinisation phenotype seen in *Rspo1* LOF murine XX embryos is not present until late in development (Maatouk et al. 2013). This suggests that studies later in gestation may be needed to discover any masculinisation phenotype, as is seen within XX patients.

6 Discussion

This thesis has described experiments aimed at improving our understanding of human disorders of sex development (DSD), especially 46,XY gonadal dysgenesis, using the mouse model to investigate the role of candidate genes identified by exome sequencing. The data presented covers the initial characterisation of three novel candidate genes, and their potential roles in gonadal development, and further characterisation of a now known testis-determining gene that was reported during the course of the research described in this thesis. Below, I will summarise what has been learned about these various candidates before moving on to discuss larger themes that have characterised my doctoral research.

6.1 *TLE3:* a candidate anti-WNT testis-determining gene

TLE3 was suggested as a candidate gene causing complete gonadal dysgenesis due to a familial case of two 46,XY sisters who were both homozygous for a rare variant (rs20050872) in *TLE3*. This variant causes a T498M substitution, predicted to be damaging. The frequency of this variant in the relevant population correlated with the XY DSD frequency, further suggesting that this was plausibly the causal mutation underlying the DSD. Further support for *TLE3*'s candidature as a testis-determining gene comes from its known links to WNT signalling. In particular, canonical WNT signalling has been shown to be crucial in ovarian development, with ectopic β-catenin expression capable of causing XY sex reversal (Maatouk et al. 2008). Studies have shown TLE3 is a known repressor of β-catenin activity, as it competitively binds with TCF4/LEF (Liu et al. 2018). TLE3's role as a repressor of WNT/ β-catenin activity further suggests it may play a role in testis determination. As we know, mutual antagonism of the two pathways is crucial for correct sex determination, and other testis-determining factors, like ZNRF3 and CBX2, also act by repressing WNT activity (Harris et al. 2018, Garcia-Moreno et al. 2019). Thus, it is plausible that loss of TLE3 function during XY gonad development might result in ectopic

canonical WNT signals that disrupt testis determination. All these factors, alongside the availability of a null allele, suggested *TLE3* was a candidate gene worth examining in a murine model.

WMISH studies found sexually dimorphic expression in 12.5-13.5 dpc gonads, with expression in XX gonads increasing after 11.5 dpc, and expression in XY gonads decreasing. Further WMISH study with *Tle3*$^{-/-}$ mice found no apparent abnormalities in XY gonads, indicating that *Tle3* is dispensable for mouse testis determination. Studies in XX *Tle3*$^{-/-}$ mice were inconclusive; a developmental delay and embryonic lethality phenotype made it difficult to harvest true 14.5 dpc ovary samples. The samples harvested were underdeveloped, which may have impacted the time-sensitive ovarian marker used for the study. As such, I was unable to confirm whether *Tle3* is involved in ovarian development using this mouse model.

The lack of a confirmed gonadal phenotype in mice does not allow us to infer that the *TLE3* variants are not the cause of the 46,XY CGD in the two sisters described above. It merely demonstrates that the use of a loss-of-function mouse model is not sufficient to cause embryonic gonadal sex reversal in mice. Whether this suggests that the human variants are not simple loss of function alleles, or whether it suggests a more fundamental difference in gonad development between mice and human, remains unclear: this is a common problem with interpreting such a negative outcome. Considerations were given to generating another model, but it was decided that further genetic manipulation was not warranted in the case of *Tle3*. This decision was made because the candidate gene arose from a single familial case that did not involve a novel mutation. Performing further genetic manipulation would have been lengthy, potentially with a low chance of success. As the candidate was not considered a strong one, it was decided not to pursue the TLE3 project any further. Decisions such as this are necessary when working with a mammalian model organism, due to their longer lifecycle and complex ethical considerations.

6.2 *Sec31a*: the problem of early lethality

SEC31A was a second candidate gene that was highlighted as responsible for a complex familial case of DSD and endocrine disorders. In contrast to *TLE3*, this family involved a *de novo* nonsense mutation of *SEC31A*, rather than a known variant. There are three affected children who all possess the mutation, Q929*, in a heterozygous state. Each child had a different phenotype: there was a 46,XY daughter with complete gonadal dysgenesis; a 46,XY son with partial gonadal dysgenesis and growth hormone deficiency, and finally, a 46,XX daughter with growth hormone deficiency and pituitary deficiency. All the children displayed other phenotypes, including mild cranio-facial abnormalities and marked dilation of the ER in their skin fibroblast cells.

These phenotypes had been determined to be consistent with loss of SEC31A function, as SEC31A is a part of the COPII complex and when other members of this complex are mutated similar phenotypes are seen. For example, mutation of *SEC23A* results in craniofacial defects and learning difficulties similar to those seen in these three siblings, in a condition known as Cranio-lenticulo-sutural dysplasia (CLSD). CLSD patients also have dilation of the ER in their skin fibroblast cells (Boyadjiev et al. 2006). Further, depletion of SEC13, a direct interacting partner of SEC31A, has been shown to cause craniofacial defects in zebrafish (Townley et al. 2008). All of these observations suggested that other phenotypes of the family in question could be caused by the mutation of *SEC31A* and highlighted it as a candidate testis determining gene. The role of my study was to confirm if the DSD phenotype could also be linked to the disruption to *SEC31A*. Unlike *Tle3*, there was no obvious connection between *SEC31A*/*Sec31a* and any known sex determining factors in either species. However, SEC31A's role within the cell is to enable transport of molecules to the cell membrane: anterograde transport. More specifically, it enables transport from the ER to the Golgi via vesicle budding. One molecule known to be transported in this way is WNT (Sun et al. 2017). This suggests a possible role for SEC31A in sex determination via the abnormal trafficking of WNT. The human *SEC31A* variant, producing a truncated protein in the patients, might in some way impact WNT signalling, causing disruption to sex

determination. The discovery of this potential connection between SEC31A and a signalling pathway that functions in sex determination supported its potential role in DSD and warranted pursuing it further by determining whether a loss of function *Sec31a* mouse model exhibited gonadal abnormalities.

I attempted to generate *Sec31a*$^{-/-}$ 14.5 dpc embryos for WMISH examination of the developing gonads. I found homozygous mutant embryos to be lethal between 3.5-6.5 dpc, around the time of implantation. This embryonic lethality associated with loss of *Sec31a* was confirmed in another study published whilst I was completing this work, which reported *Sec31a*-null *Drosophila* lethality at the larval/pupal stage (Halperin et al. 2018). To attempt to rescue the lethality phenotype, the mutant allele was bred onto a mixed genetic background, as congenic strains are often more susceptible to lethality due to reduced genetic diversity. However, even on a mixed background, these mutant embryos were not viable. To determine why the embryos were dying between 3.5-6.5 dpc, blastocysts were harvested and studied using immunofluorescence. This showed that even at 3.5 dpc, the embryos had a severe developmental delay and were unable to undergo correct lineage segregation. This suggests that a complete loss of *Sec31a* is not compatible with cellular function in the murine model, and embryos were only able to survive to 3.5 dpc due to the presence of maternal factors. In contrast to this conclusion, the study mentioned earlier (Halperin et al. 2018) reported two human patients homozygous for a null mutation, p.A927fs*61, who survived to 4 years of age. These patients had a multitude of phenotypes, including cranio-facial abnormalities, as in the heterozygous familial case previously discussed.

The murine model described here (Q929*) exhibited homozygous embryonic lethality, as did the *Drosophila* model in the above study. The question then arises: how do humans with disruptive *SEC31A* mutations survive until 4 years of age and beyond? One potential explanation are the differences in transcript complexity. Analysis of Ensembl shows the human locus encodes 41 transcripts with 28 of these known protein-coding transcripts; by contrast, the mouse locus encodes

only 12 transcripts with 7 known protein-coding. The human mutations were both located in exon 22, which is absent from 13 of the 28 protein-coding transcripts. In an attempt to model the effects of the human mutation in the mouse, the same region of sequence was removed via the deletion of exon 21, an exon that is required for 5 of 7 protein-coding transcripts. This difference in transcriptional complexity could explain the observed human viability when *SEC31A* is mutated. Another potential explanation is that SEC31A is not as important for human viability as it is for mouse and fly viability i.e. there is a fundamental difference in human biology in respect of SEC31A's role. These possibilities highlight some of the main limitations of model organism studies: they are merely a model and may not necessarily faithfully replicate the precise phenotype seen in humans.

Due to the early embryonic lethality of the *Sec31a* mutant homozygote, I attempted to study impact on gonadal development using the heterozygous model. I used two murine strains increasingly sensitised to disruptions to testis determination, B6J and B6J.Y^{AKR}, but neither showed any phenotype in the heterozygous state. The use of the heterozygote as a model makes any results inconclusive, as often the mouse requires homozygosed mutations for the production of a phenotype. Haploinsufficiency is more common in humans than in laboratory mouse strains, and previous DSD phenotypes associated with the heterozygous state are often not visible in mice until the mutant allele is homozygosed (Bouma et al. 2007). The only way to more definitively address whether *Sec31a* is required for testis determination will be to target deletion to the developing gonad using a Cre/loxP conditional targeting strategy.

6.3 *Ncor2*: a dual role in gonadal development

Ncor2 was the final novel candidate sex-determining gene examined in this thesis. It was also arguably the strongest candidate gene: at the time of the start of the study there were 11 DSD patients with *NCOR2* mutations, located across three different continents. More have been discovered since. All patients were heterozygous, and each possessed a different specific mutation to the others. Patient phenotypes were variable, and there were both XX and XY patients, suggesting a dual role for *Ncor2*

in gonadal development. The unrelated large patient cohort suggested *NCOR2* was a very strong candidate gene. This candidature was further supported by various literature studies, showing that NCOR2 has multiple connections to various known sex-related factors. Two of these include links to *Sry* and *Oct4*, both vital in testis and germ cell development, respectively. NCOR2 is a transcription coregulatory protein, acting as a scaffold to allow for recruitment of HDACs and chromatin remodelling factors (Li et al. 2000). It can recruit various deacetylases, but HDAC3 has been shown to be the main deacetylase used by NCOR2 (Perissi et al. 2010). *In vitro* studies have previously shown HDAC3 to be responsible for SRY deacetylation (Thevenet et al. 2004). If this translates to *in vivo* functionality, NCOR2 might be required for correct expression of *Sry* and its downstream targets within testis determination. Further to this testicular role, the literature study showed NCOR2 was needed for germ cell nuclear factor (GCNF) to repress *Oct4*. Repression of *Oct4* is required to allow XX germ cells to enter meiosis, and undergo correct ovarian development. In conclusion, the literature study found multiple links to known sex-determining factors and supported the strong patient data in suggesting *NCOR2* as a very strong candidate gene for human gonadal dysgenesis.

An initial WMISH study on a mixed genetic background found both an ovarian and testicular phenotype, although both were minimal. Following this, it was decided to breed the allele on three separate mouse genetic backgrounds to allow for separate studies of testis and ovarian phenotypes. Studies on B6J and B6J.Y^{AKR} determined that *Ncor2* was necessary for correct testis development, and that loss of *Ncor2* reduced expression of *Sox9* at the critical 18 ts (11.5 dpc) time-point. Studies on 129 highlighted an ovarian phenotype, with an overexpression of *Sox9* at its 18 ts time-point. These contrasting phenotypes aligned with what was seen in the patients; however, they were much more minimal, with no apparent gonadal sex reversal seen in the mouse studies. Despite the modest phenotypes observed, the *Ncor2* mouse study discussed in this thesis goes some way to confirming the role of *NCOR2* in human sex determination, and corroborating the patient data. However, it doesn't provide insight into the potential molecular function of NCOR2 within sex determination itself, or explain why the phenotypes seen in humans are much more significant.

6.4 *Znrf3* in the developing gonad

Alongside the investigation of novel candidate genes, this thesis also investigated *Znrf3,* a gene that had been actively studied in the lab before I joined and shown to result in a testis determination phenotype following genetic ablation. *Znrf3* had been brought to our attention because of human variants discovered in an exome sequencing screen of DSD patients, in the same way the other genes had been identified. Its impact on sex determination is through ZNRF3's interaction with the WNT-signalling pathway, and discovery of this factor indicated how RSPO1 functions in the ovarian pathway. Specifically, ZNRF3 works to clear FRIZZLED from the cellular membrane, thus inhibiting WNT-signalling. When RSPO1 is present, it binds ZNRF3, opposing this function. So RSPO1's role as a pro-ovarian factor is mediated by its repression of the testicular factor ZNRF3 (Zebisch and Jones 2015, Harris et al. 2018). Whilst this cell-signalling function in testis determination had been characterised in a preliminary fashion, there were still many unknowns concerning the role of *Znrf3* within the developing gonad. Previous expression studies had suggested that it was expressed at very low levels within the gonad and present in both XY and XX gonads, despite it being a pro-testis factor. I wanted to investigate the distribution and sub-cellular localisation of ZNRF3 protein within the gonad to uncover more on its specific function. Further, *Znrf3*-null gonads had been shown to be smaller than their wildtype counterparts. As cell proliferation at around 11.0 dpc is a known requirement for testis determination, I wanted to investigate any role this might be playing in the sex reversal phenotype seen in *Znrf3*-null gonads. Finally, I wanted to investigate the transcriptomic landscape in *Znrf3*-null gonads to determine whether there was any other explanation as to why loss of *Znrf3* impacts testis determination and to shed light on the general impact on gene expression of the loss of ZNRF3.

Initial investigations of commercially available antibodies against ZNRF3 were unsuccessful. The two most useful assays for antibody usage within gonadal studies are immunofluorescence and Western blot followed by co-immunoprecipitation. These enable visualisation of protein localisation within the developing gonad, and identification of interacting partners, respectively. Unfortunately, neither were

successful with commercially available antibodies, a phenomenon that is common (Voskuil 2014). As a result, I attempted to create my own anti-ZNRF3 antibody that would allow detection within the mammalian gonad. However, as with the commercial attempts, these were unsuccessful. Specificity was the main issue, with any signal also being detected in *Znrf3*-null tissue samples. To try and overcome the issue of specificity, I designed a *Znrf3-Myc-6XHis* tagged allele. This was then introduced into the endogenous mouse gene to allow for ZNRF3 visualisation using either MYC or HIS antibodies, of which there are many highly validated and reliable examples. Unfortunately, this was also unsuccessful, and any signal produced was deemed to be unspecific. Further, the tagged allele exhibited a lethality phenotype when homozygosed, suggestive of some additional genome editing effects, which could have also impacted on the failure of this allele. As with the failure of all the commercial antibodies, my inability to produce an antibody is most likely due to the protein itself. As previous studies had already suggested, expression of *Znrf3* in the developing gonad is most-likely at very low levels, making detection difficult. Further, there may be structural reasons why a transmembrane protein like ZNRF3 is difficult to detect using antibodies.

To study the impact of loss of *Znrf3* on cell proliferation, I designed a gonadal proliferation assay using EdU incorporation as a marker of proliferation (Salic and Mitchison 2008). I found that from 17-18 ts (11.5 dpc), XY gonads undergo much higher levels of proliferation than their XX counterparts, confirming previous studies done on this process (Schmahl et al. 2000, Schmahl and Capel 2003, Schmahl et al. 2004). I also showed that XY *Znrf3*-null gonads did not undergo this increase in proliferation, suggesting that they are acting more like XX gonads. However, at the critical time-point of 11.0 dpc, I showed that XY null gonads do not have significantly reduced proliferation. This indicates that the cell proliferation phenotype seen is most likely a consequence of the sex reversal phenotype, and not the cause of it. This suggests that *Znrf3*'s role may be limited to its repression of WNT-signalling, but this needed to be investigated further.

To identify any other roles *Znrf3* may have in the developing gonad at the sex-determining stage, and the general transcriptomic impact of loss of ZNRF3, I performed a bulk RNA sequencing assay on 11.5 dpc mutant and wildtype gonads. This study further confirmed *Znrf3*'s role in opposing the canonical WNT signalling pathway, and highlighted several WNT-related genes that are affected in the *Znrf3*-null gonad. It also highlighted many key members of the testis-determining pathway that were also affected in the *Znrf3*-null gonad, most likely due to the mutual antagonism between the two pathways. Further to this, is was difficult to identify any novel factors as the overall variation between the wildtype and null samples was not extensive. This was most likely due to the early stage of comparison (11.5 dpc) when differences are expected to be small, the variable phenotype of *Znrf3*-null XY gonads, and the small sample size for each genotype (n=5). *Znrf3*-null XY gonads undergo partial sex reversal, with some portions of the gonad being more testis-like and others more ovarian. The use of bulk RNAseq may have meant that any changes in the sex-reversed regions were 'drowned out' by more normal regions, making them undetectable overall; single-cell RNAseq approaches may be more suitable for identifying novel impacts, and are currently underway in the lab. Ideally, such studies would be combined with spatial information too.

6.5 Overall conclusions and future research

The work presented in this thesis only goes part of the way to investigating the role of these genes within the sex determination pathways. Further work is needed on all lines discussed to acquire a better understanding on their precise roles.

Within the *Tle3* study, the use of the knockout model may not have been the most suitable option. Here, I would suggest modelling the specific human mutation to attempt to reproduce the phenotype with more success, as the literature suggested that it could be a GOF mutation present in the patients. However, as *Tle3* is an overall weak candidate given the limited human genetics data, I would argue that it doesn't warrant further extensive study. In regards to the *Sec31a* study, the early lethality phenotype prevents any study of sex determination. As such, I would suggest the use of a conditional

model, *Sf1/Cre* (Bingham et al. 2006), to allow gene deletion to be restricted to somatic cells of the developing gonad. Further, I would recommend a deeper study into the impacts of transcript complexity, and how it could limit the mouse model. Also, as the loss of *SEC31A* in humans was not lethal as it was in mice, I would be interested in studying any paralogs or interacting partners of SEC31A. Perhaps SEC31A plays a different role in mice than it does in humans? In respect of *Znrf3,* I would be interested in pursuing single-cell RNAseq experiments, and further continuing with attempts to generate a ZNRF3 antibody or a *bona fide* tagged allele. Finally, in regards to the *Ncor2* study, I was only able to scratch the surface of any potential role in sex determination due to time constraints. Nevertheless, it is the only novel candidate gene for which I have presented positive evidence of a role in sex determination, and as such it requires further research. Here, a clear investigation is needed using all three lines, B6J, B6J.Y^{AKR} and 129, to determine the extent of the sex determination phenotypes seen. Following this, functional studies are required to highlight how *Ncor2* might be involved in both testis and ovarian determination; this could include protein-based studies alongside RNA sequencing studies.

6.6 Murine models of human disease

6.6.1 Mouse as a model for sex determination

This thesis has described specific examples of a larger project: that of understanding the aetiology of human DSDs, 46, XY gonadal dysgenesis (GD) in particular, using loss-of-function studies in the mouse. This is justified based on the large proportion of cases of human GD that remain genetically undiagnosed. The mouse has been used as a primary model for human sex determination due to the similarities in human and mouse reproductive biology, ease of access of tissue, ethical limitations of using more closely related species, and the availability of genetic technologies for manipulation of the mouse genome (Arboleda and Vilain 2011). The mechanisms of sex determination in humans and mice are highly conserved, despite the evolutionary distance between them, and there are many examples of conserved gene function. For example, *SRY* expression is the initiating factor in testis determination

in both species (Koopman 1995). However, despite this highly conserved function between the human and mouse *SRY/Sry*, there is a difference in gene expression between the two species. *Sry* expression during murine development is transient, whilst *SRY* expression in humans is constant once activated during development (Koopman et al. 1990). Another example of pathway conservation involves *RSPO1*. Loss of *RSPO1* function in humans results in XX testicular DSD (Parma et al. 2006). Moreover, duplication of *RSPO1/WNT4* in humans is associated with XY male to female sex reversal (Maatouk et al. 2008); the same has been observed in mice via the stabilisation of β-catenin (Maatouk et al. 2008). These observations suggest that *SRY* expression, and the regulation of canonical WNT signalling that it initiates, are central to both human and mouse sex determination. Indeed, most mammals rely on the same chromosomal sex determining system discussed above, the XY system, and some may make better models of human sex determination. However, the mouse provides the perfect balance between ease of use, ethical considerations and biological conservation between systems, making it the best model. As previously discussed in the introduction to this thesis, other animal groups have different sex determination systems. For example, birds use a ZW genetic system, fish use either a XY or ZW system and can have a fluid sexual identity throughout life; and ectotherms use an environment-based system. However, a theme that all these pathways appear to have in common, is the mutual antagonism between the male and female pathways (Capel 2017). This mutual antagonism is vital in maintaining commitment to cell fate, and enables correct gonadal development.

6.6.2 Laboratory mouse strain limitations

Laboratory mice were historically inbred to improve reproducibility and minimize the impact of genetic variation on studies (Gasch, Payseur and Pool 2016). Whilst this has allowed for progress in understanding cellular function, it has impaired the understanding of the role of genetic variation. Humans are incredibly genetically diverse, since they are an outbred species, so using a model with minimal genetic variation will often lead to inaccurate conclusions. In the case of *Sec31a,* the early embryonic lethality seen in the murine and *Drosophila* models was not replicated in humans. This was most likely due to the effect of genetic variation. The lack of diversity of the model genomes makes

them much more susceptible to lethality. In addition, the precise nature of the genomes of those humans harbouring *SEC31A* mutations – their individual genetic backgrounds - is likely to have a large impact on their phenotypes, in ways that we currently do not understand.

Whilst laboratory inbred strains exhibit a lack of genetic diversity, it is possible to use these inbred strains in combination as a way to address genetic diversity in humans. This is the approach taken in this thesis research. Different laboratory mouse strains tend to exhibit distinct susceptibilities to different phenotypes. As already discussed, different mouse strains show different responses to disruptions to testis determination. The B6J strain used throughout the majority of this thesis is sensitised to disruptions to testis determination. The B6J.Y^{AKR} sub-strain is even more sensitised, with wildtype embryonic testes expressing ovarian markers during transient ovotestis formation. Further studies have shown different strains to have varied brain anatomy, immune responses and behaviour (Scholz et al. 2016, Sellers et al. 2012, Halladay, Kocharian and Holmes 2017). All of this highlights the importance of choosing the correct strain for any given study, but it also highlights the limitation of the model to represent all variation present in a population. For example, the *NCOR2* study found both XX and XY patients with DSD. This suggests a role in both testis and ovarian determination. However, studying both roles on a single mouse genetic background turns out to be impossible or unwise. Studying the ovarian phenotype on a B6J background was not possible, and the phenotype was lost; whilst studying the testis phenotype on a 129 background produced a different result than on B6J. Further, studying on a mixed background reduced the severity of the phenotype altogether. Overall, the *Ncor2* study emphasised the importance of mouse strain used, both when it comes to study design, but also interpretation of the results. It also highlighted the importance that genetic variation may play in determination of phenotype within human disease. Given that there are 7 billion humans, some of those affected by DSD may have 'unusual' genomes, with rare variants at multiple loci making a (varying) contribution to the clinical phenotype. It may even be possible to examine the effect of such genetic modifiers, or oligogenic inheritance, of DSD using the mouse model, given the improving methods of genome editing.

6.6.3 Mouse model limitations

Within the mouse and human genomes there are a proportion of essential genes. These are known as essential because they cannot be removed without causing lethality. Within yeast, 20% of all genes are required for viability; these genes often encode core components of cell function such as transcription and transport (Giaever and Nislow 2014). As has been discussed, SEC31A is known to play a vital role in cell trafficking. In the case of *Sec31a,* my data have shown clearly an essential role for cellular function, which is why such an early lethality phenotype was seen when it was deleted. However, humans with homozygous mutations in *SEC31A* are reported to survive until 4 years old (Halperin et al. 2018). This suggests that *Sec31a* essentiality in mice is not conserved. In fact, many essential genes are not conserved between humans and mice. One study showed 2,394 genes which are essential in mice but not in humans (Bartha et al. 2018). This is an important observation that needs to be taken in to consideration now that more is being discovered about the differences between the two genomes. It would be useful if approaches were developed that accurately predicted the likelihood of gene essentiality before expending mice; however, there is still a lot to learn before gene essentiality can be readily predicted. In the case of *Sec31a,* the most likely explanation for the difference in essentiality is the level of transcriptional variation. The mouse gene is predicted to have 7 protein-coding transcripts, whilst the human *SEC31A* gene is predicted to have 28 protein-coding transcripts. This increased variation of the human gene may provide extra protection against mutation, and thus lethality. So, the lack of similar variation at the mouse locus, alongside the use of a null allele targeted for degradation, probably increases the risk of early lethality.

One common theme in mouse studies is the requirement for homozygosity of a mutant allele to produce a phenotype, even if the patients examined by exome sequencing are heterozygous for the discovered mutation. More study is needed to understand why this is the case, which could then enable a better prediction of the right genetic model to use for each study (Justice and Dhillon 2016). It may be due to the more diverse genetic background present in humans, meaning some humans are more prone to disease. As such, some humans heterozygous for a mutation will experience disease

whilst others won't, depending on their genetic background. One way to overcome this would be to increase the diversity present in animal experimentation. Phenotypic plasticity depends on complex gene-environment interactions (Richter 2017); by mimicking these interactions within a study, a more reliable and representable result can be produced. Systematic heterogenization works to introduce this variation into an experiment. However, this variation must be added in a systematic and controlled manner so as to maintain the number of animals used to a minimum. One such method of introducing diversity in animal experimentations, is the Collaborative Cross (Churchill et al. 2004). This provides a common reference panel of recombinant inbred strains derived from a genetically diverse set of founder strains.

Another explanation of the preponderance of heterozygous mutations in human disease is the nature of the mutant allele. Whilst my research has focussed on loss-of-function mouse mutants, there are many other types of mutant allele, including gain-of-function and dominant negative. This indicates that data concerning the nature of the human mutation is also very important when planning how to make an informative mouse model; but such data is often lacking due to general ignorance about the candidate gene and the functional domains of the protein it encodes.

The simplest way to investigate gene function is to eliminate expression of the gene (Bouabe and Okkenhaug 2013). However, this may not produce the same result as the specific human mutation that, for example, alters one amino acid. Often, eliminating expression causes a much more severe phenotype, such as lethality. With the recent development of CRISPR/Cas9 technology, it is now far easier to introduce specific point mutations into the mouse genome, enabling a precise re-creation of the patient mutation, such as a mis-sense mutation. In theory, this should be a far more reliable model for study of patient diseases; however, this is not always the case. Often, reproducing the specific point mutation observed in a patient within the mouse genome does not result in a phenotype. For example, *ZNRF3* was identified as a candidate gene for sex determination via exome sequencing and confirmed to be involved in testis determination using a null allele (Harris et al. 2018). However, when

one specific mutation seen in the patients was introduced in B6J mice, no phenotype was seen (Harris and Greenfield, unpublished data). Explanations for outcomes such as this are difficult to confirm: it may be that the particular mutation selected for modelling may not be causally responsible for the human phenotype, although the human gene and other variants still play a role; it may be that the equivalent mutation in the mouse is in a region of the mouse protein that is not especially highly conserved and is not disruptive to the protein due to an altered amino acid context – this may be the case with the aforementioned *Znrf3* mutation; or perhaps the disruption to the protein still occurs, but in a domain that is not so critical in the mouse because of alterations to interacting proteins etc. This highlights one of the realities of using CRISPR/Cas9: whilst we can now achieve a lot more in terms of genetic manipulation, this doesn't automatically correspond to more positive results. That sometimes requires better understanding of the gene and protein.

Whilst some limitations can be a result of a lack of genetic variation within mouse models, a problem which might be overcome by selection of the appropriate strains, some are merely due to the fact that mice and humans are distinct species. Humans and mice diverged from a common ancestor around 96 million years ago (Nei, Xu and Glazko 2001), with the appearance of *SRY* estimated to be between 166-148 million years ago (Wallis, Waters and Graves 2008). As such, there are genetic differences between the two that can limit the use of the mouse as a model. Despite the conserved function of *SRY* across mammals, the sequence of this gene has undergone much variation. The high mobility group (HMG)-box is the only region which has been conserved, with 80% identity between mouse and humans (Wallis et al. 2008, O'Neill and O'Neill 1999). The region 3' to the HMG-box shows a very high degree of variability between many mammalian species, suggesting a rapid level of evolution within *SRY*. Studies have shown that *SRY* genes have high K_A/K_S ratios (O'Neill and O'Neill 1999), demonstrating high levels rapid of evolution. It is suggested that these high levels are related to its residing on the Y chromosome, which undergoes faster evolution due to lack of recombination, and the function of *SRY* itself, as for an XY determining gene, quick divergence is beneficial to males in reducing competition (O'Neill and O'Neill 1999). If this is true, the same could be true for other testis-

determining factors, highlighting a major disadvantage of using a model species that diverged so long ago and revealing how little is still known about the evolution of sex-determining mechanisms (Bachtrog et al. 2014). An example, of the limitations of the mouse model, can be seen with mitogen activated protein kinase (MAPK) signalling and its relation to 46,XY DSD. A forward genetic screen highlighted the loss of *Map3k4* as the cause of XY gonadal sex reversal (Bogani et al. 2009), suggesting a role within the testis-determining pathway. Further, mice lacking *Gadd45g*, which encodes a known interacting partner of MAP3K4, also had impaired testis determination (Warr et al. 2012). Further work revealed that a GADD45γ/MAP3K4/p38 MAPK pathway is required for initiating timely *Sry* expression within the XY mouse gonad (Bashamboo and McElreavey 2015). However, no DSD patients have yet been discovered with disruptive variants of *MAP3K4*, despite its clear role in murine sex determination. Interestingly, another MAP kinase family member has been identified as responsible for DSD. *MAP3K1* mutations have been identified in six cases of 46,XY DSD (Pearlman et al. 2010); but mice lacking *Map3K1* do not show XY gonadal sex reversal (Warr et al. 2011). This example highlights evolutionary divergence, revealing the role of paralogous genes, rather than orthologues, in testis determination in the two species. In one sense, this is another example of a limitation of the mouse model. However, much depends on whether loss of *Map3k4,* and the sex reversal it causes in mice, model aspects of the consequences of *MAP3K1* mutations in human sex determination. This remains to be determined.

6.7 Exome sequencing to discover novel candidate genes

Exome sequencing is a targeted approach to identifying human variants responsible for disease, involving the sequencing of only the protein-coding region of the genome. This approach of DNA sequencing is a fast and highly cost-effective method. The exome is a highly enriched subset of the genome, making this a powerful method for detecting novel genetic causes of disease (Bamshad et al. 2011). This approach has more clinical relevance than a forward genetic screen using mice, as was evidenced in the case of *Map3k4* (Bogani et al. 2009). It is based around identifying the genetic cause

of disease in patient cohorts. However, this approach also has its limitations, including: false positives, a poor understanding of the functional impacts of rare variants, and further the cumulative effects of multiple variants. To reduce the impact of these limitations, candidate selection based on multiple non-familial cases would be ideal. As this thesis has shown, a candidate gene that has been highlighted via exome sequencing in multiple unrelated patients, such as *NCOR2*, is perhaps more likely to produce a phenotype within a murine model – although admittedly this conclusion is based on low numbers of cases. But, with this comes an added time-delay, and the result is still uncertain. More needs to be done to overcome the high false-positive rate and to improve the efficiency of exome sequencing. With the costs associated with DNA sequencing still reducing at a rapid rate, the exome sequencing approach may soon be superseded by a whole genome sequencing (WGS) approach. However, even if the whole genome is sequenced, current understanding of the how the genome functions, particularly the non-coding genome, would limit most analyses to the protein coding regions. This makes it even more important to improve the efficacy of exome sequencing. WGS would provide us with the data to discover novel roles within the non-coding regions of the genome and how these regions interact with the coding regions in terms of disease, but this potential will not be achievable until we fully understand the true functions of the exome and its variation (Bamshad et al. 2011).

6.8 Future relevance of exome sequencing and mouse model approach

Deletion of candidate genes in a murine model may not be an efficient way of discovering genes involved in sex determination and, by implication, human DSD, as suggested by this thesis. There is still a lot left to discover about the gonadal development pathway, which raises the question 'Is there a more efficient way of doing this?' A reproducibility crisis alongside growing ethical concerns surrounding animal research is making some researchers question the future of this model (Ferreira et al. 2020).

6.8.1 Humanised mouse models

Knockout mouse models are easy to make but can have a low success rate in modelling human disease, as this thesis has shown. Modelling the specific human mutation within the mouse genome is a bit more complicated and also has a low success rate due to the genetic differences between mouse and human (Harris et al. 2018, Warr et al. 2011). Over the past few years, it has become apparent that animal models are often unable to be translated into human clinical research (Robinson et al. 2019). One approach to overcome this could be a move towards humanised mouse models. Early studies with humanised mice involved grafting with human transplants. Peripheral blood mononuclear cells (PBMCs) were engrafted into mice to create an animal model for graft-versus-host disease (GVHD) (Mosier et al. 1988, Ito et al. 2009, King et al. 2009, van Rijn et al. 2003). These models also allowed the study of graft rejection and the screening of therapeutic drugs regarding this. More recently, novel genetically modified humanised mice, termed next-generation humanised mice, have been generated (Ito, Takahashi and Ito 2018, Zhu et al. 2019). Conventional humanised mice transferred with hematopoietic stems cells (HSCs) did not undergo human myeloid lineage cell differentiation; next-generation humanised mice have overcome this problem. However, other cell types such as red blood cells and platelets are still unable to completely differentiate (Ito et al. 2018). Next-generation humanised mice have shown great potential in translation into human clinical research. One study used this approach to assess the functional significance of androgen receptor (AR) genetic variation in the development of prostate cancer (Robins 2012). They found AR glutamine tract length influenced prostate cancer progression and the castration response. Humanised mice are promising but are still limited in their usefulness. They require constant identification of missing factors in the mouse to enable correct cell differentiation; they often require reduced host immunity to allow for humanisation, and there is still a lot of validation required to confirm their relevance (Walsh et al. 2017). Whilst humanised mouse models hold promise and have proved useful in other areas of research, their use in DSD research is unlikely. As the sex determination pathway is so complex, and still contains a lot of unknown factors, creating a reliable humanised mouse model for DSDs isn't

currently viable, and the current mouse model is unlikely to be replaced by this. It might, however, be useful to generate mice with human versions of the candidate gene, replacing the mouse equivalent. This may enable problems such as transcriptional complexity to be overcome: in the case of the *Sec31a* allele this could have prevented the early embryonic lethality phenotype. However, these lines are not easy to generate (Zhu et al. 2019), and they may not survive due to mouse-human gene differences. But, if they were normal, human mutations could then be introduced to test causality. Still, this is a vast amount of work and perhaps not justified for very rare diseases.

6.8.2 *In vitro* models

The use of cell lines *in vitro* to model aspects of gonad development has been of limited value due to the paucity of good cell lines. As discussed previously, the gonad consists of various cell lineages, each with a crucial role in sex determination and gonad development. The two cell lineages discussed most in this thesis are the supporting and germ cell lineages. Within the supporting cell lineage, the production of Sertoli and granulosa cells, in XY and XX gonads, respectively, is the focus of most sex determination studies. An *in vitro* study would require Sertoli/granulosa cell lines that faithfully reproduce the properties of those lineages *in vivo*, which are dynamic. A 2012 study was able to generate embryonic Sertoli-like cells via lentiviral-mediated reprogramming of fibroblasts by use of key factors DMRT1, SOX9, NR5A1, GATA4, WT1 (Buganim et al. 2012). This progress provided a model to study Sertoli pathways *in vitro*. These *in vitro* Sertoli cells had the ability to form tubule-like structures, support germ cell survival and recruit endothelial cells. However, these cells did not have the high *Fgf9* expression seen *in vivo* and also displayed highly variable levels of *Sox9* expression. This suggests that they were not identical to *in vivo* Sertoli cells, and revealed limited use for them in studying molecular processes underlying sex determination. Further, these cells were already differentiated Sertoli-like cells, making them of poor use in studying the crucial differentiation process, with its dynamic properties. An *in vitro* model fully recapitulating the human or mouse embryonic gonad was still unavailable.

More recent developments in the field of *in vitro* modelling are now not focused on the 2D model of cell line culture, but on the development of 3D organoids. Since the above 2012 study, there have been numerous attempts to develop human embryonic-like gonadal cells. Some mirrored the 2012 study, and reprogrammed fibroblasts using overexpression of transcription factors such as *GATA4* and *NR5A1* (Liang et al. 2019). Others used co-cultures of human and mouse cells in an *ex vivo* model (Rodríguez Gutiérrez, Eid and Biason-Lauber 2018, Shlush et al. 2017, Yamashiro et al. 2018). One study used co-cultures of human induced pluripotent stem cells (iPSCs) with NT2D1 cells to induce differentiation of Sertoli-like cells from fibroblasts (Rodríguez Gutiérrez et al. 2018). And finally, one study differentiated human embryonic stem cells into bipotential gonadal cells via induction of intermediate mesoderm, using sequential inactivation and activation of bone morphogenetic protein (BMP) followed by activin A and WNT signalling activation (Sepponen et al. 2017). However, despite these advancements, the generation of a stable cell line that accurately represented human embryonic gonadal cells, or the development of an organoid culture from any of these cell lines hadn't been achieved until recently (Knarston et al. 2020). This study was able to use a directed differentiation approach to drive human iPSCs differentiation, first to a bipotential gonadal supporting cell lineage and then onto a Sertoli-like cell lineage, using growth factor-mediated differentiation (Knarston et al. 2020). This novel method would allow for study of gonadal sex determination as it generates bipotential cells which become determined with maturation, something which none of the earlier studies were able to produce. Further, this 2020 study showed that the induced bipotential gonad cells were able to self-organise into 3D gonadal structures, and these organoids demonstrated more accurate expression of testis-determining genes than when the cells were grown in 2D culture (Knarston et al. 2020). This model represents a major advancement in the development of an *in vitro* model of human sex determination and, therefore, potentially of DSD. The next step would be to combine this model with germ cells differentiated from iPSCs (Yamashiro et al. 2018), and attempt a co-culture model to produce a more complete model of the gonad with both supporting and germ cell lineages (Knarston et al. 2020). The generation of such a gonadal organoid might lead to the mouse

model being abandoned altogether. Organoids provide an ethical and reproducible setting in which gonadal development can be studied. Further, they provide the option to be directly derived from patient's cells and/or have a specific mutation induced using CRISPR/Cas9 (Clevers 2016). Patient-derived organoids hold great promise, and would be easily applicable to the candidate gene approach discussed in this thesis. Organoids could be cultured directly from DSD patient cells, functional studies could then be performed to investigate the cause of gonadal abnormalities directly in the patient-derived organoids. Further, CRISPR/Cas9 could be used to correct the variants associated with DSD in these organoids, thus confirming the role of such a variant (Freedman et al. 2015, Schutgens and Clevers 2020). All that would be required is an assay, such as the ability to differentiate into a Sertoli-like cell and form testis cords, in the presence and absence of the proposed disease-causing variant. This model might out-compete the murine model of DSD as it is faster, more reproducible, less ethically contentious, and has more clinical relevance. However, such a model is not without its limitations. One major limitation of *in vitro* methods is their proneness to artefacts (Gruber and Hartung 2004); this is mainly due to differences in cell culture methodologies. But with quality control and a set standard for good cell culture practice, this can be overcome. Further, the increasing ability of machines could automate the process completely and massively reduce the risk of artefacts. Other limitations to organoid culture in respect to reproducibility involve the use of animal-based matrix extract, which can vary in composition between batches (Schutgens and Clevers 2020). But this could be overcome by culturing with clinical grade collagen, a novel method which has shown to be successful in colon organoids (Yui et al. 2012, Schutgens and Clevers 2020). Current costs of organoid culture are a further limitation, but a move to synthetic based matrices alongside an increase in demand would reduce these greatly, and make organoid study far more accessible. The use of a microwell culture system has recently been shown to be a simple, cost effective, and highly reproducible technique that can be used to generate multicellular testicular organoids (Sakib et al. 2019). This technique, developed with porcine cells, produces a system which can be used to

manipulate different cell signalling pathways in specific cell types, and represents the potential future of DSD models.

6.8.3 Is the mouse model redundant?

As discussed, there is a drive from some to move away from animal research due to the ethical problems associated with it. Whilst a reduction of animal usage in areas such as medical teaching is definitely possible, due to the advent of automated reality techniques, is this possible in regards to broader scientific research?

The implementation of the European directive to protect animals used in scientific procedures, around 10 years ago, alongside growing political pressures, has made animal research far more expensive and time consuming in regards to administrative burdens (Genzel et al. 2020). The Netherlands is leading the way in the move away from animal studies, by providing extra funding for the study of alternative methods. But the underlying knowledge enabling these advancements was gained through the use of animals in research. Further, whilst these alternatives are useful, they are unable to replicate whole body systems, which is a major limitation. For example, a drug that is effective in an organoid may prove toxic in a whole-body system due to adverse effects of other organs. Systems biology has been an important area of research for many years, and we should not forget its importance if we are discussing the role of animal research. The reproductive organs form part of such a system – the hypothalamic-pituitary-gonadal axis – and this is not something that can modelled in a dish. Indeed, the mouse has been invaluable in reproductive medicine, including the development of assisted reproductive technologies such as IVF, and so we should be very careful before making conclusions about its general value to scientific research.

In the last year, the broader importance of the animal model has been highlighted with the emergence of COVID-19. The virus causing this disease, severe acute respiratory syndrome coronavirus 2 (SARS-CoV-2), has been shown to impact multiple organs within the body including the lungs, the heart and the gut (Zuo et al. 2020). So, the use of organoids would not enable an accurate study of this complex

disease. Further, in regards to development of a therapy or vaccine, animals have proved indispensable (Genzel et al. 2020). Moving forward, a better approach might be one that involved all the approaches discussed above, perhaps with a triage design. By starting with an *in vitro* approach to studying gene function, it should be possible to first screen for the most promising candidates to a better degree than merely relying on exome sequencing data on its own; these candidates can then be studied more extensively in an animal model with greater likelihood of success.

6.9 Concluding remarks

With a view to shedding light on the causes of human DSD, this thesis has described the study of three novel candidate testis-determining genes and one known testis-determining gene in the mouse, with varied success. It has shown the importance of carefully choosing genetic background in mouse research and discussed the limitations of current approaches. I conclude that the mouse data reported here support a role for *NCOR2* in human sex determination. As such, this thesis has also shown the importance of the mouse model within sex determination research and the potential for this model moving forward, both within the field of DSDs and the wider biomedical research landscape.

Bibliography

Abbas, N., K. McElreavey, M. Leconiat, E. Vilain, F. Jaubert, R. Berger, C. Nihoul-Fekete, R. Rappaport & M. Fellous (1993) Familial case of 46,XX male and 46,XX true hermaphrodite associated with a paternal-derived SRY-bearing X chromosome. *C R Acad Sci III,* 316**,** 375-83.

Achermann, J. C., S. Domenice, T. A. Bachega, M. Y. Nishi & B. B. Mendonca (2015) Disorders of sex development: effect of molecular diagnostics. *Nat Rev Endocrinol,* 11**,** 478-88.

Agarwal, M., P. Kumar & S. J. Mathew (2015) The Groucho/Transducin-like enhancer of split protein family in animal development. *IUBMB Life,* 67**,** 472-81.

Albrecht, K. H. & E. M. Eicher (2001) Evidence that Sry is expressed in pre-Sertoli cells and Sertoli and granulosa cells have a common precursor. *Dev Biol,* 240**,** 92-107.

Ann, E. J., H. Y. Kim, M. S. Seo, J. S. Mo, M. Y. Kim, J. H. Yoon, J. S. Ahn & H. S. Park (2012) Wnt5a controls Notch1 signaling through CaMKII-mediated degradation of the SMRT corepressor protein. *J Biol Chem,* 287**,** 36814-29.

Arango, N. A., R. Lovell-Badge & R. R. Behringer (1999) Targeted mutagenesis of the endogenous mouse Mis gene promoter: in vivo definition of genetic pathways of vertebrate sexual development. *Cell,* 99**,** 409-19.

Arboleda, V. A. & E. Vilain (2011) The evolution of the search for novel genes in mammalian sex determination: from mice to men. *Mol Genet Metab,* 104**,** 67-71.

Auguste, A., A. A. Chassot, E. P. Gregoire, L. Renault, M. Pannetier, M. Treier, E. Pailhoux & M. C. Chaboissier (2011) Loss of R-spondin1 and Foxl2 amplifies female-to-male sex reversal in XX mice. *Sex Dev,* 5**,** 304-17.

Axelrod, J. D., K. Matsuno, S. Artavanis-Tsakonas & N. Perrimon (1996) Interaction Between Wingless and Notch Signaling Pathways Mediated by Dishevelled.

Bachtrog, D., J. E. Mank, C. L. Peichel, M. Kirkpatrick, S. P. Otto, T. L. Ashman, M. W. Hahn, J. Kitano, I. Mayrose, R. Ming, N. Perrin, L. Ross, N. Valenzuela & J. C. Vamosi (2014) Sex determination: why so many ways of doing it? *PLoS Biol,* 12**,** e1001899.

Bagheri-Fam, S., H. Sim, P. Bernard, I. Jayakody, M. M. Taketo, G. Scherer & V. R. Harley (2008) Loss of Fgfr2 leads to partial XY sex reversal. *Dev Biol,* 314**,** 71-83.

Bamshad, M. J., S. B. Ng, A. W. Bigham, H. K. Tabor, M. J. Emond, D. A. Nickerson & J. Shendure (2011) Exome sequencing as a tool for Mendelian disease gene discovery. *Nat Rev Genet,* 12**,** 745-55.

Barrionuevo, F., S. Bagheri-Fam, J. Klattig, R. Kist, M. M. Taketo, C. Englert & G. Scherer (2006) Homozygous inactivation of Sox9 causes complete XY sex reversal in mice. *Biol Reprod,* 74**,** 195-201.

Bartha, I., J. di Iulio, J. C. Venter & A. Telenti (2018) Human gene essentiality. *Nat Rev Genet,* 19**,** 51-62.

Bashamboo, A., P. A. Donohoue, E. Vilain, S. Rojo, P. Calvel, S. N. Seneviratne, F. Buonocore, H. Barseghyan, N. Bingham, J. A. Rosenfeld, S. N. Mulukutla, M. Jain, L. Burrage, S. Dhar, A. Balasubramanyam, B. Lee, M. C. Dumargne, C. Eozenou, J. P. Suntharalingham, K. de Silva, L. Lin, J. Bignon-Topalovic, F. Poulat, C. F. Lagos, K. McElreavey & J. C. Achermann (2016) A recurrent p.Arg92Trp variant in steroidogenic factor-1 (NR5A1) can act as a molecular switch in human sex development. *Hum Mol Genet,* 25**,** 5286.

Bashamboo, A., C. Eozenou, S. Rojo & K. McElreavey (2017) Anomalies in human sex determination provide unique insights into the complex genetic interactions of early gonad development. *Clin Genet,* 91**,** 143-156.

Bashamboo, A. & K. McElreavey (2015) Human sex-determination and disorders of sex-development (DSD). *Semin Cell Dev Biol,* 45**,** 77-83.

--- (2016) Mechanism of Sex Determination in Humans: Insights from Disorders of Sex Development. *Sex Dev,* 10**,** 313-325.

Baxter, R. M., V. A. Arboleda, H. Lee, H. Barseghyan, M. P. Adam, P. Y. Fechner, R. Bargman, C. Keegan, S. Travers, S. Schelley, L. Hudgins, R. P. Mathew, H. J. Stalker, R. Zori, O. K. Gordon, L. Ramos-Platt, A. Pawlikowska-Haddal, A. Eskin, S. F. Nelson, E. Delot & E. Vilain (2015) Exome sequencing for the diagnosis of 46,XY disorders of sex development. *J Clin Endocrinol Metab,* 100**,** E333-44.

Behringer, R. R., M. J. Finegold & R. L. Cate (1994) Mullerian-inhibiting substance function during mammalian sexual development. *Cell,* 79**,** 415-25.

Bhaskara, S., B. J. Chyla, J. M. Amann, S. K. Knutson, D. Cortez, Z. W. Sun & S. W. Hiebert (2008) Deletion of histone deacetylase 3 reveals critical roles in S phase progression and DNA damage control. *Mol Cell,* 30**,** 61-72.

Bingham, N. C., S. Verma-Kurvari, L. F. Parada & K. L. Parker (2006) Development of a steroidogenic factor 1/Cre transgenic mouse line. *Genesis,* 44**,** 419-24.

Bogani, D., P. Siggers, R. Brixey, N. Warr, S. Beddow, J. Edwards, D. Williams, D. Wilhelm, P. Koopman, R. A. Flavell, H. Chi, H. Ostrer, S. Wells, M. Cheeseman & A. Greenfield (2009) Loss of mitogen-activated protein kinase kinase kinase 4 (MAP3K4) reveals a requirement for MAPK signalling in mouse sex determination. *PLoS Biol,* 7**,** e1000196.

Bojesen, A., S. Juul & C. H. Gravholt (2003) Prenatal and postnatal prevalence of Klinefelter syndrome: a national registry study. *J Clin Endocrinol Metab,* 88**,** 622-6.

Bondy, C. A. (2009) Turner syndrome 2008. *Horm Res,* 71 Suppl 1**,** 52-6.

Bouabe, H. & K. Okkenhaug (2013) Gene targeting in mice: a review. *Methods Mol Biol,* 1064**,** 315-36.

Bouma, G. J., L. L. Washburn, K. H. Albrecht & E. M. Eicher (2007) Correct dosage of Fog2 and Gata4 transcription factors is critical for fetal testis development in mice. *Proc Natl Acad Sci U S A,* 104**,** 14994-9.

Bowles, J., L. Cooper, J. Berkman & P. Koopman (1999) Sry requires a CAG repeat domain for male sex determination in Mus musculus. *Nat Genet,* 22**,** 405-8.

Boyadjiev, S. A., J. C. Fromme, J. Ben, S. S. Chong, C. Nauta, D. J. Hur, G. Zhang, S. Hamamoto, R. Schekman, M. Ravazzola, L. Orci & W. Eyaid (2006) Cranio-lenticulo-sutural dysplasia is caused by a SEC23A mutation leading to abnormal endoplasmic-reticulum-to-Golgi trafficking. *Nat Genet,* 38**,** 1192-7.

Buganim, Y., E. Itskovich, Y. C. Hu, A. W. Cheng, K. Ganz, S. Sarkar, D. Fu, G. G. Welstead, D. C. Page & R. Jaenisch (2012) Direct reprogramming of fibroblasts into embryonic Sertoli-like cells by defined factors. *Cell Stem Cell,* 11**,** 373-86.

Bullejos, M. & P. Koopman (2001) Spatially dynamic expression of Sry in mouse genital ridges. *Dev Dyn,* 221**,** 201-5.

--- (2005) Delayed Sry and Sox9 expression in developing mouse gonads underlies B6-Y(DOM) sex reversal. *Dev Biol,* 278**,** 473-81.

Burgio, G. & L. Teboul (2020) Anticipating and Identifying Collateral Damage in Genome Editing. *Trends Genet,* 36**,** 905-914.

Callier, P., P. Calvel, A. Matevossian, P. Makrythanasis, P. Bernard, H. Kurosaka, A. Vannier, C. Thauvin-Robinet, C. Borel, S. Mazaud-Guittot, A. Rolland, C. Desdoits-Lethimonier, M. Guipponi, C. Zimmermann, I. Stévant, F. Kuhne, B. Conne, F. Santoni, S. Lambert, F. Huet, F. Mugneret, J. Jaruzelska, L. Faivre, D. Wilhelm, B. Jégou, P. A. Trainor, M. D. Resh, S. E. Antonarakis & S. Nef (2014) Loss of function mutation in the palmitoyl-transferase HHAT leads to syndromic 46,XY disorder of sex development by impeding Hedgehog protein palmitoylation and signaling. *PLoS Genet,* 10**,** e1004340.

Capel, B. (2017) Vertebrate sex determination: evolutionary plasticity of a fundamental switch. *Nat Rev Genet,* 18**,** 675-689.

Carre, G. A., P. Siggers, M. Xipolita, P. Brindle, B. Lutz, S. Wells & A. Greenfield (2018) Loss of p300 and CBP disrupts histone acetylation at the mouse Sry promoter and causes XY gonadal sex reversal. *Hum Mol Genet,* 27**,** 190-198.

Chamberlin, A., R. Huether, A. Z. Machado, M. Groden, H. M. Liu, K. Upadhyay, V. O, N. L. Gomes, A. M. Lerario, M. Y. Nishi, E. M. F. Costa, B. Mendonca, S. Domenice, J. Velasco, J. Loke & H. Ostrer (2019) Mutations in MAP3K1 that cause 46,XY disorders of sex development disrupt distinct structural domains in the protein. *Hum Mol Genet,* 28**,** 1620-1628.

Chassot, A. A., S. T. Bradford, A. Auguste, E. P. Gregoire, E. Pailhoux, D. G. de Rooij, A. Schedl & M. C. Chaboissier (2012) WNT4 and RSPO1 together are required for cell proliferation in the early mouse gonad. *Development,* 139**,** 4461-72.

Chassot, A. A., F. Ranc, E. P. Gregoire, H. L. Roepers-Gajadien, M. M. Taketo, G. Camerino, D. G. de Rooij, A. Schedl & M. C. Chaboissier (2008) Activation of beta-catenin signaling by Rspo1 controls differentiation of the mammalian ovary. *Hum Mol Genet,* 17**,** 1264-77.

Chen, J. D. & R. M. Evans (1995) A transcriptional co-repressor that interacts with nuclear hormone receptors. *Nature,* 377**,** 454-7.

Cheng, X. & H. Y. Kao (2009) G Protein Pathway Suppressor 2 (GPS2) Is a Transcriptional Corepressor Important for Estrogen Receptor α-mediated Transcriptional Regulation*. *J Biol Chem,* 284**,** 36395-404.

Churchill, G. A., D. C. Airey, H. Allayee, J. M. Angel, A. D. Attie, J. Beatty, W. D. Beavis, J. K. Belknap, B. Bennett, W. Berrettini, A. Bleich, M. Bogue, K. W. Broman, K. J. Buck, E. Buckler, M. Burmeister, E. J. Chesler, J. M. Cheverud, S. Clapcote, M. N. Cook, R. D. Cox, J. C. Crabbe, W. E. Crusio, A. Darvasi, C. F. Deschepper, R. W. Doerge, C. R. Farber, J. Forejt, D. Gaile, S. J. Garlow, H. Geiger, H. Gershenfeld, T. Gordon, J. Gu, W. Gu, G. de Haan, N. L. Hayes, C. Heller, H. Himmelbauer, R. Hitzemann, K. Hunter, H. C. Hsu, F. A. Iraqi, B. Ivandic, H. J. Jacob, R. C. Jansen, K. J. Jepsen, D. K. Johnson, T. E. Johnson, G. Kempermann, C. Kendziorski, M. Kotb, R. F. Kooy, B. Llamas, F. Lammert, J. M. Lassalle, P. R. Lowenstein, L. Lu, A. Lusis, K. F. Manly, R. Marcucio, D. Matthews, J. F. Medrano, D. R. Miller, G. Mittleman, B. A. Mock, J. S. Mogil, X. Montagutelli, G. Morahan, D. G. Morris, R. Mott, J. H. Nadeau, H. Nagase, R. S. Nowakowski, B. F. O'Hara, A. V. Osadchuk, G. P. Page, B. Paigen, K. Paigen, A. A. Palmer, H. J. Pan, L. Peltonen-Palotie, J. Peirce, D. Pomp, M. Pravenec, D. R. Prows, Z. Qi, R. H. Reeves, J. Roder, G. D. Rosen, E. E. Schadt, L. C. Schalkwyk, Z. Seltzer, K. Shimomura, S. Shou, M. J. Sillanpää, L. D. Siracusa, H. W. Snoeck, J. L. Spearow, K. Svenson, et al. (2004) The Collaborative Cross, a community resource for the genetic analysis of complex traits. *Nat Genet,* 36**,** 1133-7.

Cinque, L., A. Forrester, R. Bartolomeo, M. Svelto, R. Venditti, S. Montefusco, E. Polishchuk, E. Nusco, A. Rossi, D. L. Medina, R. Polishchuk, M. A. De Matteis & C. Settembre (2015) FGF signalling regulates bone growth through autophagy. *Nature,* 528**,** 272-5.

Clepet, C., A. J. Schafer, A. H. Sinclair, M. S. Palmer, R. Lovell-Badge & P. N. Goodfellow (1993) The human SRY transcript. *Hum Mol Genet,* 2**,** 2007-12.

Clevers, H. (2016) Modeling Development and Disease with Organoids. *Cell,* 165**,** 1586-1597.

Coleman, D. L. & K. P. Hummel (1973) The influence of genetic background on the expression of the obese (Ob) gene in the mouse. *Diabetologia,* 9**,** 287-93.

Colvin, J. S., R. P. Green, J. Schmahl, B. Capel & D. M. Ornitz (2001) Male-to-female sex reversal in mice lacking fibroblast growth factor 9. *Cell,* 104**,** 875-89.

Conover, W. J., M. E. Johnson & M. M. Johnson (1981) A Comparative Study of Tests for Homogeneity of Variances, with Applications to the Outer Continental Shelf Bidding Data. *Technometrics,* 23**,** 351-361.

Copic, A., C. F. Latham, M. A. Horlbeck, J. G. D'Arcangelo & E. A. Miller (2012) ER cargo properties specify a requirement for COPII coat rigidity mediated by Sec13p. *Science,* 335**,** 1359-62.

Correa, S. M., L. L. Washburn, R. S. Kahlon, M. C. Musson, G. J. Bouma, E. M. Eicher & K. H. Albrecht (2012) Sex reversal in C57BL/6J XY mice caused by increased expression of ovarian genes and insufficient activation of the testis determining pathway. *PLoS Genet,* 8**,** e1002569.

Coveney, D., J. Cool, T. Oliver & B. Capel (2008) Four-dimensional analysis of vascularization during primary development of an organ, the gonad. *Proc Natl Acad Sci U S A,* 105**,** 7212-7.

Cox, J. J., L. Willatt, T. Homfray & C. G. Woods (2011) A SOX9 duplication and familial 46,XX developmental testicular disorder. *N Engl J Med,* 364**,** 91-3.

Dessens, A. B., F. M. Slijper & S. L. Drop (2005) Gender dysphoria and gender change in chromosomal females with congenital adrenal hyperplasia. *Arch Sex Behav,* 34**,** 389-97.

Eggers, S. & A. Sinclair (2012) Mammalian sex determination-insights from humans and mice. *Chromosome Res,* 20**,** 215-38.

Eggers, S., K. R. Smith, M. Bahlo, L. H. Looijenga, S. L. Drop, Z. A. Juniarto, V. R. Harley, P. Koopman, S. M. Faradz & A. H. Sinclair (2015) Whole exome sequencing combined with linkage analysis identifies a novel 3 bp deletion in NR5A1. *Eur J Hum Genet,* 23**,** 486-93.

Elejalde, B. R., J. M. Opitz, M. M. de Elejalde, E. F. Gilbert, M. Abellera, L. Meisner, R. R. Lebel & J. M. Hartigan (1984) Tandem dup (1p) within the short arm of chromosome 1 in a child with ambiguous genitalia and multiple congenital anomalies. *Am J Med Genet,* 17**,** 723-30.

Ferreira, G. S., D. H. Veening-Griffioen, W. P. C. Boon, E. H. M. Moors & P. J. K. van Meer (2020) Levelling the Translational Gap for Animal to Human Efficacy Data. *Animals (Basel),* 10.

Foster, J. W., M. A. Dominguez-Steglich, S. Guioli, C. Kwok, P. A. Weller, M. Stevanovic, J. Weissenbach, S. Mansour, I. D. Young, P. N. Goodfellow & et al. (1994) Campomelic dysplasia and autosomal sex reversal caused by mutations in an SRY-related gene. *Nature,* 372**,** 525-30.

Freedman, B. S., C. R. Brooks, A. Q. Lam, H. Fu, R. Morizane, V. Agrawal, A. F. Saad, M. K. Li, M. R. Hughes, R. V. Werff, D. T. Peters, J. Lu, A. Baccei, A. M. Siedlecki, M. T. Valerius, K. Musunuru, K. M. McNagny, T. I. Steinman, J. Zhou, P. H. Lerou & J. V. Bonventre (2015) Modelling kidney disease with CRISPR-mutant kidney organoids derived from human pluripotent epiblast spheroids. *Nat Commun,* 6**,** 8715.

Fuhrmann, G., A. C. Chung, K. J. Jackson, G. Hummelke, A. Baniahmad, J. Sutter, I. Sylvester, H. R. Scholer & A. J. Cooney (2001) Mouse germline restriction of Oct4 expression by germ cell nuclear factor. *Dev Cell,* 1**,** 377-87.

Garcia-Moreno, S. A., Y. T. Lin, C. R. Futtner, I. M. Salamone, B. Capel & D. M. Maatouk (2019) CBX2 is required to stabilize the testis pathway by repressing Wnt signaling. *PLoS Genet,* 15**,** e1007895.

Gasch, A. P., B. A. Payseur & J. E. Pool (2016) The Power of Natural Variation for Model Organism Biology. *Trends Genet,* 32**,** 147-154.

Gasperowicz, M., C. Surmann-Schmitt, Y. Hamada, F. Otto & J. C. Cross (2013) The transcriptional co-repressor TLE3 regulates development of trophoblast giant cells lining maternal blood spaces in the mouse placenta. *Dev Biol,* 382**,** 1-14.

Ge, C., J. Ye, H. Zhang, Y. Zhang, W. Sun, Y. Sang, B. Capel & G. Qian (2017) Dmrt1 induces the male pathway in a turtle species with temperature-dependent sex determination. *Development,* 144**,** 2222-2233.

Genzel, L., R. Adan, A. Berns, J. van den Beucken, A. Blokland, E. Boddeke, W. M. Bogers, R. Bontrop, R. Bulthuis, T. Bousema, H. Clevers, T. Coenen, A. M. van Dam, P. M. T. Deen, K. W. van Dijk, B. J. L. Eggen, Y. Elgersma, I. Erdogan, B. Englitz, J. M. Fentener van Vlissingen, S. la Fleur, R. Fouchier, C. P. Fitzsimons, W. Frieling, B. Haagmans, B. A. Heesters, M. Henckens, S. Herfst, E. Hol, D. van den Hove, M. I. de Jonge, J. Jonkers, L. A. B. Joosten, A. Kalsbeek, M. Kamermans, H. H. Kampinga, M. J. Kas, J. A. Keijer, S. Kersten, A. J. Kiliaan, T. W. A. Kooij, S. Kooijman, W. J. H. Koopman, A. Korosi, H. J. Krugers, T. Kuiken, S. A. Kushner, J. A. M. Langermans, H. M. B. Lesscher, P. J. Lucassen, E. Lutgens, M. G. Netea, L. Noldus, J. W. M. van der Meer, F. J. Meye, J. D. Mul, K. van Oers, J. D. A. Olivier, R. J. Pasterkamp, I. Philippens, J. Prickaerts, B. J. A. Pollux, P. C. N. Rensen, J. van Rheenen, R. P. van Rij, L. Ritsma, B. H. G. Rockx, B. Roozendaal, E. M. van Schothorst, K. Stittelaar, N. Stockhofe, D. F. Swaab, R. L. de Swart, L. Vanderschuren, T. J. de Vries, F. de Vrij, R. van Wezel, C. J. Wierenga, M. Wiesmann, I. Willuhn, C. I. de Zeeuw & J. R. Homberg (2020) How the COVID-19 pandemic highlights the necessity of animal research. *Curr Biol,* 30**,** R1014-r1018.

Giaever, G. & C. Nislow (2014) The yeast deletion collection: a decade of functional genomics. *Genetics,* 197**,** 451-65.

Gonen, N., C. R. Futtner, S. Wood, S. A. Garcia-Moreno, I. M. Salamone, S. C. Samson, R. Sekido, F. Poulat, D. M. Maatouk & R. Lovell-Badge (2018) Sex reversal following deletion of a single distal enhancer of Sox9. *Science,* 360**,** 1469-1473.

Gonen, N., A. Quinn, H. C. O'Neill, P. Koopman & R. Lovell-Badge (2017) Normal Levels of Sox9 Expression in the Developing Mouse Testis Depend on the TES/TESCO Enhancer, but This Does Not Act Alone. *PLoS Genet,* 13**,** e1006520.

Gregoire, S., L. Xiao, J. Nie, X. Zhang, M. Xu, J. Li, J. Wong, E. Seto & X. J. Yang (2007) Histone deacetylase 3 interacts with and deacetylates myocyte enhancer factor 2. *Mol Cell Biol,* 27**,** 1280-95.

Griswold, M. D. (1998) The central role of Sertoli cells in spermatogenesis. *Semin Cell Dev Biol,* 9**,** 411-6.

Gruber, F. P. & T. Hartung (2004) Alternatives to animal experimentation in basic research. *Altex,* 21 Suppl 1**,** 3-31.

Gubbay, J., J. Collignon, P. Koopman, B. Capel, A. Economou, A. Munsterberg, N. Vivian, P. Goodfellow & R. Lovell-Badge (1990) A gene mapping to the sex-determining region of the mouse Y chromosome is a member of a novel family of embryonically expressed genes. *Nature,* 346**,** 245-50.

Guenther, M. G., O. Barak & M. A. Lazar (2001) The SMRT and N-CoR corepressors are activating cofactors for histone deacetylase 3. *Mol Cell Biol,* 21**,** 6091-101.

Guenther, M. G., W. S. Lane, W. Fischle, E. Verdin, M. A. Lazar & R. Shiekhattar (2000) A core SMRT corepressor complex containing HDAC3 and TBL1, a WD40-repeat protein linked to deafness. *Genes Dev,* 14**,** 1048-57.

Halladay, L. R., A. Kocharian & A. Holmes (2017) Mouse strain differences in punished ethanol self-administration. *Alcohol,* 58**,** 83-92.

Halperin, D., R. Kadir, Y. Perez, M. Drabkin, Y. Yogev, O. Wormser, E. M. Berman, E. Eremenko, B. Rotblat, Z. Shorer, L. Gradstein, I. Shelef, R. Birk, U. Abdu, H. Flusser & O. S. Birk (2018) SEC31A mutation affects ER homeostasis, causing neurological syndrome. *J Med Genet*.

Hao, H. X., Y. Xie, Y. Zhang, O. Charlat, E. Oster, M. Avello, H. Lei, C. Mickanin, D. Liu, H. Ruffner, X. Mao, Q. Ma, R. Zamponi, T. Bouwmeester, P. M. Finan, M. W. Kirschner, J. A. Porter, F. C. Serluca & F. Cong (2012) ZNRF3 promotes Wnt receptor turnover in an R-spondin-sensitive manner. *Nature,* 485**,** 195-200.

Harris, A., P. Siggers, S. Corrochano, N. Warr, D. Sagar, D. T. Grimes, M. Suzuki, R. D. Burdine, F. Cong, B. K. Koo, H. Clevers, I. Stevant, S. Nef, S. Wells, R. Brauner, B. Ben Rhouma, N. Belguith, C. Eozenou, J. Bignon-Topalovic, A. Bashamboo, K. McElreavey & A. Greenfield (2018) ZNRF3 functions in mammalian sex determination by inhibiting canonical WNT signaling. *Proc Natl Acad Sci U S A,* 115**,** 5474-5479.

Hastie, N. D. (2017) Wilms' tumour 1 (WT1) in development, homeostasis and disease. *Development,* 144**,** 2862-2872.

Hayward, P., K. Brennan, P. Sanders, T. Balayo, R. DasGupta, N. Perrimon & A. M. Arias (2005) Notch modulates Wnt signalling by associating with Armadillo/β-catenin and regulating its transcriptional activity.

Hiramatsu, R., S. Matoba, M. Kanai-Azuma, N. Tsunekawa, Y. Katoh-Fukui, M. Kurohmaru, K. Morohashi, D. Wilhelm, P. Koopman & Y. Kanai (2009) A critical time window of Sry action in gonadal sex determination in mice. *Development,* 136**,** 129-38.

Huang, B., S. Wang, Y. Ning, A. N. Lamb & J. Bartley (1999) Autosomal XX sex reversal caused by duplication of SOX9. *Am J Med Genet,* 87**,** 349-53.

Hug, N., D. Longman & J. F. Caceres (2016) Mechanism and regulation of the nonsense-mediated decay pathway. *Nucleic Acids Res,* 44**,** 1483-95.

Ito, R., I. Katano, K. Kawai, H. Hirata, T. Ogura, T. Kamisako, T. Eto & M. Ito (2009) Highly sensitive model for xenogenic GVHD using severe immunodeficient NOG mice. *Transplantation,* 87**,** 1654-8.

Ito, R., T. Takahashi & M. Ito (2018) Humanized mouse models: Application to human diseases. *J Cell Physiol,* 233**,** 3723-3728.

Jameson, S. A., Y. T. Lin & B. Capel (2012a) Testis development requires the repression of Wnt4 by Fgf signaling. *Dev Biol,* 370**,** 24-32.

Jameson, S. A., A. Natarajan, J. Cool, T. DeFalco, D. M. Maatouk, L. Mork, S. C. Munger & B. Capel (2012b) Temporal transcriptional profiling of somatic and germ cells reveals biased lineage priming of sexual fate in the fetal mouse gonad. *PLoS Genet,* 8**,** e1002575.

Jedrusik, A., A. Cox, K. B. Wicher, D. M. Glover & M. Zernicka-Goetz (2015) Maternal-zygotic knockout reveals a critical role of Cdx2 in the morula to blastocyst transition. *Dev Biol,* 398**,** 147-52.

Jensen, D. & R. Schekman (2011) COPII-mediated vesicle formation at a glance. *J Cell Sci,* 124**,** 1-4.

Jepsen, K., A. S. Gleiberman, C. Shi, D. I. Simon & M. G. Rosenfeld (2008) Cooperative regulation in development by SMRT and FOXP1. *Genes Dev,* 22**,** 740-5.

Jepsen, K., D. Solum, T. Zhou, R. J. McEvilly, H. J. Kim, C. K. Glass, O. Hermanson & M. G. Rosenfeld (2007) SMRT-mediated repression of an H3K27 demethylase in progression from neural stem cell to neuron. *Nature,* 450**,** 415-9.

Jin, Y. H., H. Kim, H. Ki, I. Yang, N. Yang, K. Y. Lee, N. Kim, H. S. Park & K. Kim (2009) Beta-catenin modulates the level and transcriptional activity of Notch1/NICD through its direct interaction. *Biochim Biophys Acta,* 1793**,** 290-9.

Johnson, E. K., I. Rosoklija, C. Finlayson, D. Chen, E. B. Yerkes, M. B. Madonna, J. L. Holl, A. B. Baratz, G. Davis & E. Y. Cheng (2017) Attitudes towards "disorders of sex development" nomenclature among affected individuals. *J Pediatr Urol,* 13**,** 608.e1-608.e8.

Jordan, B. K., M. Mohammed, S. T. Ching, E. Delot, X. N. Chen, P. Dewing, A. Swain, P. N. Rao, B. R. Elejalde & E. Vilain (2001) Up-regulation of WNT-4 signaling and dosage-sensitive sex reversal in humans. *Am J Hum Genet,* 68**,** 1102-9.

Jung, S., S. Lee, S. Kim & H. Nam (2015) Identification of genomic features in the classification of loss- and gain-of-function mutation. *BMC Med Inform Decis Mak,* 15 Suppl 1**,** S6.

Justice, M. J. & P. Dhillon. 2016. Using the mouse to model human disease: increasing validity and reproducibility. In *Dis Model Mech*, 101-3. © 2016. Published by The Company of Biologists Ltd.

Kamel, A. K., H. M. Abd El-Ghany, M. K. Mekkawy, M. M. Makhlouf, I. M. Mazen, N. El Dessouky, W. Mahmoud & S. A. Abd El Kader (2015) Sex Chromosome Mosaicism in the Gonads of DSD Patients: A Karyotype/Phenotype Correlation. *Sex Dev,* 9**,** 279-88.

Karl, J. & B. Capel (1998) Sertoli cells of the mouse testis originate from the coelomic epithelium. *Dev Biol,* 203**,** 323-33.

Kashimada, K. & P. Koopman (2010) Sry: the master switch in mammalian sex determination. *Development,* 137**,** 3921-30.

Kawase, E., K. Hashimoto & R. A. Pedersen (2004) Autocrine and paracrine mechanisms regulating primordial germ cell proliferation. *Mol Reprod Dev,* 68**,** 5-16.

Kim, K., H. Kim & D. Lee (2009) Site-specific modification of genome with cell-permeable Cre fusion protein in preimplantation mouse embryo. *Biochem Biophys Res Commun,* 388**,** 122-6.

Kim, Y., N. Bingham, R. Sekido, K. L. Parker, R. Lovell-Badge & B. Capel (2007) Fibroblast growth factor receptor 2 regulates proliferation and Sertoli differentiation during male sex determination. *Proc Natl Acad Sci U S A,* 104**,** 16558-63.

Kim, Y., A. Kobayashi, R. Sekido, L. DiNapoli, J. Brennan, M. C. Chaboissier, F. Poulat, R. R. Behringer, R. Lovell-Badge & B. Capel (2006) Fgf9 and Wnt4 act as antagonistic signals to regulate mammalian sex determination. *PLoS Biol,* 4**,** e187.

King, M. A., L. Covassin, M. A. Brehm, W. Racki, T. Pearson, J. Leif, J. Laning, W. Fodor, O. Foreman, L. Burzenski, T. H. Chase, B. Gott, A. A. Rossini, R. Bortell, L. D. Shultz & D. L. Greiner (2009)

Human peripheral blood leucocyte non-obese diabetic-severe combined immunodeficiency interleukin-2 receptor gamma chain gene mouse model of xenogeneic graft-versus-host-like disease and the role of host major histocompatibility complex. *Clin Exp Immunol,* 157**,** 104-18.

Knarston, I. M., S. Pachernegg, G. Robevska, I. Ghobrial, P. X. Er, E. Georges, M. Takasato, A. N. Combes, A. Jørgensen, M. H. Little, A. H. Sinclair & K. L. Ayers (2020) An In Vitro Differentiation Protocol for Human Embryonic Bipotential Gonad and Testis Cell Development. *Stem Cell Reports,* 15**,** 1377-1391.

Knutson, S. K., B. J. Chyla, J. M. Amann, S. Bhaskara, S. S. Huppert & S. W. Hiebert (2008) Liver-specific deletion of histone deacetylase 3 disrupts metabolic transcriptional networks. *Embo j,* 27**,** 1017-28.

Koide, T., M. Downes, R. A. Chandraratna, B. Blumberg & K. Umesono (2001) Active repression of RAR signaling is required for head formation. *Genes Dev,* 15**,** 2111-21.

Koo, B. K., M. Spit, I. Jordens, T. Y. Low, D. E. Stange, M. van de Wetering, J. H. van Es, S. Mohammed, A. J. Heck, M. M. Maurice & H. Clevers (2012) Tumour suppressor RNF43 is a stem-cell E3 ligase that induces endocytosis of Wnt receptors. *Nature,* 488**,** 665-9.

Koopman, P. (1995) The molecular biology of SRY and its role in sex determination in mammals. *Reprod Fertil Dev,* 7**,** 713-22.

Koopman, P., J. Gubbay, N. Vivian, P. Goodfellow & R. Lovell-Badge (1991) Male development of chromosomally female mice transgenic for Sry. *Nature,* 351**,** 117-21.

Koopman, P., A. Munsterberg, B. Capel, N. Vivian & R. Lovell-Badge (1990) Expression of a candidate sex-determining gene during mouse testis differentiation. *Nature,* 348**,** 450-2.

Koubova, J., D. B. Menke, Q. Zhou, B. Capel, M. D. Griswold & D. C. Page (2006) Retinoic acid regulates sex-specific timing of meiotic initiation in mice. *Proc Natl Acad Sci U S A,* 103**,** 2474-9.

Kumar, S., T. J. Cunningham & G. Duester (2016) Nuclear receptor corepressors Ncor1 and Ncor2 (Smrt) are required for retinoic acid-dependent repression of Fgf8 during somitogenesis. *Dev Biol,* 418**,** 204-215.

Lee, H., J. L. Deignan, N. Dorrani, S. P. Strom, S. Kantarci, F. Quintero-Rivera, K. Das, T. Toy, B. Harry, M. Yourshaw, M. Fox, B. L. Fogel, J. A. Martinez-Agosto, D. A. Wong, V. Y. Chang, P. B. Shieh, C. G. Palmer, K. M. Dipple, W. W. Grody, E. Vilain & S. F. Nelson (2014) Clinical exome sequencing for genetic identification of rare Mendelian disorders. *Jama,* 312**,** 1880-7.

Lee, P. A., C. P. Houk, S. F. Ahmed & I. A. Hughes (2006) Consensus statement on management of intersex disorders. International Consensus Conference on Intersex. *Pediatrics,* 118**,** e488-500.

Lejeune, F. (2017) Nonsense-mediated mRNA decay at the crossroads of many cellular pathways. *BMB Rep,* 50**,** 175-185.

Li, H., C. Leo, D. J. Schroen & J. D. Chen (1997) Characterization of receptor interaction and transcriptional repression by the corepressor SMRT. *Mol Endocrinol,* 11**,** 2025-37.

Li, J., J. Wang, Z. Nawaz, J. M. Liu, J. Qin & J. Wong (2000) Both corepressor proteins SMRT and N-CoR exist in large protein complexes containing HDAC3. *Embo j,* 19**,** 4342-50.

Liang, J., N. Wang, J. He, J. Du, Y. Guo, L. Li, W. Wu, C. Yao, Z. Li & K. Kee (2019) Induction of Sertoli-like cells from human fibroblasts by NR5A1 and GATA4. *Elife,* 8.

Lin, Y. T., L. Barske, T. DeFalco & B. Capel (2017) Numb regulates somatic cell lineage commitment during early gonadogenesis in mice. *Development,* 144**,** 1607-1618.

Linder, C. C. (2001) The influence of genetic background on spontaneous and genetically engineered mouse models of complex diseases. *Lab Anim (NY),* 30**,** 34-9.

Liu, C. F., N. Bingham, K. Parker & H. H. Yao (2009) Sex-specific roles of beta-catenin in mouse gonadal development. *Hum Mol Genet,* 18**,** 405-17.

Liu, L., Y. Zhang, C. C. Wong, J. Zhang, Y. Dong, X. Li, W. Kang, F. K. L. Chan, J. J. Y. Sung & J. Yu (2018) RNF6 Promotes Colorectal Cancer by Activating the Wnt/β-Catenin Pathway via Ubiquitination of TLE3. *Cancer Res,* 78**,** 1958-1971.

Livermore, C., M. Simon, R. Reeves, I. Stevant, S. Nef, M. Pope, A. M. Mallon, S. Wells, N. Warr & A. Greenfield (2020) Protection Against XY Gonadal Sex Reversal by a Variant Region on Mouse Chromosome 13. *Genetics,* 214**,** 467-477.

Luna-Zurita, L., B. Prados, J. Grego-Bessa, G. Luxan, G. del Monte, A. Benguria, R. H. Adams, J. M. Perez-Pomares & J. L. de la Pompa (2010) Integration of a Notch-dependent mesenchymal gene program and Bmp2-driven cell invasiveness regulates murine cardiac valve formation. *J Clin Invest,* 120**,** 3493-507.

Maatouk, D. M., L. DiNapoli, A. Alvers, K. L. Parker, M. M. Taketo & B. Capel (2008) Stabilization of beta-catenin in XY gonads causes male-to-female sex-reversal. *Hum Mol Genet,* 17**,** 2949-55.

Maatouk, D. M., L. Mork, A. A. Chassot, M. C. Chaboissier & B. Capel (2013) Disruption of mitotic arrest precedes precocious differentiation and transdifferentiation of pregranulosa cells in the perinatal Wnt4 mutant ovary. *Dev Biol,* 383**,** 295-306.

Mandel, H., R. Shemer, Z. U. Borochowitz, M. Okopnik, C. Knopf, M. Indelman, A. Drugan, D. Tiosano, R. Gershoni-Baruch, M. Choder & E. Sprecher (2008) SERKAL syndrome: an autosomal-recessive disorder caused by a loss-of-function mutation in WNT4. *Am J Hum Genet,* 82**,** 39-47.

Martineau, J., K. Nordqvist, C. Tilmann, R. Lovell-Badge & B. Capel (1997) Male-specific cell migration into the developing gonad. *Curr Biol,* 7**,** 958-68.

Mayère, C., Y. Neirijnck, P. Sararols, C. M. Rands, I. Stévant, F. Kühne, A. A. Chassot, M. C. Chaboissier, E. T. Dermitzakis & S. Nef (2021) Single-cell transcriptomics reveal temporal dynamics of critical regulators of germ cell fate during mouse sex determination. *Faseb j,* 35**,** e21452.

McElreavey, K., A. Jorgensen, C. Eozenou, T. Merel, J. Bignon-Topalovic, D. S. Tan, D. Houzelstein, F. Buonocore, N. Warr, R. G. G. Kay, M. Peycelon, J. P. Siffroi, I. Mazen, J. C. Achermann, Y. Shcherbak, J. Leger, A. Sallai, J. C. Carel, L. Martinerie, R. Le Ru, G. S. Conway, B. Mignot, L. Van Maldergem, R. Bertalan, E. Globa, R. Brauner, R. Jauch, S. Nef, A. Greenfield & A. Bashamboo (2020) Pathogenic variants in the DEAH-box RNA helicase DHX37 are a frequent cause of 46,XY gonadal dysgenesis and 46,XY testicular regression syndrome. *Genet Med,* 22**,** 150-159.

Menke, D. B., J. Koubova & D. C. Page (2003) Sexual differentiation of germ cells in XX mouse gonads occurs in an anterior-to-posterior wave. *Dev Biol,* 262**,** 303-12.

Mianne, J., L. Chessum, S. Kumar, C. Aguilar, G. Codner, M. Hutchison, A. Parker, A. M. Mallon, S. Wells, M. M. Simon, L. Teboul, S. D. Brown & M. R. Bowl (2016) Correction of the auditory phenotype in C57BL/6N mice via CRISPR/Cas9-mediated homology directed repair. *Genome Med,* 8**,** 16.

Mianne, J., G. F. Codner, A. Caulder, R. Fell, M. Hutchison, R. King, M. E. Stewart, S. Wells & L. Teboul (2017) Analysing the outcome of CRISPR-aided genome editing in embryos: Screening, genotyping and quality control. *Methods,* 121-122**,** 68-76.

Mikami, S., T. Kanaba, Y. Ito & M. Mishima (2013) NMR assignments of SPOC domain of the human transcriptional corepressor SHARP in complex with a C-terminal SMRT peptide. *Biomol NMR Assign,* 7**,** 267-70.

Mikolas, P., J. Kollarova, K. Sebkova, V. Saudek, P. Yilma, M. Kostrouchova, M. W. Krause & Z. Kostrouch (2013) GEI-8, a homologue of vertebrate nuclear receptor corepressor NCoR/SMRT, regulates gonad development and neuronal functions in Caenorhabditis elegans. *PLoS One,* 8**,** e58462.

Minucci, S. & K. Ozato (1996) Retinoid receptors in transcriptional regulation. *Curr Opin Genet Dev,* 6**,** 567-74.

Mongan, N. P., R. Tadokoro-Cuccaro, T. Bunch & I. A. Hughes (2015) Androgen insensitivity syndrome. *Best Pract Res Clin Endocrinol Metab,* 29**,** 569-80.

Morais da Silva, S., A. Hacker, V. Harley, P. Goodfellow, A. Swain & R. Lovell-Badge (1996) Sox9 expression during gonadal development implies a conserved role for the gene in testis differentiation in mammals and birds. *Nat Genet,* 14**,** 62-8.

Mosier, D. E., R. J. Gulizia, S. M. Baird & D. B. Wilson (1988) Transfer of a functional human immune system to mice with severe combined immunodeficiency. *Nature,* 335**,** 256-9.

Mottis, A., L. Mouchiroud & J. Auwerx (2013) Emerging roles of the corepressors NCoR1 and SMRT in homeostasis. *Genes Dev,* 27**,** 819-35.

Munger, S. C., D. L. Aylor, H. A. Syed, P. M. Magwene, D. W. Threadgill & B. Capel (2009) Elucidation of the transcription network governing mammalian sex determination by exploiting strain-specific susceptibility to sex reversal. *Genes Dev,* 23**,** 2521-36.

Nef, S. & J. D. Vassalli (2009) Complementary pathways in mammalian female sex determination. *J Biol,* 8**,** 74.

Nei, M., P. Xu & G. Glazko (2001) Estimation of divergence times from multiprotein sequences for a few mammalian species and several distantly related organisms. *Proc Natl Acad Sci U S A,* 98**,** 2497-502.

Nofsinger, R. R., P. Li, S. H. Hong, J. W. Jonker, G. D. Barish, H. Ying, S. Y. Cheng, M. Leblanc, W. Xu, L. Pei, Y. J. Kang, M. Nelson, M. Downes, R. T. Yu, J. M. Olefsky, C. H. Lee & R. M. Evans (2008) SMRT repression of nuclear receptors controls the adipogenic set point and metabolic homeostasis. *Proc Natl Acad Sci U S A,* 105**,** 20021-6.

O'Neill, M. J. & R. J. O'Neill (1999) Whatever happened to SRY? *Cell Mol Life Sci,* 56**,** 883-93.

Oberoi, J., L. Fairall, P. J. Watson, J. C. Yang, Z. Czimmerer, T. Kampmann, B. T. Goult, J. A. Greenwood, J. T. Gooch, B. C. Kallenberger, L. Nagy, D. Neuhaus & J. W. Schwabe (2011) Structural basis for the assembly of the SMRT/NCoR core transcriptional repression machinery. *Nat Struct Mol Biol,* 18**,** 177-84.

Ordentlich, P., M. Downes, W. Xie, A. Genin, N. B. Spinner & R. M. Evans (1999) Unique forms of human and mouse nuclear receptor corepressor SMRT. *Proc Natl Acad Sci U S A,* 96**,** 2639-44.

Pannetier, M., A. A. Chassot, M. C. Chaboissier & E. Pailhoux (2016) Involvement of FOXL2 and RSPO1 in Ovarian Determination, Development, and Maintenance in Mammals. *Sex Dev,* 10**,** 167-184.

Park, E. J., D. J. Schroen, M. Yang, H. Li, L. Li & J. D. Chen (1999) SMRTe, a silencing mediator for retinoid and thyroid hormone receptors-extended isoform that is more related to the nuclear receptor corepressor. *Proc Natl Acad Sci U S A,* 96**,** 3519-24.

Parma, P., O. Radi, V. Vidal, M. C. Chaboissier, E. Dellambra, S. Valentini, L. Guerra, A. Schedl & G. Camerino (2006) R-spondin1 is essential in sex determination, skin differentiation and malignancy. *Nat Genet,* 38**,** 1304-9.

Pearlman, A., J. Loke, C. Le Caignec, S. White, L. Chin, A. Friedman, N. Warr, J. Willan, D. Brauer, C. Farmer, E. Brooks, C. Oddoux, B. Riley, S. Shajahan, G. Camerino, T. Homfray, A. H. Crosby, J. Couper, A. David, A. Greenfield, A. Sinclair & H. Ostrer (2010) Mutations in MAP3K1 cause 46,XY disorders of sex development and implicate a common signal transduction pathway in human testis determination. *Am J Hum Genet,* 87**,** 898-904.

Pei, L., M. Leblanc, G. Barish, A. Atkins, R. Nofsinger, J. Whyte, D. Gold, M. He, K. Kawamura, H. R. Li, M. Downes, R. T. Yu, H. C. Powell, J. B. Lingrel & R. M. Evans (2011) Thyroid hormone receptor repression is linked to type I pneumocyte-associated respiratory distress syndrome. *Nat Med,* 17**,** 1466-72.

Perissi, V., K. Jepsen, C. K. Glass & M. G. Rosenfeld (2010) Deconstructing repression: evolving models of co-repressor action. *Nat Rev Genet,* 11**,** 109-23.

Pesce, M., X. Wang, D. J. Wolgemuth & H. Scholer (1998) Differential expression of the Oct-4 transcription factor during mouse germ cell differentiation. *Mech Dev,* 71**,** 89-98.

Pierce, S. B., K. Gersak, R. Michaelson-Cohen, T. Walsh, M. K. Lee, D. Malach, R. E. Klevit, M. C. King & E. Levy-Lahad (2013) Mutations in LARS2, encoding mitochondrial leucyl-tRNA synthetase, lead to premature ovarian failure and hearing loss in Perrault syndrome. *Am J Hum Genet,* 92**,** 614-20.

Rahmoun, M., R. Lavery, S. Laurent-Chaballier, N. Bellora, G. K. Philip, M. Rossitto, A. Symon, E. Pailhoux, F. Cammas, J. Chung, S. Bagheri-Fam, M. Murphy, V. Bardwell, D. Zarkower, B. Boizet-Bonhoure, P. Clair, V. R. Harley & F. Poulat (2017) In mammalian foetal testes, SOX9 regulates expression of its target genes by binding to genomic regions with conserved signatures. *Nucleic Acids Res,* 45**,** 7191-7211.

Reilly, S. M., P. Bhargava, S. Liu, M. R. Gangl, C. Gorgun, R. R. Nofsinger, R. M. Evans, L. Qi, F. B. Hu & C. H. Lee (2010) Nuclear receptor corepressor SMRT regulates mitochondrial oxidative metabolism and mediates aging-related metabolic deterioration. *Cell Metab,* 12**,** 643-53.

Richter, S. H. (2017) Systematic heterogenization for better reproducibility in animal experimentation. *Lab Anim (NY),* 46**,** 343-349.

Riethmacher, D., V. Brinkmann & C. Birchmeier (1995) A targeted mutation in the mouse E-cadherin gene results in defective preimplantation development. *Proc Natl Acad Sci U S A,* 92**,** 855-9.

Robins, D. M. (2012) Androgen receptor gene polymorphisms and alterations in prostate cancer: of humanized mice and men. *Mol Cell Endocrinol,* 352**,** 26-33.

Robinson, N. B., K. Krieger, F. M. Khan, W. Huffman, M. Chang, A. Naik, R. Yongle, I. Hameed, L. N. Girardi & M. Gaudino (2019) The current state of animal models in research: A review. *Int J Surg,* 72**,** 9-13.

Rodríguez Gutiérrez, D., W. Eid & A. Biason-Lauber (2018) A Human Gonadal Cell Model From Induced Pluripotent Stem Cells. *Front Genet,* 9**,** 498.

Romereim, S. M. & A. S. Cupp (2016) Mesonephric Cell Migration into the Gonads and Vascularization Are Processes Crucial for Testis Development. *Results Probl Cell Differ,* 58**,** 67-100.

Saftig, P. & A. Haas (2016) Turn up the lysosome. *Nat Cell Biol,* 18**,** 1025-7.

Sakib, S., Y. Yu, A. Voigt, M. Ungrin & I. Dobrinski (2019) Generation of Porcine Testicular Organoids with Testis Specific Architecture using Microwell Culture. *J Vis Exp*.

Salic, A. & T. J. Mitchison (2008) A chemical method for fast and sensitive detection of DNA synthesis in vivo. *Proc Natl Acad Sci U S A,* 105**,** 2415-20.

Schmahl, J. & B. Capel (2003) Cell proliferation is necessary for the determination of male fate in the gonad. *Dev Biol,* 258**,** 264-76.

Schmahl, J., E. M. Eicher, L. L. Washburn & B. Capel (2000) Sry induces cell proliferation in the mouse gonad. *Development,* 127**,** 65-73.

Schmahl, J., Y. Kim, J. S. Colvin, D. M. Ornitz & B. Capel (2004) Fgf9 induces proliferation and nuclear localization of FGFR2 in Sertoli precursors during male sex determination. *Development,* 131**,** 3627-36.

Schmidt, D., C. E. Ovitt, K. Anlag, S. Fehsenfeld, L. Gredsted, A. C. Treier & M. Treier (2004) The murine winged-helix transcription factor Foxl2 is required for granulosa cell differentiation and ovary maintenance. *Development,* 131**,** 933-42.

Scholz, J., C. LaLiberté, M. van Eede, J. P. Lerch & M. Henkelman (2016) Variability of brain anatomy for three common mouse strains. *Neuroimage,* 142**,** 656-662.

Schutgens, F. & H. Clevers (2020) Human Organoids: Tools for Understanding Biology and Treating Diseases. *Annu Rev Pathol,* 15**,** 211-234.

Sekido, R. & R. Lovell-Badge (2008) Sex determination involves synergistic action of SRY and SF1 on a specific Sox9 enhancer. *Nature,* 453**,** 930-4.

Sellers, R. S., C. B. Clifford, P. M. Treuting & C. Brayton (2012) Immunological variation between inbred laboratory mouse strains: points to consider in phenotyping genetically immunomodified mice. *Vet Pathol,* 49**,** 32-43.

Sepponen, K., K. Lundin, K. Knuus, P. Väyrynen, T. Raivio, J. S. Tapanainen & T. Tuuri (2017) The Role of Sequential BMP Signaling in Directing Human Embryonic Stem Cells to Bipotential Gonadal Cells. *J Clin Endocrinol Metab,* 102**,** 4303-4314.

Sharpe, R. M. (2020) Androgens and the masculinization programming window: human-rodent differences. *Biochem Soc Trans,* 48**,** 1725-1735.

Shimizu, H., I. Astapova, F. Ye, M. Bilban, R. N. Cohen & A. N. Hollenberg (2015) NCoR1 and SMRT play unique roles in thyroid hormone action in vivo. *Mol Cell Biol,* 35**,** 555-65.

Shlush, E., L. Maghen, S. Swanson, S. Kenigsberg, S. Moskovtsev, T. Barretto, A. Gauthier-Fisher & C. L. Librach (2017) In vitro generation of Sertoli-like and haploid spermatid-like cells from human umbilical cord perivascular cells. *Stem Cell Res Ther,* 8**,** 37.

Siggers, P., G. A. Carre, D. Bogani, N. Warr, S. Wells, H. Hilton, C. Esapa, M. K. Hajihosseini & A. Greenfield (2014) A novel mouse Fgfr2 mutant, hobbyhorse (hob), exhibits complete XY gonadal sex reversal. *PLoS One,* 9**,** e100447.

Sinclair, A. H., P. Berta, M. S. Palmer, J. R. Hawkins, B. L. Griffiths, M. J. Smith, J. W. Foster, A. M. Frischauf, R. Lovell-Badge & P. N. Goodfellow (1990) A gene from the human sex-determining region encodes a protein with homology to a conserved DNA-binding motif. *Nature,* 346**,** 240-4.

Smith, C. A., K. N. Roeszler, T. Ohnesorg, D. M. Cummins, P. G. Farlie, T. J. Doran & A. H. Sinclair (2009) The avian Z-linked gene DMRT1 is required for male sex determination in the chicken. *Nature,* 461**,** 267-71.

Smith, P. J. 2016. EdU and BrdU incorporation resolve their differences. In *Cell Cycle*, 1527-8.

Smyth, C. M. & W. J. Bremner (1998) Klinefelter syndrome. *Arch Intern Med,* 158**,** 1309-14.

Soh, Y. Q., J. P. Junker, M. E. Gill, J. L. Mueller, A. van Oudenaarden & D. C. Page (2015) A Gene Regulatory Program for Meiotic Prophase in the Fetal Ovary. *PLoS Genet,* 11**,** e1005531.

Stevant, I., F. Kuhne, A. Greenfield, M. C. Chaboissier, E. T. Dermitzakis & S. Nef (2019) Dissecting Cell Lineage Specification and Sex Fate Determination in Gonadal Somatic Cells Using Single-Cell Transcriptomics. *Cell Rep,* 26**,** 3272-3283.e3.

Stevant, I., Y. Neirijnck, C. Borel, J. Escoffier, L. B. Smith, S. E. Antonarakis, E. T. Dermitzakis & S. Nef (2018) Deciphering Cell Lineage Specification during Male Sex Determination with Single-Cell RNA Sequencing. *Cell Rep,* 22**,** 1589-1599.

Sun, J., S. Yu, X. Zhang, C. Capac, O. Aligbe, T. Daudelin, E. M. Bonder & N. Gao (2017) A Wntless-SEC12 complex on the ER membrane regulates early Wnt secretory vesicle assembly and mature ligand export. *J Cell Sci,* 130**,** 2159-2171.

Szenker-Ravi, E., U. Altunoglu, M. Leushacke, C. Bosso-Lefevre, M. Khatoo, H. Thi Tran, T. Naert, R. Noelanders, A. Hajamohideen, C. Beneteau, S. B. de Sousa, B. Karaman, X. Latypova, S. Basaran, E. B. Yucel, T. T. Tan, L. Vlaeminck, S. S. Nayak, A. Shukla, K. M. Girisha, C. Le Caignec, N. Soshnikova, Z. O. Uyguner, K. Vleminckx, N. Barker, H. Kayserili & B. Reversade (2018) RSPO2 inhibition of RNF43 and ZNRF3 governs limb development independently of LGR4/5/6. *Nature,* 557**,** 564-569.

Tam, Y. H., Y. S. Wong, K. K. Pang, K. F. To, A. K. Yiu, H. Y. Wong, S. Y. Tsui, J. W. Mou, K. W. Chan & K. H. Lee (2016) Tumor risk of children with 45,X/46,XY gonadal dysgenesis in relation to their clinical presentations: Further insights into the gonadal management. *J Pediatr Surg,* 51**,** 1462-6.

Tang, H., J. Brennan, J. Karl, Y. Hamada, L. Raetzman & B. Capel (2008) Notch signaling maintains Leydig progenitor cells in the mouse testis. *Development,* 135**,** 3745-53.

Thevenet, L., C. Mejean, B. Moniot, N. Bonneaud, N. Galeotti, G. Aldrian-Herrada, F. Poulat, P. Berta, M. Benkirane & B. Boizet-Bonhoure (2004) Regulation of human SRY subcellular distribution by its acetylation/deacetylation. *Embo j,* 23**,** 3336-45.

Toublanc, J. E., C. Boucekkine, N. Abbas, D. Barama, E. Vilain, K. McElreavey, M. Toublanc & M. Fellous (1993) Hormonal and molecular genetic findings in 46,XX subjects with sexual ambiguity and testicular differentiation. *Eur J Pediatr,* 152 Suppl 2**,** S70-5.

Townley, A. K., Y. Feng, K. Schmidt, D. A. Carter, R. Porter, P. Verkade & D. J. Stephens (2008) Efficient coupling of Sec23-Sec24 to Sec13-Sec31 drives COPII-dependent collagen secretion and is essential for normal craniofacial development. *J Cell Sci,* 121**,** 3025-34.

Toyooka, Y., N. Tsunekawa, Y. Takahashi, Y. Matsui, M. Satoh & T. Noce (2000) Expression and intracellular localization of mouse Vasa-homologue protein during germ cell development. *Mech Dev,* 93**,** 139-49.

Uhlenhaut, N. H., S. Jakob, K. Anlag, T. Eisenberger, R. Sekido, J. Kress, A. C. Treier, C. Klugmann, C. Klasen, N. I. Holter, D. Riethmacher, G. Schutz, A. J. Cooney, R. Lovell-Badge & M. Treier (2009) Somatic sex reprogramming of adult ovaries to testes by FOXL2 ablation. *Cell,* 139**,** 1130-42.

Unger, S., G. Scherer & A. Superti-Furga. 1993. Campomelic Dysplasia. In *GeneReviews((R)),* eds. M. P. Adam, H. H. Ardinger, R. A. Pagon, S. E. Wallace, L. J. H. Bean, K. Stephens & A. Amemiya. Seattle (WA): University of Washington, Seattle

University of Washington, Seattle. GeneReviews is a registered trademark of the University of Washington, Seattle. All rights reserved.

Vainio, S., M. Heikkila, A. Kispert, N. Chin & A. P. McMahon (1999) Female development in mammals is regulated by Wnt-4 signalling. *Nature,* 397**,** 405-9.

van Rijn, R. S., E. R. Simonetti, A. Hagenbeek, M. C. Hogenes, R. A. de Weger, M. R. Canninga-van Dijk, K. Weijer, H. Spits, G. Storm, L. van Bloois, G. Rijkers, A. C. Martens & S. B. Ebeling (2003) A new xenograft model for graft-versus-host disease by intravenous transfer of human peripheral blood mononuclear cells in RAG2-/- gammac-/- double-mutant mice. *Blood,* 102**,** 2522-31.

Van Schoore, G., F. Mendive, R. Pochet & G. Vassart (2005) Expression pattern of the orphan receptor LGR4/GPR48 gene in the mouse. *Histochem Cell Biol,* 124**,** 35-50.

Vidal, V. P., M. C. Chaboissier, D. G. de Rooij & A. Schedl (2001) Sox9 induces testis development in XX transgenic mice. *Nat Genet,* 28**,** 216-7.

Villanueva, C. J., L. Vergnes, J. Wang, B. G. Drew, C. Hong, Y. Tu, Y. Hu, X. Peng, F. Xu, E. Saez, K. Wroblewski, A. L. Hevener, K. Reue, L. G. Fong, S. G. Young & P. Tontonoz (2013) Adipose subtype-selective recruitment of TLE3 or Prdm16 by PPARgamma specifies lipid storage versus thermogenic gene programs. *Cell Metab,* 17**,** 423-35.

Voskuil, J. (2014) Commercial antibodies and their validation. *F1000Res,* 3**,** 232.

Wallis, M. C., P. D. Waters & J. A. Graves (2008) Sex determination in mammals--before and after the evolution of SRY. *Cell Mol Life Sci,* 65**,** 3182-95.

Walsh, N. C., L. L. Kenney, S. Jangalwe, K. E. Aryee, D. L. Greiner, M. A. Brehm & L. D. Shultz (2017) Humanized Mouse Models of Clinical Disease. *Annu Rev Pathol,* 12**,** 187-215.

Wang, N. & J. L. Tilly (2010) Epigenetic status determines germ cell meiotic commitment in embryonic and postnatal mammalian gonads. *Cell Cycle,* 9**,** 339-49.

Wansleeben, C., H. Feitsma, M. Montcouquiol, C. Kroon, E. Cuppen & F. Meijlink (2010) Planar cell polarity defects and defective Vangl2 trafficking in mutants for the COPII gene Sec24b. *Development,* 137**,** 1067-73.

Warr, N., D. Bogani, P. Siggers, R. Brixey, H. Tateossian, A. Dopplapudi, S. Wells, M. Cheeseman, Y. Xia, H. Ostrer & A. Greenfield (2011) Minor abnormalities of testis development in mice lacking the gene encoding the MAPK signalling component, MAP3K1. *PLoS One,* 6**,** e19572.

Warr, N., G. A. Carre, P. Siggers, J. V. Faleato, R. Brixey, M. Pope, D. Bogani, M. Childers, S. Wells, C. L. Scudamore, M. Tedesco, I. del Barco Barrantes, A. R. Nebreda, P. A. Trainor & A. Greenfield (2012) Gadd45gamma and Map3k4 interactions regulate mouse testis determination via p38 MAPK-mediated control of Sry expression. *Dev Cell,* 23**,** 1020-31.

Warr, N., P. Siggers, D. Bogani, R. Brixey, L. Pastorelli, L. Yates, C. H. Dean, S. Wells, W. Satoh, A. Shimono & A. Greenfield (2009) Sfrp1 and Sfrp2 are required for normal male sexual development in mice. *Dev Biol,* 326**,** 273-84.

Washburn, L. L. & E. M. Eicher (1989) Normal testis determination in the mouse depends on genetic interaction of a locus on chromosome 17 and the Y chromosome. *Genetics,* 123**,** 173-9.

Weber, C., Y. Zhou, J. G. Lee, L. L. Looger, G. Qian, C. Ge & B. Capel (2020) Temperature-dependent sex determination is mediated by pSTAT3 repression of Kdm6b. *Science,* 368**,** 303-306.

Wieacker, P., D. Missbach, S. Jakubiczka, S. Borgmann & N. Albers (1996) Sex reversal in a child with the karyotype 46,XY, dup (1) (p22.3p32.3). *Clin Genet,* 49**,** 271-3.

Wu, Y., J. Zhang, B. Peng, D. Tian, D. Zhang, Y. Li, X. Feng, J. Liu, J. Li, T. Zhang, X. Liu, J. Lu, B. Chen & S. Wang (2019) Generating viable mice with heritable embryonically lethal mutations using the CRISPR-Cas9 system in two-cell embryos. *Nat Commun,* 10**,** 2883.

Xie, Y., R. Zamponi, O. Charlat, M. Ramones, S. Swalley, X. Jiang, D. Rivera, W. Tschantz, B. Lu, L. Quinn, C. Dimitri, J. Parker, D. Jeffery, S. K. Wilcox, M. Watrobka, P. LeMotte, B. Granda, J. A. Porter,

V. E. Myer, A. Loew & F. Cong (2013) Interaction with both ZNRF3 and LGR4 is required for the signalling activity of R-spondin. *EMBO Rep,* 14**,** 1120-6.

Xu, F., K. Li, M. Tian, P. Hu, W. Song, J. Chen, X. Gao & Q. Zhao (2009) N-CoR is required for patterning the anterior-posterior axis of zebrafish hindbrain by actively repressing retinoid signaling. *Mech Dev,* 126**,** 771-80.

Yamashiro, C., K. Sasaki, Y. Yabuta, Y. Kojima, T. Nakamura, I. Okamoto, S. Yokobayashi, Y. Murase, Y. Ishikura, K. Shirane, H. Sasaki, T. Yamamoto & M. Saitou (2018) Generation of human oogonia from induced pluripotent stem cells in vitro. *Science,* 362**,** 356-360.

Yang, X. J., V. V. Ogryzko, J. Nishikawa, B. H. Howard & Y. Nakatani (1996) A p300/CBP-associated factor that competes with the adenoviral oncoprotein E1A. *Nature,* 382**,** 319-24.

Yang, X. Y., X. Y. Zhou, Q. Q. Wang, H. Li, Y. Chen, Y. P. Lei, X. H. Ma, P. Kong, Y. Shi, L. Jin, T. Zhang & H. Y. Wang (2013) Mutations in the COPII vesicle component gene SEC24B are associated with human neural tube defects. *Hum Mutat,* 34**,** 1094-101.

Yao, H. H., W. Whoriskey & B. Capel (2002) Desert Hedgehog/Patched 1 signaling specifies fetal Leydig cell fate in testis organogenesis. *Genes Dev,* 16**,** 1433-40.

Yokoyama, T., Y. Miura, A. Yamamoto, C. Hasegawa, K. Kawanishi, N. Takada, T. Omotehara, T. Hirano, Y. Mantani, T. Miki & N. Hoshi (2019) Genetic differences between C57BL/6 substrains affect the process of testis differentiation in YPOS mice. *J Vet Med Sci,* 81**,** 608-11.

Yoshiki, A. & K. Moriwaki (2006) Mouse phenome research: implications of genetic background. *Ilar j,* 47**,** 94-102.

You, S. H., H. W. Lim, Z. Sun, M. Broache, K. J. Won & M. A. Lazar (2013) Nuclear receptor co-repressors are required for the histone-deacetylase activity of HDAC3 in vivo. *Nat Struct Mol Biol,* 20**,** 182-7.

Yu, J., Y. Li, T. Ishizuka, M. G. Guenther & M. A. Lazar (2003) A SANT motif in the SMRT corepressor interprets the histone code and promotes histone deacetylation. *Embo j,* 22**,** 3403-10.

Yui, S., T. Nakamura, T. Sato, Y. Nemoto, T. Mizutani, X. Zheng, S. Ichinose, T. Nagaishi, R. Okamoto, K. Tsuchiya, H. Clevers & M. Watanabe (2012) Functional engraftment of colon epithelium expanded in vitro from a single adult Lgr5^{+} stem cell. *Nat Med,* 18**,** 618-23.

Zebisch, M. & E. Y. Jones (2015) ZNRF3/RNF43--A direct linkage of extracellular recognition and E3 ligase activity to modulate cell surface signalling. *Prog Biophys Mol Biol,* 118**,** 112-8.

Zhang, J., M. Kalkum, B. T. Chait & R. G. Roeder (2002) The N-CoR-HDAC3 nuclear receptor corepressor complex inhibits the JNK pathway through the integral subunit GPS2. *Mol Cell,* 9**,** 611-23.

Zhang, R. R., Y. H. Gui & X. Wang (2015) [Role of the canonical Wnt signaling pathway in heart valve development]. *Zhongguo Dang Dai Er Ke Za Zhi,* 17**,** 757-62.

Zhao, L., E. T. Ng, T. L. Davidson, E. Longmuss, J. Urschitz, M. Elston, S. Moisyadi, J. Bowles & P. Koopman (2014) Structure-function analysis of mouse Sry reveals dual essential roles of the C-terminal polyglutamine tract in sex determination. *Proc Natl Acad Sci U S A,* 111**,** 11768-73.

Zhao, L., C. Wang, M. L. Lehman, M. He, J. An, T. Svingen, C. M. Spiller, E. T. Ng, C. C. Nelson & P. Koopman (2018) Transcriptomic analysis of mRNA expression and alternative splicing during mouse sex determination. *Mol Cell Endocrinol,* 478**,** 84-96.

Zhou, S. & S. D. Hayward. 2001. Nuclear Localization of CBF1 Is Regulated by Interactions with the SMRT Corepressor Complex. In *Mol Cell Biol*, 6222-32.

Zhu, F., R. R. Nair, E. M. C. Fisher & T. J. Cunningham (2019) Humanising the mouse genome piece by piece. *Nat Commun,* 10**,** 1845.

Zuo, T., F. Zhang, G. C. Y. Lui, Y. K. Yeoh, A. Y. L. Li, H. Zhan, Y. Wan, A. C. K. Chung, C. P. Cheung, N. Chen, C. K. C. Lai, Z. Chen, E. Y. K. Tso, K. S. C. Fung, V. Chan, L. Ling, G. Joynt, D. S. C. Hui, F. K. L. Chan, P. K. S. Chan & S. C. Ng (2020) Alterations in Gut Microbiota of Patients With COVID-19 During Time of Hospitalization. *Gastroenterology,* 159**,** 944-955.e8.

Appendices

Appendix 1: *Sec31a* 1055del and 423del sequence surrounding the deletion.

SEC31A-DEL1055: Deletion of 1055nt including exon ENSMUSE00001292836:

GTTGCTGCAAAGCATACACTACCATGCATCAGGATGCAAAGAGTCTGTGTGGGTGTGTGTAGGTGCCCTGTAC
TTTGTGTGTGTGCAGGGGTGAGTGTGTGGGTACTCTGTATCTTCTGTGGGGTTGTGTGT

[1055 nt deletion]

GCAATAAGATGCACCGAGCAGGCAGATGAATGCCGAGTAGGGACTGGAGAGGAACGAGGAAGAAGCGAGA
GCATATATAATCATCTATATAATCAGGTGACAGTTCTATATAGTGTTATATATAGTCAGTGAGCAGATATACCT
GTGTGTCAGAGGGAGAGGCTGCAGGTGGATGGCTGGGGAGGGCAGTGGGAGTTTTG

SEC31A-DEL423: Deletion of 423 nt replaced by 4 nt including exon ENSMUSE00001292836:

CGTTGCTGCAAAGCATACACTACCATGCATCAGGATGCAAAGAGTCTGTGTGGGTGTGTGTAGGTGCCCTGTA
CTTTGTGTGTGTGCAGGGGTGAGTGTGTGGGTACTCTGTATCTTCTGTGGGGTTGTGTGTAGGTGCCCTGTAC
TTTCGTGTGGGTGAGCATGGGTGAGTGTGTGGGTGCCCTGTATCTTCTGTGTGGGTGAATGTGTGGGTGCCC
TGTACGCTGTGTGTGGGTGAGCATGTGGGTGCCCTGTATCTTGTGTGTGGGTGAGCATGGGTGTGTGTGGGT
GCCCTGTATCTTCTGTGTGGGTGAATGTGTGGGTGCCCTGTACTCTGTGTGTGGGTGAGCATGTGGGTGCCCT
GTATCTTGTGTGTGGGTGAGCATGTCAGTGTGTGTCTCTCTTGTGTCTATTCCCCACCTCCCCACTCTCTGTGGG
TGCTAGAAACTGAACACT

[423 nt deletion replaced by 4nt] gagg

GACTGTAGTGAATGGCAGCAGCAATGGCCTCATAACAGCAACACTGTGGTAACACCAGAAGTTTCATCTCTAC
TAACTTCCATTTACTGCTCCGGACTCTGGGGATAAATAGCATAAGGGGACTTTTGGTTTTCTTCCATTTCTGCAA
TGCTTACAAGAAAGAGAAACATCTTCATAAAATTCAATTTAAACCATTATTTGAACCTTGGTTGAGATTTTTCTA
GCTCTAGTAAATTTAGAACTGCAGAAGAAGAGAAAGGATAAGAGAATCAATTAATAGCACTAAAAATTGCCA
CCTGTATCCCACCAGCAATAAGATGCACCGAGCAGGCAGATGAATGCCGAGTAGGGACTGGA

Appendix 2: Ontology Table highlighting the ontologies affected by loss of *Znrf3* in RNA sequencing analysis of 11.5 dpc gonads.

DATABASE	ONTOLOGY TERM	XY vs XX	XY vs XYDEL	XX vs XXDel
GO:BP	gonad development	6.78E-05	na	na
GO:BP	development of primary sexual characteristics	7.98E-05	na	na
GO:BP	male gonad development	8.90E-05	na	na
GO:BP	development of primary male sexual characteristics	9.26E-05	na	na
GO:BP	developmental process involved in reproduction	0.000209041	na	na
GO:BP	male sex differentiation	0.00022878	na	na
GO:BP	sex differentiation	0.000229215	na	0.028869809
GO:BP	reproductive structure development	0.000359607	na	na
GO:BP	reproductive system development	0.000388854	na	na
GO:BP	regulation of male gonad development	0.000502985	na	na
GO:BP	sex determination	0.001232966	na	na
GO:BP	reproductive process	0.001517876	na	na
GO:BP	reproduction	0.00152759	na	na
GO:BP	male sex determination	0.002334385	na	na
GO:BP	regulation of gonad development	0.006384338	na	na
GO:BP	renal vesicle induction	0.009961382	na	na
GO:BP	histone lysine demethylation	0.016708446	na	na
GO:BP	histone demethylation	0.018481688	na	na
GO:BP	protein dealkylation	0.022391858	na	na
GO:BP	protein demethylation	0.022391858	na	na
GO:BP	positive regulation of macromolecule metabolic process	0.024377305	na	na
GO:BP	metanephric tubule formation	0.033148438	na	na
GO:BP	positive regulation of gene expression	0.036487989	na	na
GO:BP	positive regulation of multicellular organismal process	0.043027855	0.00081066	na
GO:BP	C21-steroid hormone metabolic process	na	0.00075744	0.008818517
GO:BP	tissue development	na	0.003015799	na
GO:BP	steroid metabolic process	na	0.000363142	0.026468776
GO:BP	bone morphogenesis	na	0.02295126	na
GO:BP	animal organ development	na	5.13E-06	na
GO:BP	positive regulation of cell differentiation	na	0.021856535	na
GO:BP	gonadotropin secretion	na	0.023736034	na
GO:BP	anatomical structure morphogenesis	na	0.014768828	na
GO:BP	metanephros development	na	na	0.008963261
GO:BP	alcohol metabolic process	na	na	0.005690817
GO:BP	positive regulation of cell communication	na	na	0.034414055
GO:BP	steroid biosynthetic process	na	0.004102265	na
GO:BP	cellular developmental process	na	0.003121385	na
GO:BP	regulation of hormone levels	na	0.000485139	0.000267293
GO:BP	osteoblast differentiation	na	0.022072627	na
GO:BP	multicellular organism development	na	9.88E-08	na
GO:BP	primary alcohol metabolic process	na	0.037513103	0.004449257
GO:BP	developmental process	na	3.23E-06	na
GO:BP	positive regulation of developmental process	na	0.00644402	na
GO:BP	multicellular organismal process	na	3.86E-05	na
GO:BP	cell population proliferation	na	na	0.006658425
GO:BP	positive regulation of signal transduction	na	na	0.020956788
GO:BP	regulation of developmental process	na	0.035575631	na
GO:BP	hydrogen peroxide catabolic process	na	0.034732251	na
GO:BP	response to toxic substance	na	0.022042453	na
GO:BP	hormone metabolic process	na	3.87E-05	0.031464717
GO:BP	cellular response to growth factor stimulus	na	0.031033901	na
GO:BP	nephron epithelium development	na	na	0.027024737
GO:BP	response to lipid	na	0.00105758	na
GO:BP	tertiary alcohol metabolic process	na	0.034732251	na
GO:BP	gas transport	na	1.01E-07	na
GO:BP	response to oxygen-containing compound	na	0.001865847	na
GO:BP	cellular hormone metabolic process	na	0.000344058	0.001593107
GO:BP	hepatocyte differentiation	na	na	0.035331049
GO:BP	cell differentiation	na	0.001680214	na
GO:BP	organic hydroxy compound metabolic process	na	na	0.00162464
GO:BP	regulation of osteoblast differentiation	na	0.008854818	na
GO:BP	response to endogenous stimulus	na	0.007047714	na
GO:BP	regulation of biological quality	na	5.71E-05	na
GO:BP	cellular ketone metabolic process	na	na	0.036163801
GO:BP	progesterone metabolic process	na	na	0.029808098

GO:BP	response to chemical	na	7.23E-05	na
GO:BP	fibrinolysis	na	na	0.035331049
GO:BP	enzyme linked receptor protein signaling pathway	na	0.009178797	na
GO:BP	response to organic cyclic compound	na	0.039046028	na
GO:BP	coagulation	na	na	0.011295439
GO:BP	anatomical structure development	na	2.08E-06	na
GO:BP	follicle-stimulating hormone secretion	na	0.001383199	na
GO:BP	positive regulation of signaling	na	na	0.035827522
GO:BP	lipid metabolic process	na	0.009611902	na
GO:BP	positive regulation of osteoblast differentiation	na	0.023791121	na
GO:BP	kidney epithelium development	na	na	0.005219995
GO:BP	cellular response to chemical stimulus	na	3.50E-05	na
GO:BP	blood coagulation	na	na	0.010182568
GO:BP	oxygen transport	na	3.41E-07	na
GO:BP	response to organic substance	na	0.003656511	na
GO:BP	regulation of multicellular organismal process	na	0.003308132	na
GO:BP	system development	na	1.12E-07	na
GO:BP	gastrulation	na	na	0.021512615
GO:BP	hemostasis	na	na	0.010914016
HP	Maculopapular exanthema	na	0.031003041	na
HP	Hypernatriuria	na	0.028892479	na
HP	Abnormal urine sodium concentration	na	0.043982466	na
HP	Abnormal circulating androgen level	0.000614989	na	na
HP	Functional abnormality of male internal genitalia	0.022478318	na	na
HP	Decreased circulating androgen level	0.016688739	na	na
HP	Male infertility	0.021304153	na	na
HP	Y-linked inheritance	0.000217272	na	na
HP	Extramedullary hematopoiesis	na	0.000418162	na
HP	Aplasia/Hypoplasia of the vagina	0.032144491	na	na
HP	Abnormal serum testosterone level	0.000456676	na	na
HP	Hypercoagulability	na	0.013859693	na
HP	Azoospermia	0.002717865	na	na
HP	Male hypogonadism	0.004091368	na	na
HP	Sex reversal	0.00740368	na	na
HP	Sparse axillary hair	0.00796574	na	na
HP	Primary amenorrhea	0.020537745	na	na
HP	Abnormality of secondary sexual hair	0.030997487	na	na
HP	Abnormal spermatogenesis	0.00382167	na	na
HP	Infertility	0.01030524	na	na
HP	Spontaneous hemolytic crises	na	0.031003041	na
HP	Spherocytosis	na	0.008980245	na
HP	Abnormality of the axillary hair	0.010691846	na	na
HP	Abnormality of the pubic hair	0.008809136	na	na
HP	Sparse pubic hair	0.008809136	na	na
HP	Absence of secondary sex characteristics	0.021304153	na	na
KEGG	Malaria	na	0.011036953	na
KEGG	Pancreatic secretion	na	0.037330796	na
KEGG	Signaling pathways regulating pluripotency of stem cells	na	0.022921691	na
KEGG	Ovarian steroidogenesis	na	0.018247416	0.004826118
REAC	Retinoid metabolism and transport	na	na	5.06E-05
REAC	O2/CO2 exchange in erythrocytes	na	0.000858802	na
REAC	G alpha (i) signalling events	na	na	0.017532941
REAC	Physiological factors	na	na	0.023856824
REAC	Visual phototransduction	na	na	0.001961896
REAC	Metabolism of steroid hormones	na	0.00812754	na
REAC	Metabolism of fat-soluble vitamins	na	na	8.79E-05
REAC	Metabolism of vitamins and cofactors	na	na	0.043177735
REAC	Regulation of TLR by endogenous ligand	na	na	0.003066429
REAC	Erythrocytes take up oxygen and release carbon dioxide	na	0.00012486	na
REAC	Erythrocytes take up carbon dioxide and release oxygen	na	0.000858802	na
REAC	Metabolism of steroids	na	0.03296437	na
REAC	Glycoprotein hormones	na	0.007140966	na
REAC	Scavenging by Class B Receptors	na	na	0.023856824
REAC	Peptide hormone biosynthesis	na	0.016914346	na
WP	Blood Clotting Cascade	na	na	0.004655991

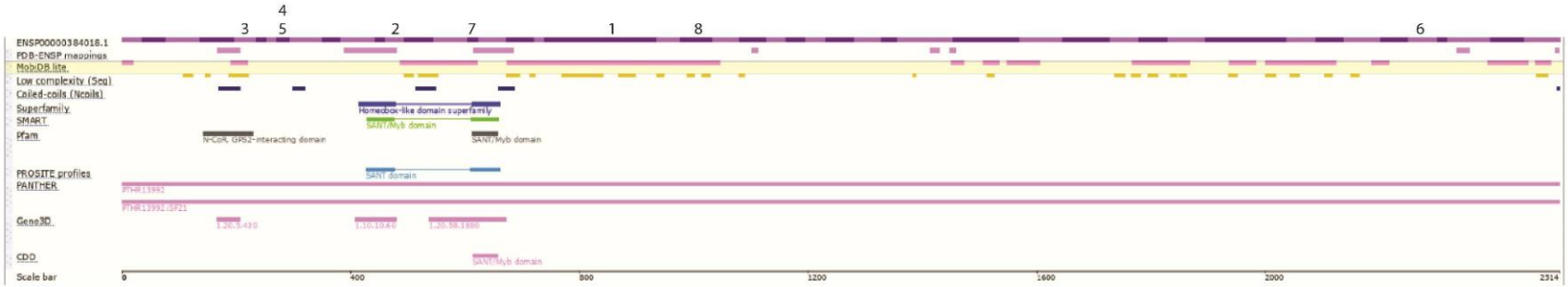

Origin	Phenotype	Mutation	Zygosity	Population: Minor Allele Frequency	
Belgium	46,XY CGD	p.His1862Leu	heterozygous	Novel	
North Africa	46,XY DSD, cardiac anomalies, dysmorphia	p.Gly1166Arg	homozygous	East Asian: 0.0007096	1
North Africa	46,XY CGD	p.Thr1586Met	heterozygous	Latino: 0.00002921	2
North Africa	46,XY syndromic DSD	p.Asp2075Asn	heterozygous	East Asian: 0.0001542	3
North Africa	46,XY CGD	p.Arg1947Gln	heterozygous	very rare variant rs932680959	4
India	46,XX male	p.Ile1109Phe	Heterozygous	de novo, novel	8
Tunisia	46,XX male	p.Asn1665His	Heterozygous	Novel	
Egypt	46,XX male	p.Arg1905Cys	heterozygous	East Asian: 0.00007980: inherited from father	5
UK	46,XY CGD	p.Arg224Cys	heterozygous	South Asian: 0.00006571	6
Egypt	46,XX male	p.Arg1352His	heterozygous	European non-Finnish: 0.008008	7
Ukraine	46,XY DSD	p.Arg2234Gln	heterozygous	very rare variant rs764050780	

Appendix 3. Location of Patient mutations on *NCOR2*

Diagram depicting the locations of some of the patients, presenting with DSD, mutations on *NCOR2*

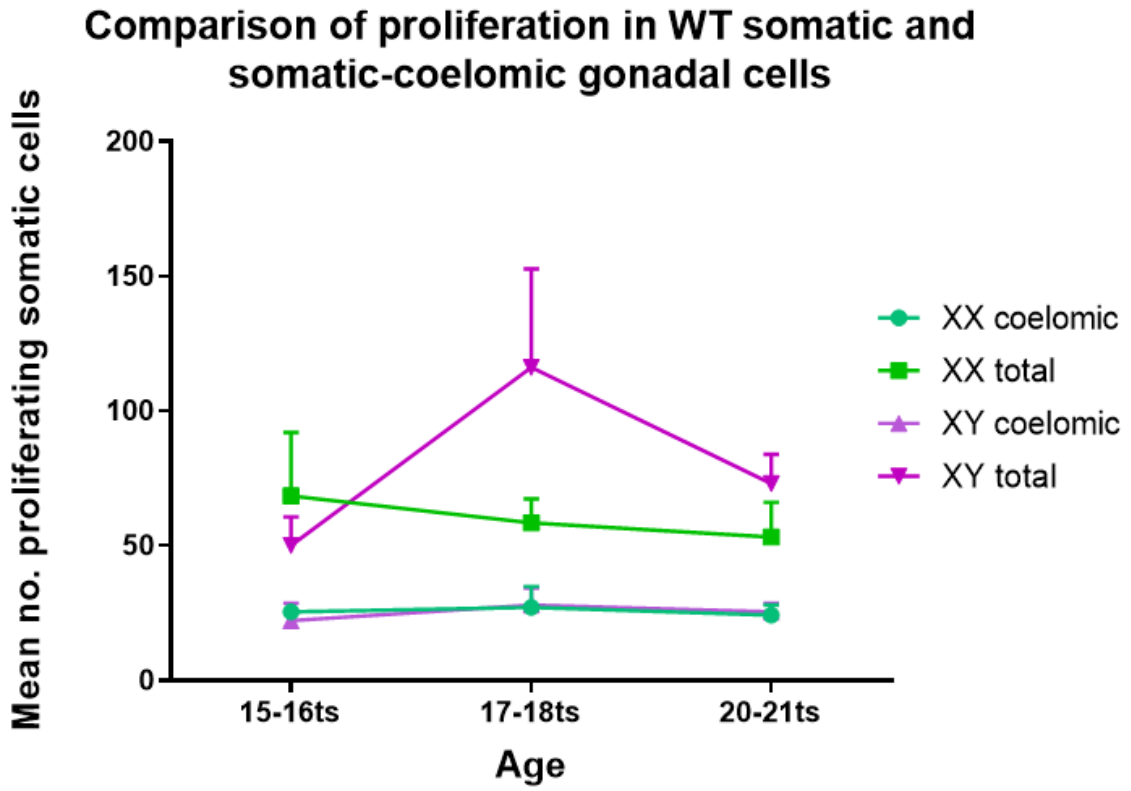

Appendix 4. Analysis of cell proliferation in the coelomic cells of the gonad.
Proliferation in the coelomic cells of the gonad was equal in both XX and XY wild-type gonads throughout development. N=5-6.